Pelton, A. D. and Blander, M. (1984) in *Second International Symposium on Metallurgical Slags & Fluxes*, eds Fine, A. H. and Gaskell, D. R. (Met. Soc. AIME, New York), p. 281.
Pelton, A. D. (1988) *CALPHAD*, **12**, 127.
Pelton, A. D. and Blander, M. (1986a) *Met. Trans. B*, **17B**, 805.
Pelton, A. D. and Blander, M. (1986b) in *Computer Modelling of Phase Diagrams*, ed. Bennett, L. H. (TMS, Warrendale), p. 19.
Pelton, A. D. and Blander, M. (1988) *CALPHAD*, **12**, 97.
Pettifor, D. G. (1995) private communication.
Pitzer, K. S. (1973) *J. Phys. Chem.*, **77**, 268.
Pitzer, K. S. (1975) *J. Soln. Chem.*, **4**, 249.
Pitzer, K. S. and Brewer, L. (1961) *Thermodynamics; 2nd Edition* (McGraw-Hill, New York).
Pitzer, K. S. and Kim, J. J. (1974) *J. Am. Chem. Soc.*, **96**, 5701.
Pitzer, K. S. and Mayorga, G. (1973) *J. Phys. Chem.*, **77**, 2300.
Predel, B. and Oehme, G. (1974) *Z. Metallkde*, **65**, 509.
Richardson, F. D. (1956) *Trans. Farad. Soc.*, **52**, 1312.
Sastri, P. and Lahiri, A. K. (1985) *Met. Trans. B*, **16B**, 325.
Sastri, P. and Lahiri, A. K. (1986) *Met. Trans. B*, **17B**, 105.
Saunders, N. (1989) *Z. Metallkde.*, **80**, 894.
Saunders, N. (1996) *CALPHAD*, **4**, 491.
Selleby, M. (1996) unpublished research.
Sharma, R. C. and Chang, Y. A. (1979) *Met. Trans. B.*, **10B**, 103.
Sommer, F. (1977) *CALPHAD*, **2**, 319.
Sommer, F. (1980) *Z. Metallkde*, **71**, 120.
Sommer, F. (1982) *Z. Metallkde.*, **73**, 72 and 77.
Sundman, B. (1985) private communication.
Sundman, B. (1994) unpublished research.
Sundman, B. (1996) private communication.
Sundman, B. and Mohri, T. (1990) *Z. Metallkde*, **81**, 251.
Sundman, B. and Ågren, J. (1981) *J. Phys. Chem. Solids*, **42**, 297.
Taylor, J. R. and Dinsdale, A. T. (1990) *CALPHAD*, **14**, 71.
Temkin, M. (1945) *Acta Phys. Chim. USSR*, **20**, 411.
Tomiska, J. (1980) *CALPHAD*, **4**, 63.
Toop, G. W. (1965) *Trans. Met. Soc. Aime*, **233**, 855.
Toop, G. W. and Samis, C. S. (1962) *Can. Met. Quart.*, **1**, 129.
Villars, P. and Calvert, L. D. (1991) *Pearson's Handbook of Crystallographic Data for Intermetallic Phases; 2nd Edition* (ASM International, Materials Park, OH).
Wagner, C. (1951) *Thermodynamics of Alloys*, Addison-Wesley, Reading, Mass.
Yokokawa, T. and Niwa, T. (1969) *Trans. Japan Inst. Met.*, **10**, 1.
Zemaitis, J. F. (1980) in *Themodynamics of Aqueous Systems with Industrial Applications*, ed. Newman, S. A. (American Chemical Society), p. 227.

Chapter 6
Phase Stabilities

Chapter 6
Phase Stabilities

6.1. INTRODUCTION

The CALPHAD approach is based on the axiom that complete Gibbs energy versus composition curves can be constructed for all the structures exhibited by the elements right across the whole alloy system. This involves the extrapolation of *G/x* curves of many phases into regions where they are either metastable or unstable and, in particular, *the relative Gibbs energy for various crystal structures of the pure elements of the system must therefore be established.* By convention these are referred to as *lattice stabilities* and the Gibbs energy differences between all the various potential crystal structures in which an element can exist need to be characterised as a function of temperature, pressure and volume.

The basic question is how to perform extrapolations so as to obtain a consistent set of values, taking into account various complications such as the potential presence of mechanical instability. Additional complications arise for elements which have a magnetic component in their Gibbs energy, as this gives rise to a markedly non-linear contribution with temperature. This chapter will concern itself with various aspects of these problems and also how to estimate the thermodynamic properties of metastable solid solutions and compound phases, where similar problems arise when it is impossible to obtain data by experimental methods.

6.2. THERMOCHEMICAL ESTIMATIONS

6.2.1 General procedure for allotropic elements

Allotropic elements, which exhibit different crystal forms within accessible temperatures and pressures, allow the Gibbs energies to be measured for at least some of the possible alternative structures. Such data, although of necessity restricted to particular regimes of temperature and pressure, were therefore used as the platform for all the initial efforts in this field. The elements Mn (Weiss and Tauer 1958), Ti and Zr (Kaufman 1959a) and Fe (Kaufman *et al.* 1963) thus provided the basis for obtaining the first lattice stabilities for phase-diagram calculations. However, in order to make the CALPHAD approach universally applicable, a knowledge of the relative stability of the most frequently occurring crystal structures is also required for elements which do not manifest allotropy under normally accessible conditions

of temperature and pressure. Kaufman's conviction that a reliable set of basic lattice stabilities could be assembled was undoubtedly the key concept for the whole CALPHAD approach.

As with all physical phenomena, an agreed reference state has to be established for each element or component. In order to have a firm foundation, this has generally been taken as the crystal structure in which that element exists at standard temperature and pressure.

This ensures that thermochemical (TC) lattice stabilities are firmly anchored to the available experimental evidence. Although the liquid phase might be considered a common denominator, this raises many problems because the structure of liquids is difficult to define; it is certainly not as constant as popularly imagined. It is therefore best to anchor the framework for lattice stabilities in the solid state.

Figure 6.1(a) shows the relative position of the experimentally determined Gibbs energy curves for Ti, which includes segments that refer to the stable low-temperature c.p.h. α-phase, the high temperature b.c.c. β-phase and the liquid phase. Figure 6.1(b) shows curves where properties have been extrapolated to cover regions where, although the phases are metastable, properties can be estimated by extrapolation from alloys which stabilise one or other of the phases in binary systems.

It is clearly desirable to see if the total curve can be de-convoluted into parts that can be identified with a specific physical property so that trends can be established for the many cases where data for metastable structures are not experimentally accessible. In principle, the TC lattice stability of an element in a specified crystal structure β relative to the standard state α can be comprehensively expressed as follows (Kaufman and Bernstein 1970):

$$G^{\alpha\to\beta}_{\text{Total}} = H^{\alpha\to\beta}_{T=0} + G^{\alpha\to\beta}_{\text{Debye}}\, f(\theta_\alpha, \theta_\beta, T) + G^{\alpha\to\beta}_{\text{Elec}}\, f(\gamma_\alpha, \gamma_\beta, T) + G^{\alpha\to\beta}_{\text{Lambda}}\, f(\lambda_\alpha, \lambda_\beta, T) + G^{\alpha\to\beta}_{s1,s2}\, f(E_\alpha, E_\beta) + G^{\alpha\to\beta}_{P}\, f(V_\alpha, V_\beta, P). \quad (6.1)$$

Here $H^{\alpha\to\beta}_{T=0}$ is the enthalpy of transformation at 0 K, $f(\theta, \gamma, \lambda, E)$ denote functions for the components associated with Debye temperature (θ), electronic specific heat (γ), lambda transitions such as magnetism (λ) and contributions (E) related to multiple electronic states, $s1$,$s2$..., while $f(P, V_\alpha, V_\beta)$ refers to the function which generates the pressure contribution.

It may of course be unnecessary to consider all these terms and the equation is much simplified in the absence of magnetism and multiple electronic states. In the case of Ti, it is possible to deduce values of the Debye temperature and the electronic specific heat for each structure; the pressure term is also available and lambda transitions do not seem to be present. Kaufman and Bernstein (1970) therefore used Eq. (6.2), which yields the results shown in Fig. 6.1(c).

References are listed on pp. 173–178.

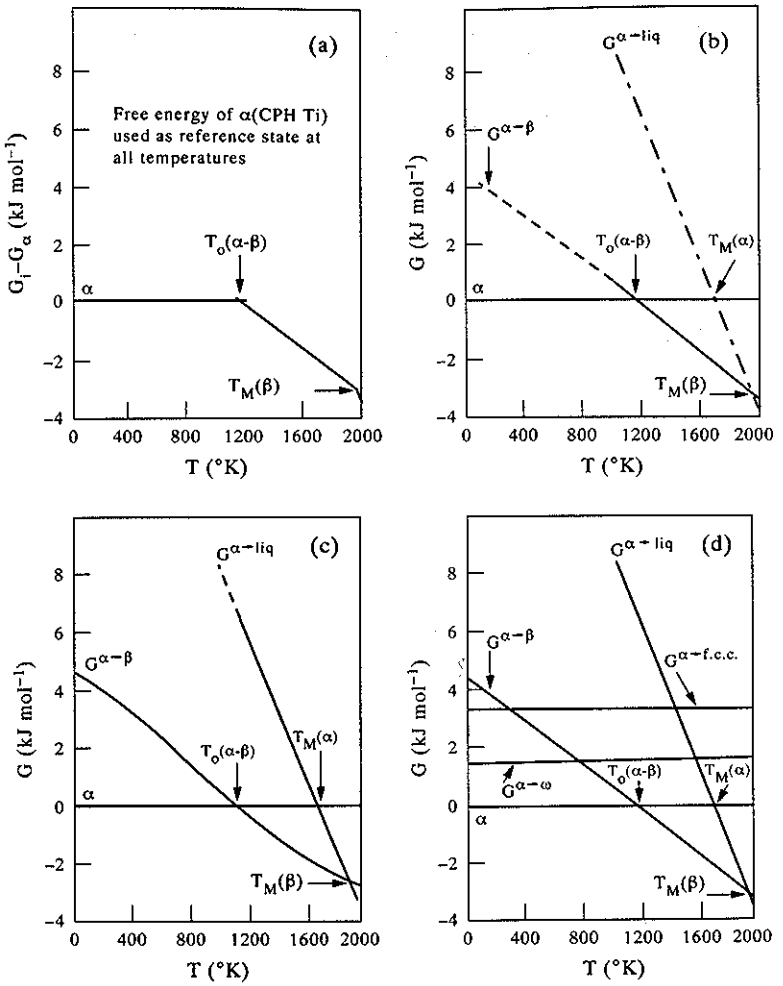

Figure 6.1. Gibbs free energy curves for Ti (a) α, β and liquid segments corresponding to the stable regions of each phase; (b) extrapolated extensions into metastable regions; (c) characterisation from Kaufman (1959a) using equation (6.2); and (d) addition of the G curves for ω and f.c.c. structures (from Miodownik 1985).

$$G^{\alpha\to\beta}_{\text{Ti}} = H^{\alpha\to\beta}_{T=0} + \frac{9}{8}(\theta^\beta - \theta^\alpha) + \left[f\left(\frac{\theta^\beta}{T}\right) - f\left(\frac{\theta^\alpha}{T}\right)\right] + 10^{-4}\frac{R}{T}\left[\left(\frac{3T}{(2-\theta^\beta)}\right)^2 - \left(\frac{3T}{(2-\theta^\alpha)}\right)^2\right] - \frac{T^2}{2}(\gamma^\beta - \gamma^\alpha). \quad (6.2)$$

The right-hand side can be separated into five parts. The first part is the enthalpy at 0 K, the second represents the zero point energy, the third is the Debye energy term, the fourth is an approximation for the $C_p - C_v$ correction while the last part arises from the difference in electronic specific heats.

6.2.2 *General procedure for non-allotropic elements*

With the exception of a few allotropic elements, the necessary input parameters to Eqs (6.1) or (6.2) are not available to establish the lattice stabilities of metastable structures. Therefore an alternative solution has to be found in order to achieve the desired goal. This has evolved into a standard format where the reference or ground state Gibbs energy is expressed in the form of general polynomials which reproduce assessed experimental C_p data as closely as possible. An example of such a standard formula is given below (Dinsdale 1991):

$$G_m[T] - H_m^{\mathrm{SER}} = a + bT + cT\ln(T) + \sum_2^n d_n T^n. \tag{6.3}$$

The left-hand term is defined as the Gibbs energy relative to the standard element reference (SER) state where H_m^{SER} is the enthalpy of the element or substance in its defined reference state at 298.15 K, a, b, c and d_n are coefficients and n represents a set of integers, typically taking the values of 2, 3 and –1. From Eq. (6.3) further thermodynamic properties of interest can be obtained.

$$S = -b - c - c\ln(T) - \sum n d_n T^{n-1} \tag{6.3a}$$

$$H = a - cT - \sum (n-1)\, d_n T^n \tag{6.3b}$$

$$C_p = -c - \sum n(n-1)\, d_n T^{n-1}. \tag{6.3c}$$

Other phases are then characterised relative to this ground state, using the best approximation to Eq. (6.1) that is appropriate to the available data. For instance, if the electronic specific heats are reasonably similar, there are no lambda transitions and $T >> \theta_D$, then the entropy difference between two phases can be expressed just as a function of the difference in their Debye temperatures (Domb 1958):

$$S_{T>>\theta}^{\alpha\to\beta} \approx \log_{\mathrm{e}} \frac{\theta_\beta}{\theta_\alpha}. \tag{6.4}$$

Combined with the 0 K enthalpy difference, the Gibbs energy of metastable phases can then be obtained by adding terms of the form (A–BT) to the reference state value or, more specifically:

$$G^{\alpha\to\beta} = H^{\alpha\to\beta} - TS^{\alpha\to\beta} \tag{6.5}$$

References are listed on pp. 173–178.

where $H^{\alpha\to\beta}$ and $S^{\alpha\to\beta}$ are taken as constant with respect to temperature. A linear model as shown in Fig. 6.1(b) is therefore a reasonable approximation at temperatures above θ_D. If the Debye temperatures are close enough, then the linear model will also give a reasonable description of the lattice stabilities below the Debye temperature (Miodownik 1986) and can be used to estimate a value of $H_{T=0}^{\alpha\to\beta}$, since this will be equal to the enthalpy of transformation measured at high temperature. Such linear expressions form the basis of many listed metastable lattice stability values but, in the longer term, it is desirable to return to a mode of representation for the unary elements which re-introduces as many physically definable parameters as possible. This is currently being pursued (Chase *et al.* 1995) by using either the Debye or Einstein equation where

$$C_{\mathrm{Debye}} = 9R\left(\frac{T}{\theta_D}\right)^3 \int_0^{\theta_D} \frac{x^4 \mathrm{e}^x}{(\mathrm{e}^x - 1)^2}\,\mathrm{d}x \tag{6.6}$$

and $x = h\nu/RT$, or

$$C_{\mathrm{Einstein}} = 3R\left(\frac{\theta_E}{T}\right)^2 \frac{\mathrm{e}^{\theta_E/T}}{[\mathrm{e}^{\theta_E/T} - 1]^2}. \tag{6.7}$$

Empirical fitting coefficients can be added ($a_i (i = 1, 2 \ldots)$) so that the C_p is given by

$$C_{\mathrm{fit}} = C_{\mathrm{Debye,\,Einstein}} + \sum_i a_i T^i. \tag{6.8}$$

The excess term should allow the total Gibbs energy to be fitted to match that of Eq. (6.3) while at the same time incorporating a return to the inclusion of $f(\theta)$ and $f(\gamma)$ in the lattice stabilities. With the increased potential for calculating metastable Debye temperatures and electronic specific heats from first principles (Haglund *et al.* 1993), a further step forward would be to also replace Eq. (6.5) by some function of Eq. (6.8).

Expressions for the liquid phase are complicated by the presence of a glass transition temperature (T_g). A simple linear model for the liquid should not, therefore, be used close to and below T_g and the curve representing the properties of the liquid phase in Fig. 6.1(b) has subsequently not been extended to 0 K. Further algorithms can be added to the high temperature linear treatment to provide for the effect of the liquid → glass transition if required (Ågren *et al.* 1995). However, regardless of what happens close to and below T_g, an extrapolated curve based on the concept of a retained liquid phase at 0 K will certainly yield the correct Gibbs energy at high temperatures. A similar situation occurs with relation to a magnetic transition, where it is physically impossible to retain the high-temperature paramagnetic configuration below the corresponding critical Curie (or Neel) temperature. Nevertheless, the procedure that has been generally adopted is to define a Gibbs energy curve for the paramagnetic state which covers the whole range of temperatures, and then add a magnetic Gibbs energy to it.

In addition to the melting point of the β phase and the α/β allotropic transformation temperature in Fig. 6.1(b), there is a further intersection between the Gibbs energy of α and liquid phases. This corresponds to the metastable melting point of the α phase. A linear model will then dictate that the entropy of melting for α is defined by the entropies of melting and transformation at the two other critical points (Ardell 1963),

$$S^{\alpha\to L} = S^{\alpha\to\beta} + S^{\beta\to L}. \tag{6.9}$$

This is a reasonable assumption providing the metastable melting point is well above both the θ_D of the solid and the T_g of the liquid. Eq. (6.9) has the following corollary:

$$H^{\alpha\to\beta} = T_f^{\alpha} S^{\alpha\to L} - T_f^{\beta} S^{\beta\to L}. \tag{6.10}$$

If the procedure adopted to determine the melting characteristics of the metastable phase is reversed, this provides a possible route for establishing TC lattice stabilities in cases where the metastable allotrope is not experimentally accessible. Moreover this is so even where the Gibbs energy curve for the metastable crystal structure does not intersect the Gibbs energy curve of the ground state structure (Fig. 6.1(d)). At first sight this does not seem particularly useful, because there is still a requirement for two unknown parameters T_f^{Φ} and $\Delta S^{\Phi\to L}$, where Φ is the experimentally inaccessible allotrope. However, the next two sections show how meaningful estimates can be obtained for these two parameters.

6.2.2.1 The van Laar technique for estimating melting points. T_f^{Φ} can be obtained by extrapolation from the liquidus of alloy systems which contain a phase of structure Φ by a technique originally suggested by van Laar (1908) but not considered seriously until resuscitated by Hume-Rothery and Raynor (1940). It is described succinctly in the following extract from their paper:

> *"... the b.c.c. structure of the beta phase (in copper alloys) may be regarded as derived from a hypothetical b.c.c. form of copper, which in pure copper is less stable than the f.c.c. structure, but which becomes more stable when sufficient solute is present to raise the electron concentration. From this point of view, which was already discussed by Rosenhain in 1926, the actual phase diagram may be regarded as arising in the way shown in Fig. 6.2, where the broken lines represent the extrapolation of the beta phase solidus and liquidus into the region where the phase is no longer stable."*

It was therefore appropriate that the first attempt to produce lattice stabilities for non-allotropic elements dealt with Cu, Ag and Zn (Kaufman 1959b). It is also significant that, because of the unfamiliarity of the lattice stability concept, this paper did not appear as a mainstream publication although the work on Ti and Zr (Kaufman 1959a) was published virtually at the same time. It was also realised that the reliability of metastable melting points derived by extrapolation were best

References are listed on pp. 173–178.

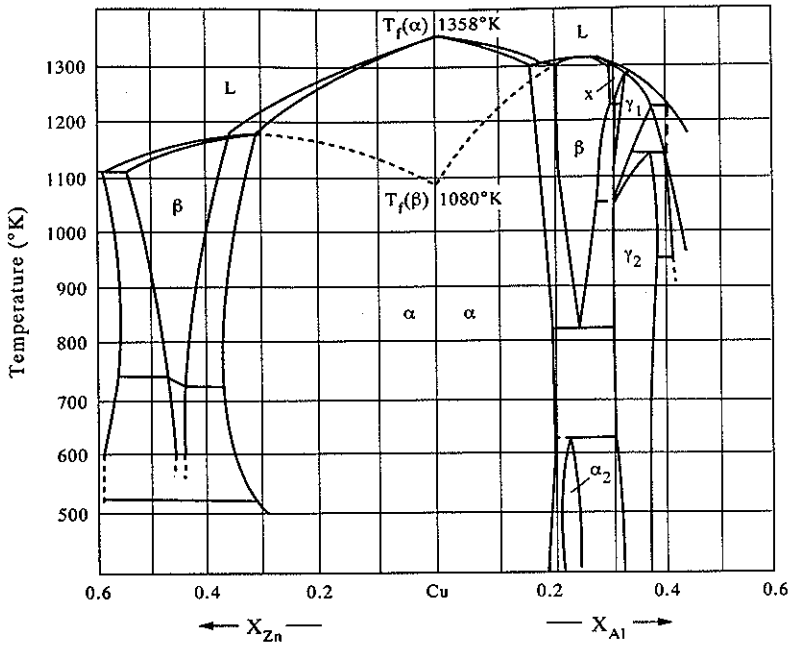

Figure 6.2. Illustration of the proposal by Rosenhain (1926) for Cu alloys containing α- and β-phases. The broken lines represent the extrapolation of the transus lines into the region where the β-phase is no longer stable, terminating at the metastable melting point of b.c.c. Cu (from Miodownik 1986).

obtained by combining the results from a number of different systems. Figure 3.6 from Kaufman and Bernstein (1970) shows this philosophy in action for the case of b.c.c. Re.

6.2.2.2 The estimation of metastable entropies of melting. Many of the lattice stabilities listed in the first embryonic database (Kaufman 1967) were obtained by combining the extrapolated values of melting points with an estimate for the entropy of fusion (S^f) based on Richard's rule. This dates to the last century and states that all metals should exhibit an entropy of fusion approximately equal to the gas constant R. However, with the accumulation of new experimental data for a wider range of elements, this was seen to be an over-simplification. Different crystal structures appear to have characteristic entropies of fusion with b.c.c. structures generally showed the lowest values of S^f, with higher values for f.c.c., c.p.h. and various structures of increasingly lower symmetry (Chalmers 1959, Gschneider 1961). An additional trend relates to the variation of S^f with melting point (Miodownik 1972a, Sawamura 1972). This was initially taken to be linear but, when more recent values for the higher melting-point elements were included, this

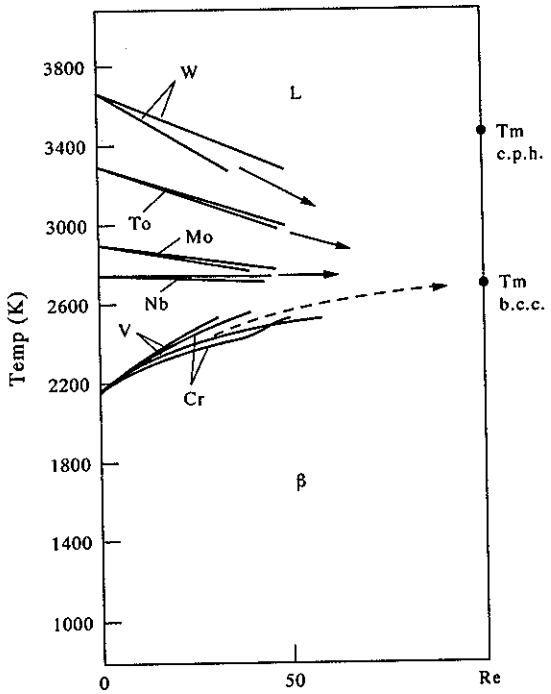

Figure 6.3. Convergence of metastable melting point of Re derived by extrapolation from a number of different systems (from Kaufman and Bernstein 1970, p. 66).

temperature dependence was shown to be markedly non-linear (Fig. 6.4(a)) (Miodownik 1986, Saunders *et al.* 1988). There is nevertheless a linear relationship between S^f and H^f with an intercept value, for $H^f = 0$, which is consistent with the 'structural entropy' term as originally suggested by Miodownik (1972a). As might be expected, there is a similar but smaller intercept value in the corresponding plot that relates S and H for allotropic transformations.

In order to use such empirical correlations as a general method for estimating lattice stabilities, it is necessary to establish whether properties of metastable phases will follow a similar trend to their stable counterparts. In the case of many transition metals (Miodownik 1972a) this certainly seems to be a useful working assumption. However, it is apparent that S^f for the high-temperature b.c.c. structures of the rare earths are anomalously low (Gschneider 1961, 1975) and some of the actinides show a similar effect; S^f for *β-Pu* is, for example, only 3.09 J mol^{-1} K^{-1} (Dinsdale 1991). It has been suggested that electrons in partially occupied *f*-levels can contribute an extra entropy component to the b.c.c. phase in rare earths and actinides (Kmetko and Hill 1976), while Tiwari (1978) suggested that the cumulative entropy of all prior transformations is a more constant quantity

References are listed on pp. 173–178.

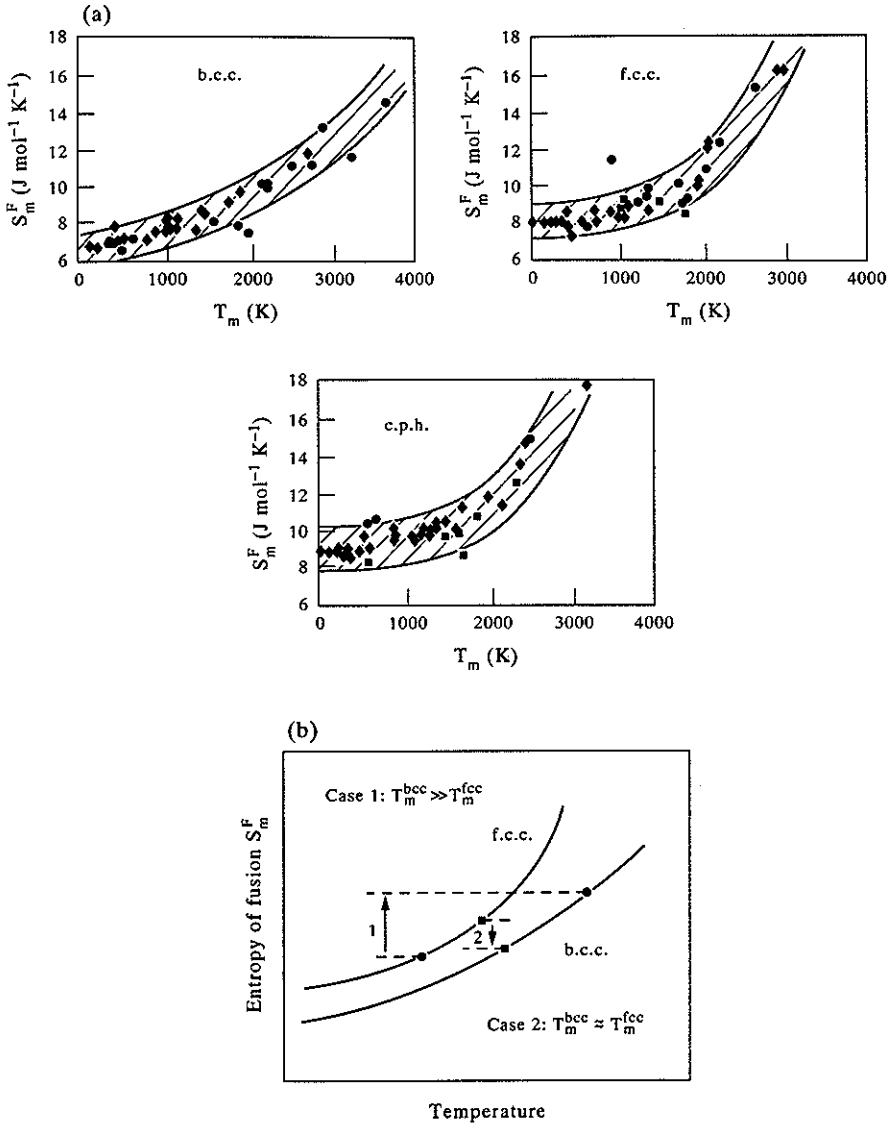

Figure 6.4. (a) Variation of the entropy of fusion with melting point for different crystal structures (from Saunders *et al.* 1988) and (b) schematic illustration of the possibility of a change in value and sign for the entropy of transformation if the metastable structure has a low melting point (from Miodownik 1992).

than the individual component entropies of transformation. But this begs the question of how to estimate the entropies associated with specific transformations.

On the whole it seems reasonable to use plots such as shown in Fig. 6.4(a) to estimate values for S^f of experimentally inaccessible phases, bearing in mind the exceptional elements discussed in the previous paragraph. However, an alternative procedure (Grimwall *et al.* 1987, Fernandez Guillermet and Hillert 1988, Fernandez Guillermet and Huang 1988) is to use the *average* S^f value deduced for each crystal class from the available experimental data (Gschneider 1964).

The values of $S^{\alpha\rightarrow\beta}$ deduced from both approaches will be similar for low-melting-point elements, or when the melting points of the stable and metastable elements are close together. However, they diverge significantly when there is an appreciable difference between the melting points of the stable and metastable structures. This is because using S^f vs temperature plots as shown in Fig. 6.4(b) predicts that there would be a change in the magnitude and, potentially, of the sign of $S^{\alpha\rightarrow\beta}$ when differences in melting temperatures become large (Saunders *et al.* 1988), while the use of an average S^f for the different classes of crystal structure automatically defines that $S^{\alpha\rightarrow\beta}$ will be constant.

It is worth considering whether the trends shown in Fig. 6.4 have any theoretical basis. Originally the intercept values were empirically rationalised in terms of numbers of nearest neighbours (Miodownik 1972a). An electron structure approach used by Friedel (1974) yields the right sign for $S^{\text{f.c.c.}\rightarrow\text{b.c.c.}}$, but the predicted magnitude is too high and applying this approach to the other crystal structures does not yield meaningful results. Relating S^f to differences in θ_D (see Eq. (6.4)) is a more fruitful approach (Grimwall and Ebbsjo 1975, Grimwall 1977). A relation between the intercept values of S^f in Fig. 6.4(a) and the Debye temperature can be invoked using the structural dependence of the constant (C_L) in the well-known Lindemann equation

$$\theta_D = C_L V_a^{-1/3} T_f^{1/2} M^{-1/2} \tag{6.11}$$

where V_a is the atomic volume, T_f the melting point and M the atomic weight. A dimensional analysis indicates that C_L^2 has the same dimensions as entropy, and Table 6.1 shows that S^f and C_L^2 are closely proportional (Achar and Miodownik 1974). This accounts for the empirical finding that a further set of constant values for C_L can be obtained if the allotropic transformation temperature is substituted for the melting point in the Lindemann equation (Cho and Puerta 1976).

However, most of the examples quoted in these earlier papers do not include the higher melting-point elements such as W, where a detailed treatment shows that the total entropy (at least of the solid phases) must include many other components such as the electronic specific heat, anharmonicity terms and the temperature dependence of θ_D (Grimwall *et al.* 1987, Moroni *et al.* 1996). An estimate for the Debye temperature of the high-temperature β phase was included in the seminal

References are listed on pp. 173–178.

Table 6.1. Correlation between the entropy of fusion S^f (extrapolated to $T_m = 0$) and the Lindemann constant (C_L) for various crystal structures (from Achar and Miodownik 1974)

Structure of solid phase	Lindemann constant (C_L)	Function of C_L ($10^{-4}\,C_L^2$)	Entropy of fusion (S^f)
b.c.c. (A2)	118	1.4	1.6
f.c.c. (A1)	138	1.9	1.9
c.p.h. (A3)	169	2.8	2.3
Bi (A7)	197	3.9	4.0
Diamond (A4)	215	4.6	4.6

paper on Ti and Zr (Kaufman 1959a), but the treatment did not take into account the inherent mechanical instability of the high temperature phase. More recent work has shown that, in the case of these elements, suitable anharmonic contributions can stabilise the b.c.c. phase in Ti and Zr and that the vibrational entropy contribution accounts for 70% of $S^{\alpha\rightarrow\beta}$ at the allotropic transformation temperature (Ho and Harman 1990, Petry *et al.* 1991). As, in this case, the mechanical instability is only marginal the treatment of Kaufman (1959a) may be considered a good approximation. However, when there is a much more marked instability, as in the case for tungsten (Fernandez Guillermet *et al.* 1995, Einarsdotter *et al.* 1997) any vibrational entropies calculated from Debye temperatures may be totally inappropriate.

6.2.2.3 Determination of transformation enthalpies in binary systems. Just as consistent values of T_m for elements can be obtained by back-extrapolation from binary systems, so it is possible to obtain values of $H^{\alpha\rightarrow\beta}$ by extrapolating the enthalpy of mixing vs composition in an alloy system where the phase has a reasonable range of existence. The archetypal use of this technique was the derivation of the lattice stability of f.c.c. Cr from the measured thermodynamic properties of the Ni-based f.c.c. solid solution (γ) in the Ni–Cr system (Kaufman 1972). If it is assumed that the f.c.c. phase is a regular solution, the following expression can be obtained:

$$RT \ln \frac{a_{\text{Cr}}^{\gamma}}{x_{\text{Cr}}} = G_{\text{Cr}}^{\text{b.c.c.}\rightarrow\text{f.c.c.}} + \Omega x_{\text{Ni}}^2 \tag{6.12}$$

where the left-hand side refers to the activity coefficient of Cr in the Ni solid solution, γ, the right-hand side contains the 'lattice stability' value for f.c.c. Cr while Ω is the regular solution interaction parameter.

Plotting $a_{\text{Cr}}^{\gamma}/x_{\text{Cr}}$ vs x_{Ni}^2 then leads to a straight line with an intercept equal to the Gibbs energy difference between the f.c.c. and b.c.c. forms of Cr, at the temperature where measurements were made (Fig. 6.5), while the slope of the line yields the associated regular solution interaction parameter. The lattice stability and the interaction parameter are conjugate quantities and, therefore, if a different magnitude

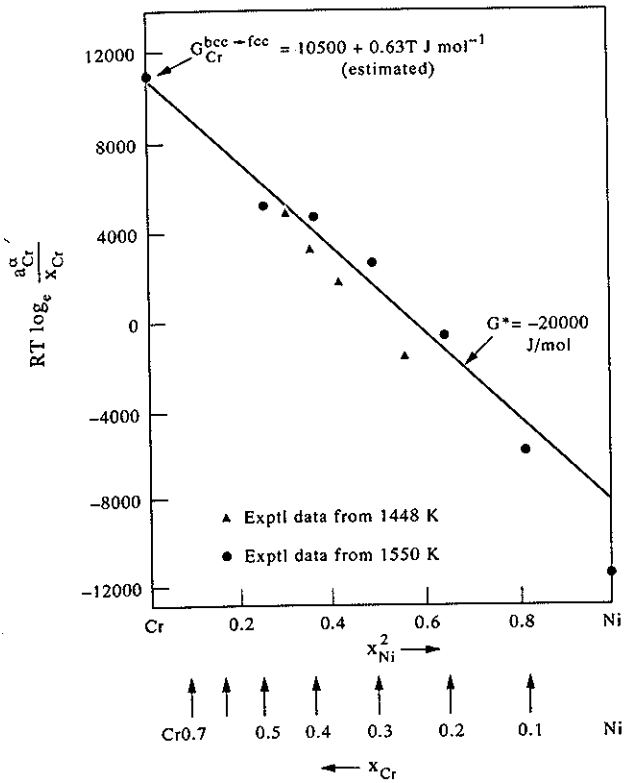

Figure 6.5. Plot of the activity coefficient of f.c.c. Cr (relative to pure b.c.c. Cr) vs the square of the atomic fraction of Ni to establish the lattice stability of f.c.c. Cr (adapted from Kaufman 1972).

for the lattice stability is adopted, the results can only be fitted by using a more complex solution model (e.g. sub-regular). In the case of Ni–Cr, the use of a regular solution model leads to a lattice stability for f.c.c. Cr which coincides closely with the value obtained independently through liquidus extrapolations (Saunders *et al.* 1988).

However, on the basis of calculations of lattice stabilities from spectroscopic data, Brewer (1967, 1979) has consistently maintained that interaction coefficients can change drastically with composition, and that extrapolated lattice stabilities obtained with simple models should therefore be considered as only 'effective' values. While this may indeed be true when mechanical instability occurs, many of the assumptions which underlie Brewer's methodology are questionable. A core principle of the spectroscopic approach is the derivation of 'promotion energies' which require the definition of both ground and excited levels. Assumptions concerning the relevant excited state have always been strongly coloured by adherence to the empirical views of Engel (1964) and Brewer (1967). By definition, the choice

References are listed on pp. 173–178.

of atomic ground states ignores all band-structure effects, and calculations by Moruzzi and Marcus (1988a) for the 3D transition elements highlight the omitted factors. It is interesting to note that there have been progressive changes in underlying assumptions over the years (Brewer 1975, Kouvetakis and Brewer 1993) and the lattice stabilities obtained by this route are now much closer to those currently produced by the more conventional TC method.

6.2.2.4 Utilisation of Stacking-Fault Energies. Experimental values of stacking-fault energies (SFE) offer a method of providing energy differences between stable and metastable close-packed structures. A rigorous relationship involves modelling the interface between the fault and the matrix, but a good working formula can be established by assuming that this interfacial energy term is constant for a given class of alloys (Miodownik 1978c).

$$\lambda = 2(G_s^{\text{f.c.c.}\rightarrow\text{c.p.h.}} + \sigma) \tag{6.13}$$

where

$$G_s^{\text{f.c.c.}\rightarrow\text{c.p.h.}} = \frac{10^7}{N^{1/3}}\left[\rho/M\right]^{2/3} G_m^{\text{f.c.c.}\rightarrow\text{c.p.h.}} \tag{6.14}$$

$G_s^{\text{f.c.c.}\rightarrow\text{c.p.h.}}$ is the Gibbs energy difference/unit area between the f.c.c. and c.p.h. phases in mJ m^{-2}, σ is the energy of the dislocation interface, ρ is the density in g cm^{-3}, M the molecular weight in grammes and $G_m^{\text{f.c.c.}\rightarrow\text{c.p.h.}}$ the Gibbs energy in J mol^{-1}. Eqs (6.13) and (6.14) were originally used to predict the SFE of a wide range of stainless steels, but they have also been used, in reverse, to estimate values of $G^{\text{f.c.c.}\rightarrow\text{c.p.h.}}$ of some f.c.c. elements (Saunders *et al.* 1988) where they provide values which are in excellent agreement (Miodownik 1992) with those obtained by FP methods (Crampin *et al.* 1990, Xu *et al.* 1991).

Although this method is essentially restricted to a particular sub-set of lattice stabilities, it nevertheless provides an additional experimental input, especially in cases where it is not possible to access the metastable phase by other methods. It is therefore disappointing that there are no *experimental* values of the SFE available for Ru or Os, which could provide confirmation of $G^{\text{c.p.h.}\rightarrow\text{f.c.c.}}$ obtained by other methods. High SFE values have, however, been both observed and predicted for Rh and Ir, which is indirect confirmation for a larger variation of $G_m^{\text{f.c.c.}\rightarrow\text{c.p.h.}}$ with *d*-shell filling than proposed by Kaufman and Bernstein (1970).

6.2.3 Summary of the current status of thermochemical estimates

While all extrapolative methods have some disadvantages, there is no doubt that remarkably consistent values have been obtained through combining extrapolations from various different TC methods. This has led to the consolidation of lattice stabilities of a large number of elements (Dinsdale 1991). The driving force for such

a compilation is that, *if lattice stabilities are allowed to become floating parameters, characterisations of different sub-systems will become incompatible when joined in a multi-component database, even though the individual characterisations are internally self-consistent.* This leads to inconsistencies when such data bases are subsequently combined and invalidates subsequent calculations.

Individual lattice stabilities have nonetheless to be continuously scrutinised as there are many good scientific reasons to consider revisions at periodic intervals; some of these are discussed below:

(1) Although changes in stable melting temperature are now quite rare, and generally rather small, this is not the case for values of S^f, where relatively large changes have been reported in the last decade for a number of high-melting-point elements. This can cause large changes in values of lattice stabilities estimated from S^f in conjunction with extrapolated metastable melting points and using Eq. (6.10) (Miodownik 1986, Saunders *et al.* 1988).

(2) Estimations of metastable melting points are invariably problematical. They are inherently semi-quantitative in nature and depend on the extent of the required extrapolation of stable liquidus lines which can be far away from the element for which the extrapolation is being made.

(3) The use of linear models for many metastable allotropes, which incorporate temperature independent enthalpy and entropies of transformation, has proved adequate so far because calculations have tended to be made for elevated temperatures, where the effect of incorporating more complex models seems marginal. However, as requirements increase for handling non-equilibrium transformations at lower temperatures, it is clearly necessary to have more accurate information for extrapolated Gibbs energy curves. If this requires substantial revisions of lattice stabilities to be made, there is clearly a premium on adding any further effects (e.g., those arising from the liquid → glass transition) onto existing Gibbs energy expressions so as to avoid changes in well-substantiated high-temperature data (Agren *et al.* 1995). If high-temperature data were also to change this would inevitably require major re-calculation of many systems.

(4) The increasing availability of electron energy calculations for lattice stabilities has produced alternative values for enthalpy differences between allotropes at 0 K which do not rely on the various TC assumptions and extrapolations. Such calculations can also provide values for other properties such as the Debye temperature for metastable structures, and this in turn may allow the development of more physically appropriate non-linear models to describe low-temperature Gibbs energy curves.

6.3. *AB INITIO* ELECTRON ENERGY CALCULATIONS

Ideally, the 0 K values of the relative enthalpy for various crystal structures can be

References are listed on pp. 173–178.

obtained by *ab initio* (*first-principles*) electron energy calculations, using merely atomic numbers and the desired atomic geometry as input. However, such methods did not have sufficient accuracy at the time lattice stabilities were first brought into use. An apocryphal analogy is that to obtain lattice stabilities by calculating the difference in total energy of two crystal structures, is like determining the weight of a ship's captain by first weighing the ship empty and then weighing the ship with the captain on the bridge!

Even as late as 1971 some methods were still unable to predict the correct ground state for elements such as Zn, while the scatter obtained from various calculation routes was far too high for *ab initio* phase stabilities to be introduced into a TC database (Kaufman 1972). However, owing to a combination of improved modelling and the availability of more powerful computers, results have become increasingly more consistent (Pettifor 1977, Skriver 1985, Watson *et al.* 1986, Paxton *et al.* 1990, Asada and Terakura 1993). In many cases, the values obtained from first principles (FP) have confirmed the values obtained by the thermochemical (TC) methods outlined in the previous section. The convergence of FP and TC values for the 0 K enthalpy is of great potential benefit to both the CALPHAD and physics communities for the following reasons.

1. Despite the success of phase-diagram calculations, there is still a considerable reluctance by sections of the scientific community to accept that TC lattice stabilities represent a real physical entity as distinct from an operational convenience. This inevitably creates doubts concerning the ultimate validity of the calculations. It is therefore important to verify that TC lattice stabilities, largely derived by extrapolation, can be verified by *ab initio* calculations and placed on a sound physical basis.

2. From the physicist's point of view, agreement with the CALPHAD figures for metastable allotropes represents one of the few ways of assessing the validity of their technique which is based on the principle that, *once a theoretical model is developed, there are no further adjustable input parameters other than the atomic number and a fixed geometry for relative atomic positions*. However, just as a number of different extrapolative techniques have been used in the TC approach, so a variety of assumptions have been used to solve the Schrödinger equation for a complex ensemble of atoms, combining different levels of accuracy with solutions that can be attained on a realistic time scale. A selection is given in Table 6.2. As many methods were developed in parallel, the order in which they are listed should not be considered important.

The most significant assumptions made in these various electron energy calculations are indicated in the various acronyms listed in Table 6.2. These can be permutated in many combinations and a proper comparison of these methods is beyond the scope of the present article. Excellent review articles (Pettifor 1977, Turchi and Sluiter 1993, de Fontaine 1996) are available if further detail is required. Other references of particular interest are those which compare the results

Table 6.2. Selection of various methods used to produce first-principles (FP) values for the relative stability at 0 K of different crystal structures

EPM	Empirical pseudo-potential method	Heine and Weaire (1971)
CPA	Coherent potential approximation	Ehrenreich and Schwartz (1976)
GPM	Generalised perturbation method	Ducastelle and Gautier (1976)
FRO	Frozen core approximation	Yin (1982)
GPT	Generalised pseudo-potential theory	Moriarty and McMahan (1982)
CFT	Concentration-functional theory	Gyorffy and Stocks (1983)
LMTO	Linear muffin tin orbital	Skriver (1983)
FLAPW	Full potential linearised augmented plane wave	Jansen and Freeman (1984)
ASA	Atomic spherical wave approximation	Skriver (1985)
LASTO	Linear augmented slater type orbital	Watson *et al.* (1986)
LSDA	Local spin density approximation	Moruzzi *et al.* (1986)
ECM	Embedded cluster method	Gonis *et al.* (1987)
GGA	Generalised gradient approach	Asada and Terakura (1993)
BOP	Bond order approximation	Pettifor *et al.* (1995)

of making different combinations for specific groups of elements, see for example Moriarty and McMahan (1982), Fernando *et al.* (1990) and Asada and Terakura (1993).

6.3.1 Comparison between FP and TC lattice stabilities

Despite the variety of assumptions that have been used, some general trends for the resultant lattice stabilities have been obtained for various crystal structures across the periodic table. The mean values of such (FP) lattice stabilities can therefore be compared with the equivalent values determined by thermochemical (TC) methods. Such a comparison shows the following important features (Miodownik 1986, Watson *et al.* 1986, Saunders *et al.* 1988, Miodownik 1992):

(1) In the main there is reasonable agreement for the sign and the magnitude of the lattice stabilities for elements whose bonding is dominated by sp electrons (Table 6.3) (see also Figs 6 and 7 of Saunders *et al.* 1988). In the case of elements such as Na, Ca and Sr, predictions have even included a reasonable estimate of their transition temperatures. Good agreement is also obtained for Group IVB elements such as Ge and Si (Table 6.4). The agreement for these elements is particularly striking because the values obtained by TC methods entailed large extrapolations, and for the case of Si(f.c.c.) a virtual, negative melting point is implied. At first sight such a prediction could be considered problematical. However, it can be interpreted in terms of the amorphous state being more stable at low temperatures than the competing f.c.c. crystalline configuration, and it does not contravene the third law as it is either metastable or unstable compared to the stable A4 structure. In the case of W and Mo there is now experimental evidence that supports this viewpoint (Chen and Liu 1997).

References are listed on pp. 173–178.

Table 6.3. Comparison of lattice stabilities (kJ mol^{-1}) obtained by TC and FP routes for elements whose bonding is dominated by sp electrons

Element	Method	b.c.c. → c.p.h.	f.c.c. → c.p.h.	Reference
Al	Pseudopotentials	–4.6	+5.5	Moriarty and McMahan (1982)
	TC	–4.6	+5.5	Kaufman and Bernstein (1970)
				Saunders *et al.* (1988)
Mg	Pseudopotentials	–2.7	–0.8	Moriarty and McMahan (1982)
	LMTO	–1.2	–0.9	Moriarty and McMahan (1982)
	TC	–3.1	–2.6	Saunders *et al.* (1988)
Zn	Pseudopotentials	–7.5	–1.7	Moriarty and McMahan (1982)
	LAPW	–9.2	–1.6	Singh and Papaconstantopoulos (1990)
	TC	–2.9	–3.0	Dinsdale (1991)
Be	Pseudopotentials	–8.1	–7.2	Lam *et al.* (1984)
	LMTO	–6.4	–5.9	Skriver (1982)
	TC	–6.8	–6.3	Saunders *et al.* (1988)

Table 6.4. Comparison of lattice stabilities for Si and Ge (kJ mol^{-1}) obtained by TC and FP routes for transformations from A4 to A1 (f.c.c.), A2 (b.c.c.), A3 (c.p.h.) and A5 (β-Sn)

		Structure				
Element	Method	A1	A2	A3	A5	Reference
Si	TC	51	47	49		Saunders *et al.* (1988)
	TC	50	42	51		Kaufman and Bernstein (1970)
	FP	55	51	53	26	Yin (1982)
	FP					Goodwin *et al.* (1989)
Ge	TC	36	34	35		Saunders *et al.* (1988)
	TC	36			28	Miodownik (1972b)
	FP	44	42	43	24	Yin (1982)
	FP					Goodwin *et al.* (1989)

(2) A sinusoidal variation of the 0 K energy difference between b.c.c. and close-packed structures is predicted across the transition metal series, in agreement with that obtained by TC methods (Saunders *et al.* 1988). For the most part magnitudes are in reasonable agreement, but for some elements FP lattice stabilities are as much as 3–10 times larger than those obtained by any TC methods (Fig. 6.6).
(3) FP methods inherently lead to a marked sinusoidal variation of $H^{\text{f.c.c.}\rightarrow\text{c.p.h.}}$ across the periodic table (Pettifor 1977) and for Group V and VI elements, electron energy calculations predict $H^{\text{f.c.c.}\rightarrow\text{c.p.h.}}$ of *opposite sign* to those obtained by TC methods. It is worth noting, however, that a sinusoidal variation is reproduced by one of the more recent TC estimates (Saunders *et al.* 1988) although displaced on the energy axis (Fig. 6.7).

Some reconciliation can be achieved by considering the effect of changing

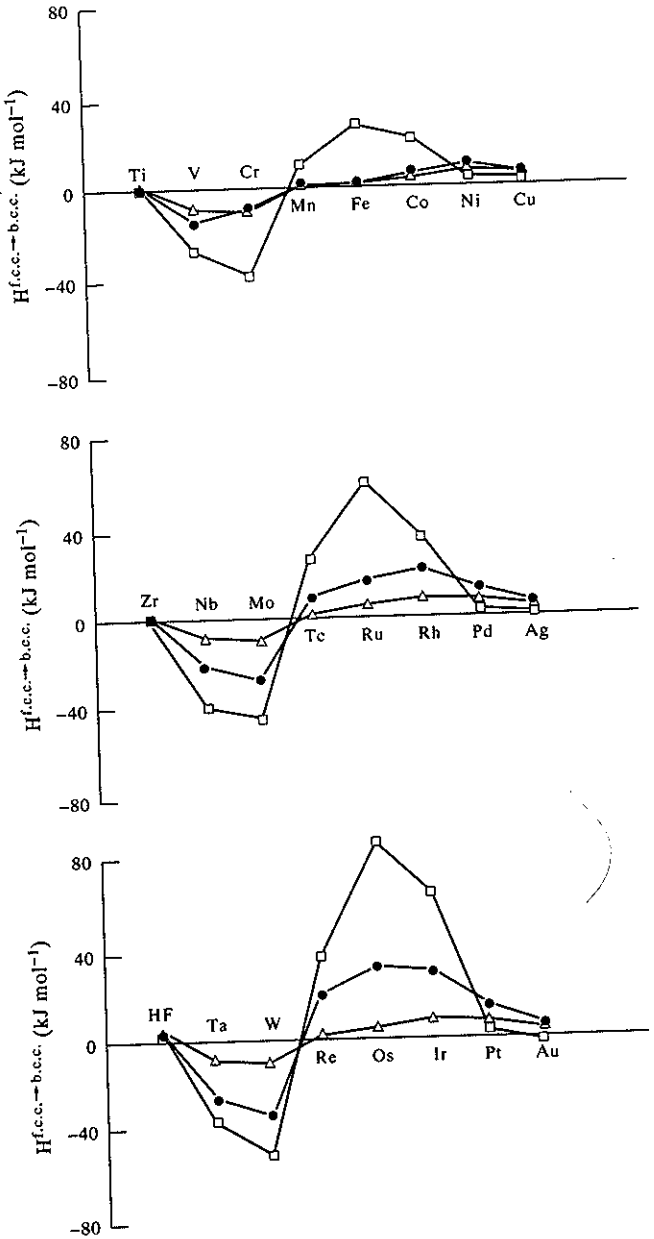

Figure 6.6. Variation of the enthalpy difference between f.c.c. and b.c.c. structures obtained by various TC and FP routes. • Saunders *et al.* (1988); △ Kaufman and Bernstein (1970); □ Skriver (1985).

References are listed on pp. 173–178.

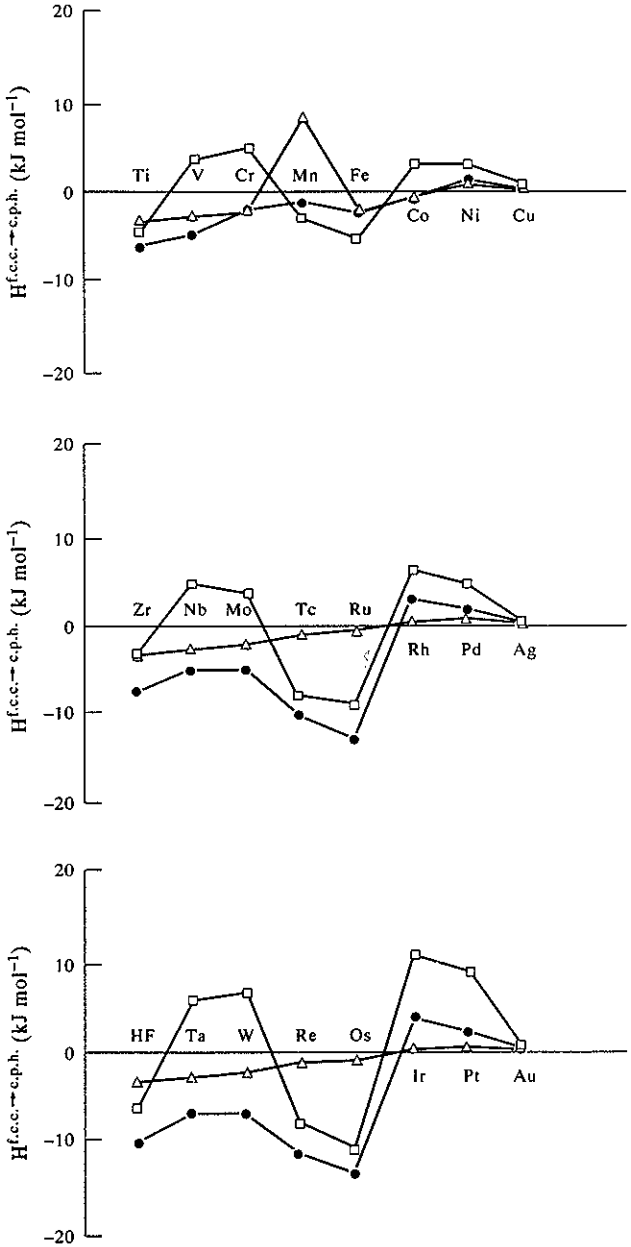

Figure 6.7. Variation of the enthalpy difference between f.c.c. and c.p.h. structures obtained by various TC and FP routes. • Saunders *et al.* (1988); △ Kaufman and Bernstein (1970); □ Skriver (1985).

the c/a ratio (Fernando *et al.* 1990), as some of the hexagonal phases seem to be most stable at c/a ratios which depart substantially from the ideal close-packed value (~1.63). This factor is of significance in the case of elements like Cd and Zn where $c/a \sim 1.8$ and it is clearly not appropriate to equate the Gibbs energies of the ideal and non-ideal hexagonal forms (Singh and Papaconstantopoulus 1990). Making this kind of adjustment could reverse the sign of $H^{\text{f.c.c.}\rightarrow\text{c.p.h.}}$ for Nb but does not really make much impact on the situation for Mo, Ta and W. Likewise a change in volume within reasonable limits does not resolve the issue (Fernando *et al.* 1990).

(4) In the past, electron energy calculations have failed dramatically for magnetic elements since spin polarisation was not included. However, this can now be taken into account quite extensively (Moruzzi and Marcus 1988b, 1990, Asada and Terakura 1993) and calculations can reproduce the correct ground states for the magnetic elements.

6.3.2 Reconciliation of the difference between FP and TC lattice stabilities for some of the transition metals

Several approaches have been made in order to remove the outstanding conflicts between FP and TC lattice stabilities. Niessen *et al.* (1983) proposed a set of compromise values, which are also listed in de Boer *et al.* (1988), but these do not constitute a solution to this problem. These authors merely combined the two sets of values in relation to an arbitrary reference state in order to refine their predictions for heats of formation (see Section 6.6.1.1).

The accuracy with which a phase diagram can be fitted with competing values of phase stabilities appeared, at one time, to be a fairly obvious route to discover whether the TC or FP values were closer to reality. Tso *et al.* (1989) calculated the Ni–Cr phase diagram using a series of different values for the lattice stability of f.c.c. Cr. They were able to reasonably reproduce the phase diagram with energy differences close to those proposed by electron energy calculations. However, they could only do so by introducing a compensating change in the Gibbs energy of mixing for the f.c.c. phase, which had to become large and negative in sign. It is difficult to accept such a proposal for the enthalpy of mixing for f.c.c. alloys when the liquid exhibits almost ideal behaviour and the b.c.c. phase has mainly positive interactions. In addition, calculations of mixing energy by using *d*-band electron models (Colinet *et al.* 1985, Pasturel *et al.* 1985) supports values much closer to those already in use by CALPHAD practitioners.

A series of publications by various authors used a similar process to establish which lattice stability gave the best fit for particular phase diagrams (Anderson *et al.* 1987, Fernandez Guillermet and Hillert 1988, Fernandez Guillermet and Huang 1988, Kaufman 1993, Fernandez Guillermet and Gustafson 1985). Au–V formed a particularly useful test vehicle (Fernandez Guillermet and Huang 1988, Kaufman

References are listed on pp. 173–178.

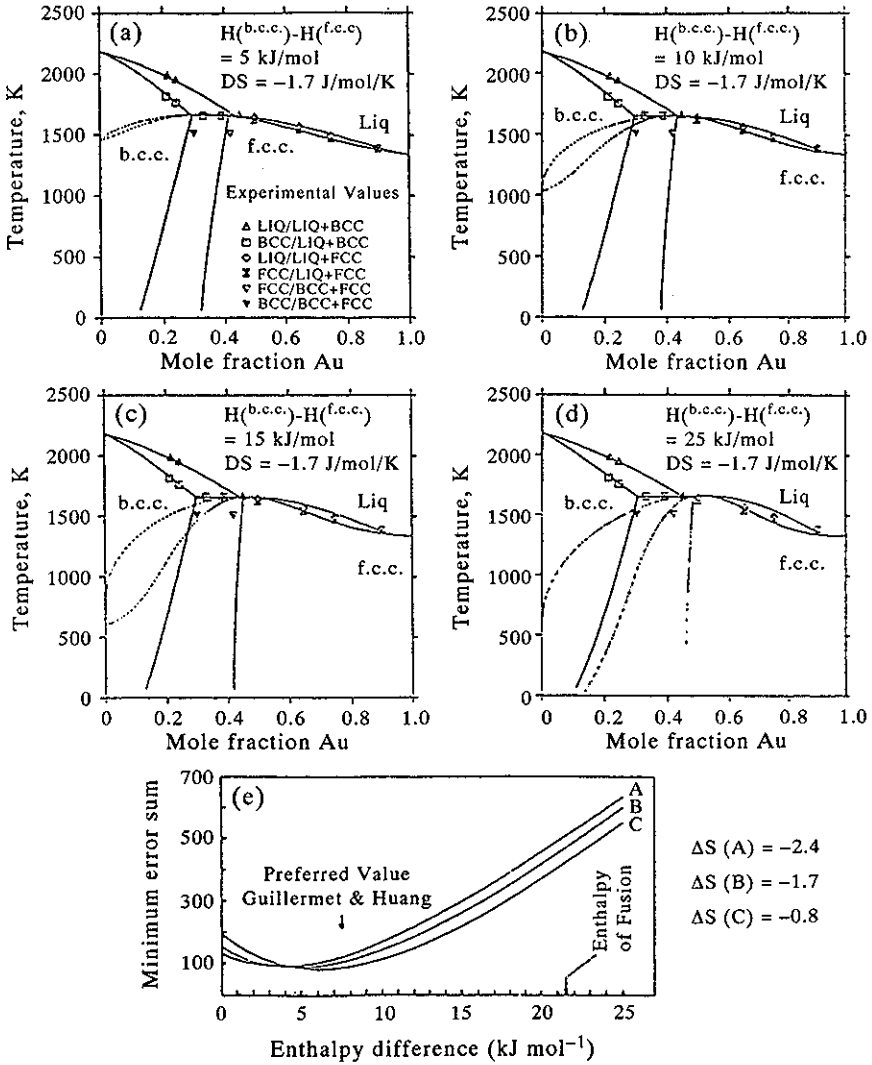

Figure 6.8. (a–d) The effect of varying the f.c.c.–b.c.c. V lattice stability on the matching of experimental and calculated phase boundaries in the Au–V system (after Fernandez Guillermet and Huang 1988) and (e) the effect of varying $\Delta S^{\text{b.c.c.}\rightarrow\text{f.c.c.}}$ on the minimum error sum, giving a preferred value of 7.5 kJ mol^{-1}.

1993) as V was one of the elements which showed a serious discrepancy (Fig. 6.8). Using a regular solution model and restricting the range of S^f, such an analysis (Fernandez Guillermet and Huang 1988) suggested that the optimum values of

$G^{b.c.c.\rightarrow f.c.c.}$ were markedly lower than those obtained by electron energy calculations (Fernandez Guillermet and Huang 1988) and also significantly lower than proposed by Saunders *et al.* (1988). The permitted range of lattice stability values can be increased by changing these constraints, in particular letting S^f vary as shown in Fig. 6.4(a), but any values still exclude FP predictions.

This impasse was eventually resolved by taking into consideration the calculated elastic constants of metastable structures in addition to their energy difference at 0 K. Craievich *et al.* (1994), Craievich and Sanchez (1995) and Guillermet *et al.* (1995), using independent calculations, have suggested that the difference between TC and *ab initio* predictions may be associated with mechanical instabilities in the metastable phase. This point had been raised earlier by Pettifor (1988) and has the following consequence as reported by Saunders *et al.* (1988):

> *"... the analogy with titanium and zirconium is useful. In these elements there is a reported lattice softening in the b.c.c. allotrope near the c.p.h. → b.c.c. transformation temperature. This instability is reflected by a substantial C_p difference between the c.p.h. and b.c.c. structures which effectively destabilises the b.c.c. phase with decreasing temperature. High-temperature extrapolations which ignore this, then overestimate the low temperature stability of the b.c.c. phase. As ab initio calculations give values for heats of transformation at 0 K, comparison with high-temperature phase diagram and thermodynamic extrapolations will produce different results."*

Furthermore, such instabilities will extend into the alloy system up to a critical composition and must therefore be taken into account by any effective solution-phase modelling. In the case of Ni–Cr , it is predicted that mechanical instability, as defined by a negative value of $c' = 1/2(c_{11} - c_{12})$, will occur between 60 and 70 at%Cr (Craievich and Sanchez 1995), so beyond this composition the f.c.c. phase cannot be considered as a competing phase.

While this concept of mechanical instability offers a potential explanation for the large discrepancies between FP and TC lattice stabilities for some elements, the calculations of Craeivich *et al.* (1994) showed that such instabilities also occur in many other transition elements where, in fact, FP and TC values show relatively little disagreement. *The key issue is therefore a need to distinguish between 'permissible' and 'non-permissible' mechanical instability.* Using the value of the elastic constant C' as a measure of mechanical instability, Craievich and Sanchez (1995) have found that the difference between the calculated elastic constant C' for f.c.c. and b.c.c. structures of the transition elements is directly proportional to the FP value of $H^{b.c.c.\rightarrow f.c.c.}$ (Fig. 6.9(a)).

The position of Ti and Zr is again important in this context. While the b.c.c. phase in these elements has long been known to indicate mechanical instability at 0 K, detailed calculations for Ti (Petry 1991) and Zr (Ho and Harmon 1990) show that it is stabilised at high temperatures by additional entropy contributions arising from low values of the elastic constants (soft modes) in specific crystal directions. This concept had already been raised in a qualitative way by Zener (1967), but the

References are listed on pp. 173–178.

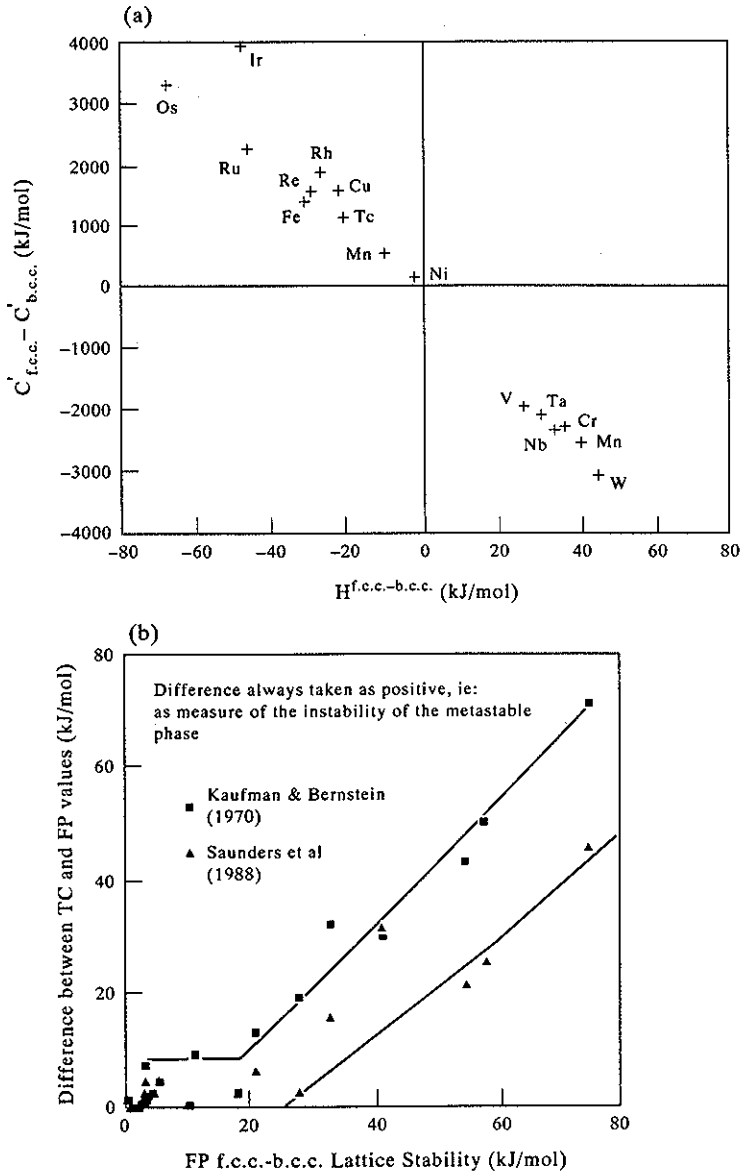

Figure 6.9. (a) Proportionality of calculated values of $\Delta H^{f.c.c.-b.c.c.}$ to the associated elastic instability as measured by the elastic constant C′ (Private Communication from Craievich and Sanchez 1995). (b) The difference between TC and FP lattice stabilities plotted vs the absolute value of the calculated FP lattice stability. When combined with Fig. 6.8 this suggests a critical value of the elastic instability that cannot be compensated for by thermal contributions.

key issue is to find out whether there is a maximum value to the additional entropy that is available to counterbalance specific values of mechanical instability at 0 K. This would be consistent with the observation that major discrepancies between FP and TC lattice stabilities only seem to arise when the mechanical instability rises beyond a critical value (Fig. 6.9(b)). This is also consistent with the findings of (Fernandez Guillermet *et al.* 1995), who could only reproduce the phase diagram for W–Pt by invoking an empirical and highly anomalous value of $S^{\text{f.c.c.}\rightarrow\text{b.c.c.}}$ which would also have to exhibit a strong temperature dependence to avoid the appearance of f.c.c. W as a stable phase below the melting point.

The effect of incorporating a more complex entropy function has also been examined by Chang *et al.* (1995) using the Ni–Cr system as a test vehicle. Here an anomalous entropy contribution was *simulated* by incorporating a dual Debye temperature function, linked to the critical composition at which the elastic constants had been calculated to change sign in this system. The resulting lattice stability for the f.c.c. phase nicely shows how this approach rationalises the extrapolated liquidus derived using the van Laar method and values that would be consistent with a FP approach. Figure 6.10 shows that the phase diagram in the stable region does not suffer inaccuracies by using high FP values as happened in the earlier attempts on Au–V (Fig. 6.8). It should, however, be emphasised that the equations used by Chang *et al.* (1995) to define the Gibbs energy of f.c.c. Cr are highly empirical and require a whole new set of adjustable parameters, such as a critical temperature which defines the onset of mechanical instability. This poses an

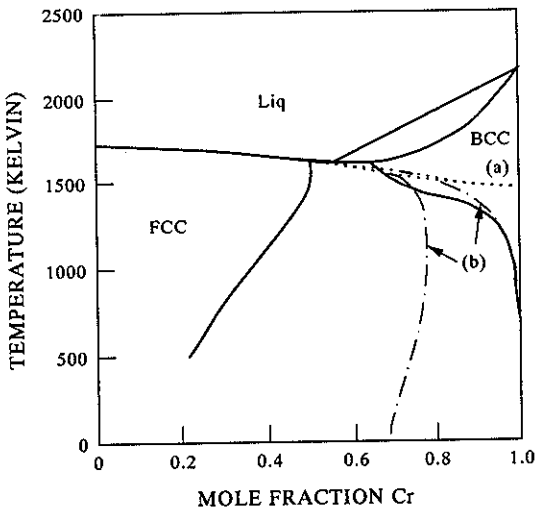

Figure 6.10. Comparison of the extrapolated liquidus/solidus lines relating to the f.c.c. phase in Ni–Cr alloys, derived by (a) using the van Laar method and (b) the trajectory obtained using the modified FP approach used by Chang *et al.* (1995).

References are listed on pp. 173–178.

exciting challenge to provide a sounder basis for a treatment that can encompass low-temperature mechanical instability. The present situation concerning FP and TC lattice stabilities can probably be described as follows.

1. Thermochemical methods generate lattice stabilities based on high-temperature equilibria that yield self-consistent multi-component phase-diagram calculations. However, as they are largely obtained by extrapolation, this means that in *some* cases they should only be treated as *effective lattice stabilities.* Particular difficulties may occur in relation to the liquid → glass transition and instances of mechanical instability.
2. By contrast, electron energy calculations have the inherent capability of yielding accurate values for many metastable structures at 0 K but have little or no capability of predicting the temperature dependence of the Gibbs energy, especially in cases where mechanical instabilities are involved.

Although the two methodologies are complementary, attempts at producing Gibbs energy curves which combine the two approaches are currently still empirical and would, in practice, be very difficult to incorporate in a general CALPHAD calculation. *A more fundamental treatment of various entropy contributions is required to achieve proper integration. Until this is realised in practice, the use of TC lattice stability values as well established operational parameters, valid at high temperatures and for most CALPHAD purposes, is likely to continue for the foreseeable future.*

6.4. THE BEHAVIOUR OF MAGNETIC ELEMENTS

The treatment outlined so far has not included the magnetic Gibbs energy contributions in Eq. (6.1) because the ground state of the majority of elements is paramagnetic. This, however, is certainly not the case for some key 3d transition elements, which exhibit various forms of magnetic behaviour not only in the ground state but also in one or more allotropes. Fe is a classic example and since ferrous metallurgy has been a major driving force in the development of phase diagram calculations, one of the first steps was to establish the magnitude of the magnetic component on the Gibbs energy. The basic factors that control this are detailed in Chapter 8, but it is worthwhile here to review some of the implications for specific elements, with particular emphasis on Fe.

6.4.1 Fe

Considerable information is available on the magnetic parameters associated with three different crystal structures of Fe which are b.c.c. and f.c.c. at ambient pressures and c.p.h. which is observed at high pressures. Table 6.5 gives the corresponding values of the maximum enthalpy and entropy contributions due to

Table 6.5. Maximum values of the magnetic enthalpy and entropy for various allotropes of Fe, Co and Ni based on data and methodology drawn from Miodownik (1977) and additional data from de Fontaine *et al.* (1995). Structures in brackets correspond to metastable forms that have not been observed in the *TP* diagram of the element

Element	Structure	H^{mag} (kJ mol^{-1})	S^{mag} (J mol^{-1} K^{-1})
Fe	b.c.c.	9.13	9.72
	f.c.c.	0.32	4.41
	c.p.h.	0	0
Co	(b.c.c.)	11.17	8.56
	f.c.c.	10.69	8.56
	c.p.h.	9.66	8.26
Ni	(b.c.c.)	1.91	3.37
	f.c.c.	2.27	4.01
	(c.p.h.)	0.94	3.48

magnetism, H^{mag}_{max} and S^{mag}_{max} respectively, and Fig. 6.11(a) shows how this affects the total Gibbs energy for the three structures in Fe. At high temperatures Fe behaves like many other allotropic elements, solidifying in a b.c.c. lattice, (δ-Fe). As the temperature is reduced, there is a transition to the f.c.c. γ-Fe phase which has both a lower energy and a lower entropy. However because of G^{mag} the b.c.c. phase reappears at lower temperature as α-Fe. While the Curie temperature of α-Fe, 770°C, is actually 140°C below the α/γ transformation temperature at 910°C, there is already sufficient short-range magnetic order to cause the transformation. A consequence of this unique behaviour is that the value of $G^{b.c.c.\rightarrow f.c.c.}$ remains exceedingly small in the region between the two transition points and never exceeds 50–60 J mol^{-1} (see Fig. 6.11(b)). This means that small changes in Gibbs energy, due to alloying, will substantially alter the topography of the γ-phase region in many Fe-base systems. If the alloying element also significantly affects the Curie temperature, the proximity of the latter to the α/γ transus will mean that this boundary is disproportionately altered in comparison to the γ/δ transus. This latter point can be shown to account for the otherwise puzzling asymmetric effects of alloying additions on the two transition points (Zener 1955, Miodownik 1977, Miodownik 1978b).

Because it is the basis of so many important commercial systems, the allotropy of Fe has been re-examined at frequent intervals. There is relatively more experimental information available for α-Fe, as this is the ground state, and relatively little controversy about characterising this phase. There is also little difference between the various proposals for $G^{b.c.c.\rightarrow f.c.c.}$ in the temperature range where γ-Fe is stable, because of the need to reproduce the two well-known transformation temperatures $T^{\alpha/\gamma}$ and $T^{\gamma/\delta}$ and their associated enthalpies of transformation (Fig. 6.11(b)). There are, however, different points of view regarding the extrapolation of the Gibbs energy of the γ-phase to low temperatures, which relate to different weightings given to various specific heat measurements, assumptions made

References are listed on pp. 173–178.

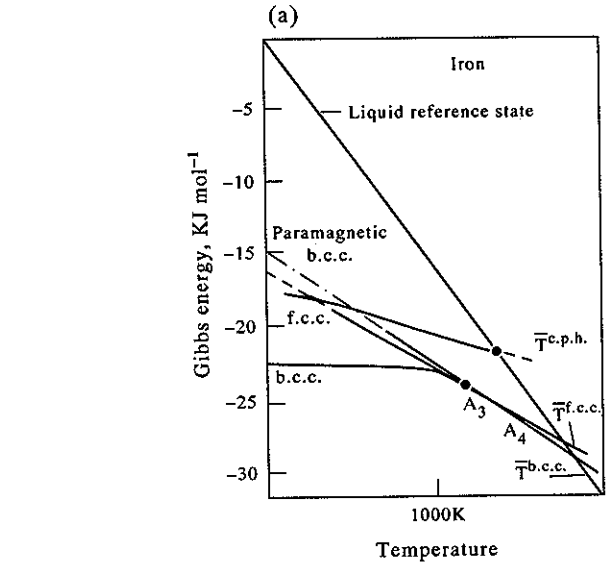

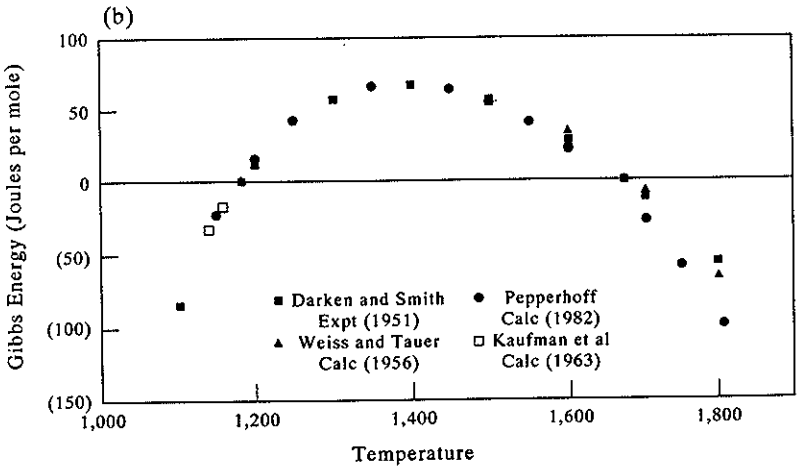

Figure 6.11. General overview of the relative stability of the f.c.c. and b.c.c. phases in pure Fe (a) over the whole temperature range (Miodownik 1978b) and (b) in the critical high-temperature region between the two critical points denoted A3 and A4, based on the work of Darken and Smith (1951), Weiss and Tauer (1956), Bendick and Pepperhoff (1982) and Kaufman *et al.* (1963).

regarding the magnetic description of γ-Fe, and the significance placed on data derived from low-temperature martensitic transformations (Fig. 6.12).

Johannson (1937) is generally credited with the earliest calculations of $G^{b.c.c.\rightarrow f.c.c.}$, which were based on the specific heat measurements of Austin (1932).

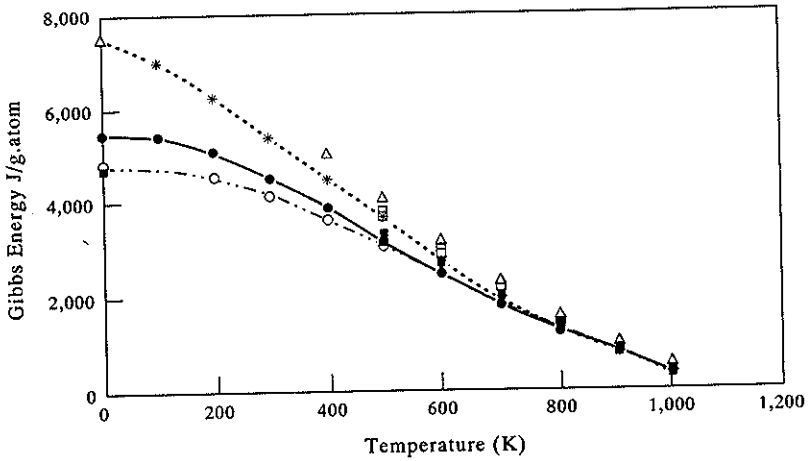

Figure 6.12. Effect of different models on the Gibbs energy difference between the f.c.c. and b.c.c. phases in pure iron. Data (□) of Darken and Smith (1951), (△) Weiss and Tauer (1956), (•) Kaufman *et al.* (1963), (⊡) Orr and Chipman (1967), (▲) Ågren (1979), (○) Bendick and Pepperhoff (1982), (⋆) Fernandez Guillermet and Gustafson (1985), (■) Chang *et al.* (1985).

Relevant data extracted from activity measurements in the Fe–C phase were later included in the assessment by Zener (1946) and Darken and Smith (1951). All this work followed a traditional approach solely based on thermodynamic data derived under equilibrium conditions. By contrast, Kaufman and Cohen (1958) showed that the data of Johannson (1937) were more consistent with information derived from Fe-based martensite transformations than the interpretation used by Darken and Smith (1951). Together with the work of Svechnikov and Lesnik (1956) *this was a notable attempt to combine thermodynamic information derived from low-temperature metastable transformations with those from more traditional sources.*

Another such departure was the attempt by Weiss and Tauer (1956) to deconvolute the global value of $G^{\text{b.c.c.}\rightarrow\text{f.c.c.}}$ into magnetic, vibrational and electronic components. This represented the first attempt to obtain *a physical explanation* for the overall effect. An even more comprehensive approach by Kaufman *et al.* (1963) led to the further inclusion of two competing magnetic states for γ-Fe. Since the computer programmes available at that time could not handle such a sophisticated approach, the relevant values of $G^{\text{b.c.c.}\rightarrow\text{f.c.c.}}$ were converted into polynomial form and subsequently used for the calculations of key Fe-base diagrams such as Fe–Ni, Fe–Co and Fe–Cr (Kaufman and Nesor 1973).

Subsequent reassessments now took divergent routes. Ågren (1979) used thermodynamic data largely drawn from Orr and Chipman (1967) and re-characterised the magnetic component of the α-phase with the Hillert and Jarl model (see Chapter 8). The concept of two competing states in the γ-phase was abandoned as Orr and

References are listed on pp. 173–178.

Chipman (1967) favoured a high value for $H^{\text{b.c.c.}\rightarrow\text{f.c.c.}}$ and a suitable fit could be obtained without invoking the added complications of this model. The Ågren treatment has been further refined in the most recent assessment of the *T–P* properties of Fe made by Fernandez Guillermet and Gustafson (1985). By contrast, both Miodownik (1978b) and Bendick and Pepperhoff (1982) pursued further evidence for the existence of two gamma states from other physical properties and built alternative assessments for Fe around this concept.

Although attention has tended to concentrate on the equilibrium between α- and γ-Fe, the hexagonal variant, ε, has also to be considered. This can only be accessed experimentally in pure Fe when the b.c.c. phase is destabilised by pressure or alloying additions. The extrapolated properties of ε-Fe are consistent with it being paramagnetic, or very weakly anti-ferromagnetic, and so magnetism will provide a negligible contribution to its stability. Nevertheless, the extrapolation of SFE versus composition plots confirms that the ε-Fe becomes more stable than the γ-Fe at low temperatures, despite the magnetic contributions in the γ-phase (see Fig. 8.11 of Chapter 8). Hasegawa and Pettifor (1983) developed a model based on spin-fluctuation theory which accounts for the *T–P* diagram of Fe without invoking any differences in vibrational entropy or multiple magnetic states, but their theory predicts that both close-packed states should exhibit a temperature-induced local moment. The f.c.c. phase then behaves in a way which is rather similar to that predicted by the phenomenological two-γ-state model (Kaufman *et al.* 1963). The prediction of a high-temperature moment for the ε-phase is, however, at variance with the assumptions or predictions of most other workers who consider that the ε-phase has a zero or negligibly low moment. Various other models have been proposed which break down the total Gibbs energy in different ways, for instance by placing a different emphasis on the contribution of vibrational and electronic terms (Grimwall 1974). Both the Pettifor–Hasegewa and the Grimwall models can account for the some of the necessary qualitative features exhibited by the allotropy of Fe, but the intrinsic assumptions of these two approaches are incompatible with each other.

The various approaches were again reviewed by Kaufman (1991) who quoted further evidence for the two-gamma-state concept, but virtually all current databases incorporate the data generated by Fernandez Guillermet and Gustafson (1985) (Fig. 6.12). This has certainly been well validated in phase-diagram calculations, and it is hard to see how it could be improved at elevated temperatures. However, the differences that appear at low temperatures may be important in relation to metastable equilibria such as martensite transformations which, since the early work of Kaufman and Cohen (1956, 1958), have tended to be excluded from any optimisation procedure. Certainly there seems to be no doubt about the existence of many competing combinations of crystal structure and magnetic moments (Asada and Terakura 1993) (Fig. 6.13) which suggest that there must be room for an improved model.

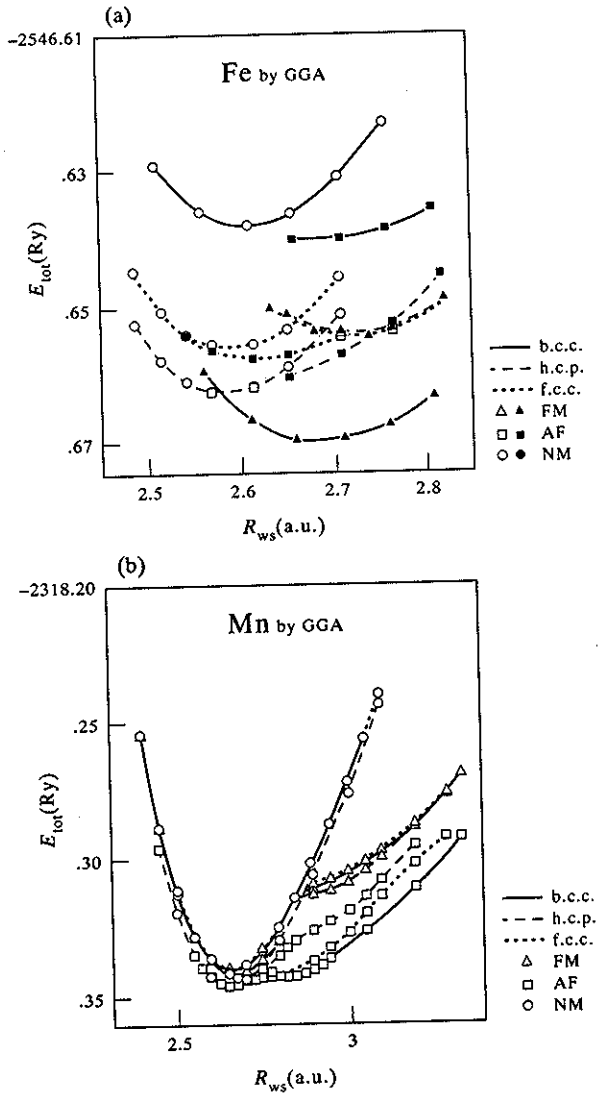

Figure 6.13. Enthalpy vs volume plots for f.c.c., b.c.c. and c.p.h. for (a) Fe and (b) Mn, incorporating the effect of assuming different magnetic interactions. △ ferromagnetic, □ anti-ferromagnetic, ○ non magnetic (from Asada and Terakura 1993).

6.4.2 Co

Table 6.5 shows that $Co^{c.p.h.}$ has a high value of H_{max}^{mag}, so it is tempting to say that, as with Fe, the low-temperature allotrope forms are due to strong stabilisation by magnetic forces. However this is not the case, as $Co^{f.c.c.}$ is also ferromagnetic with very similar values of β and T_c. The magnetic contributions virtually cancel each other out in this case, although the f.c.c./c.p.h. transformation temperature will clearly be sensitive to small changes in magnetic parameters on alloying. The magnetic properties of metastable b.c.c. Co were derived indirectly by Inden (1975) as part of a calculation involving ordering in b.c.c. Fe–Co alloys. Interestingly, these values are substantially confirmed by more recent FP calculations. Table 8.2 and Fig. 8.11 of Chapter 8 can be consulted for further details.

References are listed on pp. 173–178.

6.4.3 Ni

Ni does not exhibit any allotropy with respect to either temperature or pressure, which implies that its f.c.c. structure must be significantly more stable than the nearest competitors. This is consistent with values for $G^{f.c.c.\rightarrow c.p.h.}$ derived from SFE measurements and changes in SFE with alloying also suggest that there is a magnetic component in $G^{f.c.c.\rightarrow c.p.h.}$. Since the magnetic enthalpy is much smaller than for Fe or Co, this in turn implies that that $Ni^{c.p.h.}$ is paramagnetic or has a low T_c (Miodownik 1978a). However, FP calculations imply a value of β not much lower than for $Ni^{f.c.c.}$, which would indicate that Ni behaves much like Co. Further experimental information on the magnetic properties of $Ni^{c.p.h.}$, possibly from thin films, would clearly be desirable.

6.4.4 Mn

Experimentally Mn solidifies as the b.c.c. δ-Mn phase, which then transforms to f.c.c. γ-Mn on cooling. This is entirely analogous to the behaviour of Fe. However, it then undergoes two further low-temperature transitions to β-Mn and α-Mn which are complex crystal structures with large unit cells. De-convoluting the experimental data into separate contributions is difficult. Three of the phases are anti-ferromagnetic with widely differing values of the saturation magnetisation at 0 K, and there are also significant differences in the Debye temperatures and electronic specific heat. It is therefore difficult to make a consistent characterisation which matches all these observations. By concentrating on matching phase transition temperatures and Debye temperature data, Fernandez Guillermet and Huang (1990) were forced to use *effective* magnetisation values which could be as low as ⅓ of those experimentally observed. This makes it impossible to estimate the real role of any magnetic factors in their treatment.

By contrast, in an earlier assessment, Weiss and Tauer (1958) decided to use the measured magnetisation values as a primary input over the whole temperature range, but then had to depart from the experimentally observed Debye temperatures. Interestingly, their treatment led to the conclusion that the G curves for β-Mn and γ-Mn would also intersect twice so that the behaviour of Fe could no longer be

considered unique. However in this scenario it is γ-Mn that has the largest magnetic component, while the stability of β-Mn is dictated by a larger electronic specific heat. The finding by Gazzara *et al.* (1964) that the value of the saturation magnetisation for α-Mn (and other anti ferromagnetic materials) can be temperature dependent may have to be taken into account in order to finally reconcile what are otherwise different interpretations of the same data. The relative Gibbs energy curves for b.c.c., f.c.c. and c.p.h. Mn as calculated by Asada and Terakura (1993) are shown in Fig. 6.13(b).

6.5. THE EFFECT OF PRESSURE

6.5.1 Basic addition of a PΔV *term*

It is commonplace to assume a form of the Gibbs energy function which excludes the pressure variable for solid-state phase transformations, as the magnitude of the $P\Delta V$ term is small at atmospheric pressures. This is of course not the case in geological systems, or if laboratory experiments are deliberately geared to high-pressure environments. Klement and Jayaraman (1966) provide a good review of the data available at the time when some of the earliest CALPHAD-type calculations were made (Kaufman and Bernstein 1970, Kaufman 1974). Much work was also carried out on specific alloy systems such as Fe–C (Hilliard 1963) and the Tl–In system (Meyerhoff and Smith 1963).

The extra pressure term to be added to the Gibbs energy can be expressed as

$$G_m^{\alpha\to\beta} = \int_0^P V_m^{\alpha\to\beta} \mathrm{d}P \tag{6.15}$$

where $V_m^{\alpha\to\beta}$ is the change in molar volume due to the transformation of α to β. Although this can be considered as constant to a first approximation, this will no longer be true at high pressures, and several empirical descriptions have been developed, depending on the pressure range in question. Bridgman (1931) used a simple second-power polynomial to define the effect of pressures up to 3 GPa:

$$V_m = V_0 + V_1 P + V_2 P^2 \tag{6.16}$$

where $V_{0,1,2}$ are temperature dependent and have to be determined by experiment. If the entropy, enthalpy and volume differences between these phases are assumed independent of temperature and pressure is not excessive, then Eq. (6.15) will obviously reduce to:

$$G_m^{\alpha\to\beta} = PV_m^{\alpha\to\beta} \tag{6.17}$$

where P and $V_m^{\alpha\to\beta}$ are given in GPa and m^3 respectively. This simple treatment also leads to the familiar Clapeyron equation where the slope of the temperature vs pressure plot for the transformation $\alpha \to \beta$ is given by:

$$\frac{\mathrm{d}T}{\mathrm{d}P} = \frac{V^{\alpha\to\beta}}{S^{\alpha\to\beta}}. \tag{6.18}$$

References are listed on pp. 173–178.

Table 6.6. Linear Gibbs energy equations for some non-transition elements that include a pressure term taken (Kaufman and Bernstein 1970). Values are applicable only at temperatures >300 K

Element	Transformation	ΔH (J mol^{-1})	$-T\Delta S$ (S = J mol^{-1}; $T = K$)	$+P\Delta V$ ($P = GPa$; $V = m^3$)
Ca	f.c.c.→b.c.c.	243	–0.33T	+0.01P
Sr	f.c.c.→b.c.c.	837	–0.96T	–0.10P
Be	c.p.h.→b.c.c.	4602	–3.01T	–0.18P
Yb	f.c.c.→b.c.c.	3180	–2.97T	–0.80P
Ba	f.c.c.→c.p.h.	4351	+3.35T	–0.74P
Pb	f.c.c.→c.p.h.	2510	–0.42T	–0.18P
C	A4→Graphite	1255	–4.77T	+1.76P

Note: Although current values of ΔH and ΔS are different in later references this will not affect the pressure term.

Some examples of equations based on adding a simple $P\Delta V$ term to the definition of lattice stabilities are given in Table 6.6 (adapted from Kaufman and Bernstein 1970).

6.5.2 Making the volume a function of T *and* P

These earlier treatments have now been superseded by a more general approach, where the molar volume of each phase as a function of temperature and pressure is expressed as a function of the compressibility χ (Fernandez Guillermet *et al.* 1985).

$$V_m^{T,P} = V_0(1 + nP\chi)^{-1/n} \exp\left(\alpha_0 T + \tfrac{1}{2}\alpha_1 T^2\right) \tag{6.19}$$

where V_0 is an empirically fitted parameter with the dimensions of volume and α_0 and α_1 are parameters obtained from fitting the experimental lattice parameter and dilatometric data such that

$$\alpha_{P=0}^T = \alpha_0 + \alpha_1 T \tag{6.20}$$

where $\alpha_{P=0}^T$ is the thermal expansivity at zero pressure as a function of temperature. χ is also expressed as a function of temperature using the polynomial

$$\chi = \chi_0 + \chi_1 T + \chi_2 T^2. \tag{6.21}$$

At constant temperature, Eq. (6.19) reduces to the simpler expression suggested much earlier by Murnaghan (1944).

$$V_m^{T,P} = \frac{V_m^{T,P=0}}{(1 + nP\chi^{T,P=0})^{1/n}} \tag{6.21}$$

where $V_m^{T,P=0}$ and $\chi^{T,P=0}$ are, respectively, the molar volume and isothermal compressibility at zero pressure. G_m as a function of both temperature and pressure can then be obtained by adding the following expression to Eq. (6.3):

$$G_m^{T,P} - H_m^{\mathrm{SER}} = a + bT + cT\log_e(T) + \sum \mathrm{d}T^m + \int_0^P V_m^{T,P}\mathrm{d}P \tag{6.22}$$

where

$$\int_0^P V_m^{T,P}\mathrm{d}P = V_0\left\{(1 + nP\chi)^{(n-1)/n} - 1\right\}\frac{\exp\left(\alpha_0 T + \frac{1}{2}\alpha_1 T^2\right)}{\chi(n-1)}. \tag{6.23}$$

Available experimental data for various solid–liquid and solid–solid state transformations has been successfully fitted for C, Mo and W (Fernandez Guillermet *et al.* 1985) and Fe (Fernandez Guillermet and Gustafson 1985) using the above expression. It gives better results than Eq. (6.16) at high pressures and also has the advantage that Eq. (6.19) can be inverted to give an expression for P^{T,V_m}. This in turn allows an explicit function to be written for the Helmholtz energy. Another approach that has been considered recently is the Rose equation of state (Rosen and Grimwall 1983). This however requires the additional input the expansion coefficient and the pressure derivative of the bulk modulus. With the increasing availability of such quantities from first-principles calculations, this may well become the basis for future formulations (Burton *et al.* 1995).

Depending on the data available, Eqs (6.17)–(6.23) reproduce experimental pressure effects with considerable accuracy in many cases. In particular, Eq. (6.18) can be used to confirm entropy data derived using more conventional techniques and can also provide data for metastable allotropes. Ti again provides a leading example, as pressure experiments revealed that the ω-phase, previously only detected as a metastable product on quenching certain Ti alloys, could be stabilised under pressure (Fig. 6.14). Extrapolation of the β/ω transus line yields the metastable allotropic transformation temperature at which the β-phase would transform to ω in the absence of the α-phase, while the slope of the transus lines can be used to extract a value for the relevant entropy via Eq. (6.18).

6.5.3 *Effect of competing states*

All of the above approaches assume that missing pressure data can be estimated from consistent periodic trends and that individual phases do not exhibit anomalous behaviour. This is reasonable when the alternative crystal structures are each associated with specific energy minima, but there can be some important exceptions

References are listed on pp. 173–178.

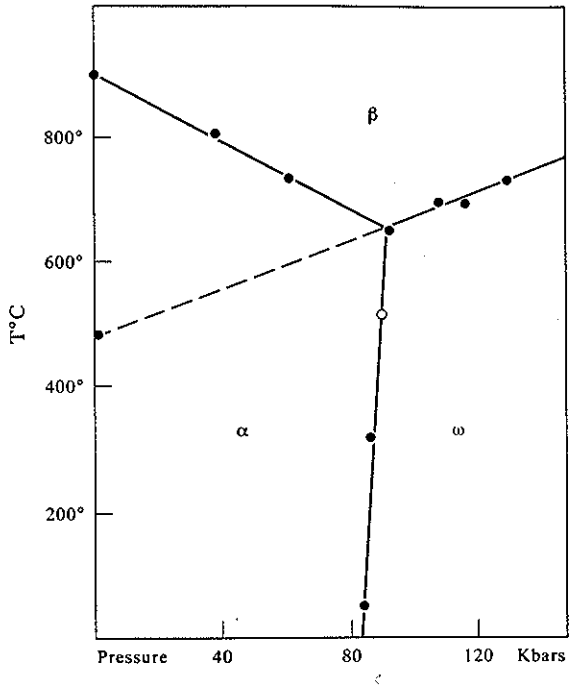

Figure 6.14. T–P diagram for Ti showing experimental data from Bundy (1965b) and Jayaraman (1966) and the extrapolation of the β–ω transus to yield the metastable $T^{\beta-\omega}$ at atmospheric pressure (from Vanderpuye and Miodownik 1970).

to this general rule. For example, in magnetic systems it is possible to obtain markedly different combinations of exchange and correlation forces in the *same* crystal structure (Fig. 6.13) although the two structures can differ in energy by only a small amount (Asada and Terakura 1993). The possibility of Schottky excitations between alternative states can then produce an anomalous changes in volume with temperature and pressure. Although it is always possible to handle such a situation by a choice of suitable coefficients in Eq. (6.23), an alternative treatment is to explicitly determine the effect on the Gibbs energy of having a combination of states. This was attempted for γ-Fe using the following additional relationships (Kaufman *et al.* 1963, Blackburn *et al.* 1965):

$$V^{\gamma_1 \rightarrow \gamma_2} = f^{\gamma_2} V_T^{\gamma_2} - f^{\gamma_1} V_T^{\gamma_1} \tag{6.24}$$

$$\frac{f_{T,P}^{\gamma_2}}{f_{T,P}^{\gamma_1}} = \alpha \exp^{-\Delta G/RT} \tag{6.25}$$

$$E_P^{\gamma_1 \rightarrow \gamma_2} = E_{P=0}^{\gamma_1 \rightarrow \gamma_2} + PV^{\gamma_1 \rightarrow \gamma_2} \tag{6.26}$$

$$G_{T,P}^{\gamma_1 \rightarrow \gamma_2} = 100PV_T^{\gamma_1} + RT\ln(1 - f^{\gamma_2}). \tag{6.27}$$

Here $V^{\gamma_1}, V^{\gamma_2}$ and $f^{\gamma_1}, f^{\gamma_2}$ refer to the molar volume and fractions of each state, $E^{\gamma_1 \rightarrow \gamma_2}$ is the difference in energy between the two states and $G^{\gamma_1 \rightarrow \gamma_2}$ is the extra increment of Gibbs energy resulting from the existence of the two states. Including this term, the γ/ε temperature–pressure transus for pure iron *was then quantitatively predicted before this was verified experimentally* by Bundy (1965a) (Fig. 6.15). The fit is clearly not as good as that which can be obtained by Fernandez Guillermet and Gustafson (1985) using Eqs (6.3) and (6.23), but on the other hand these authors *included the experimental pressure data in their optimisation* and did not make any specific provision for the possibility of multiple states. Which treatment is to be preferred depends on whether priority is to be given to the development of simple universally applicable algorithms or to more physically realistic models.

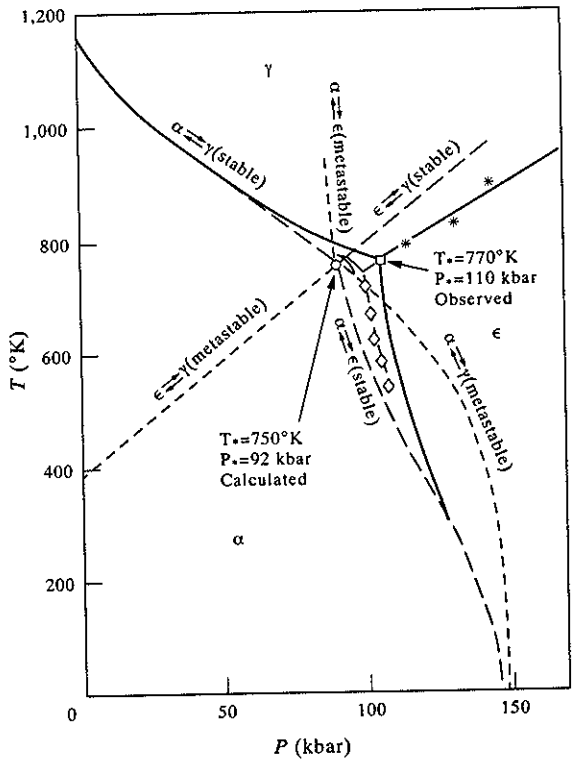

Figure 6.15. Comparison of experimental T–P diagram for Fe (Bundy 1965) * with calculated phase boundaries from Blackburn *et al.* (1965) and Fernandez Guillermet and Gustafson (1985) ◇.

References are listed on pp. 173–178.

Data derived from pressure experiments on semi-conducting elements by Klement and Jayamaran (1966) and Minomura (1974) have also been useful in obtaining confirmation that the entropies associated with transitions in Si, Ge and Sn form a consistent pattern, supporting the concept that each crystallographic transformation tends to have a characteristic associated entropy change (Miodownik 1972a, 1972b). Similarly, extrapolations from pressure data on alloys can be used to obtain estimates of lattice stabilities at $P = 0$, which can then be compared with estimates obtained by other routes, such as SFE measurements.

Calculation of the critical pressure required to cause a phase transformation at 0 K can also be obtained from first-principle calculations. Assuming the various phases exhibit normal elastic behaviour the tangency rule can be applied to energy vs volume plots to yield values for the critical pressure that would generate a phase transformation:

$$P_{\text{crit}} = \frac{\delta G}{\delta V}. \tag{6.28}$$

However, if there are large variations in the elastic constants with pressure, this can seriously affect P_{crit} by as much as an order of magnitude (Lam *et al.* 1984).

6.6. DETERMINATION OF INTERACTION COEFFICIENTS FOR ALLOYS AND STABILITY OF COUNTER-PHASES

The determination of individual binary equilibrium diagrams usually only involves the characterisation of a limited number of phases, and it is possible to obtain some experimental thermodynamic data on each of these phases. However, when handling multi-component systems or/and metastable conditions there is a need to characterise the Gibbs energy of many phases, some of which may be metastable over much of the composition space.

This requires a methodology for characterising a large range of metastable solutions and compounds which, by definition are difficult, if not impossible, to access experimentally. The available methods involve various levels of compromise between simplicity and accuracy and can be categorised by the choice of atomic properties used in the process.

At one end of the spectrum are first-principles methods where the only input requirements are the atomic numbers Z_A, Z_B, ... the relevant mole fractions and a specified crystal structure. This is a simple extension to the methods used to determine the lattice stability of the elements themselves. Having specified the atomic numbers, and some specific approximation for the interaction of the relevant wave functions, there is no need for any further specification of attractive and repulsive terms. Other properties, such as the equilibrium atomic volumes, elastic moduli and charge transfer, result automatically from the global minimisation of

the energy for the total assembly of electrons and ions (Zunger 1980a, 1980b, Pettifor 1992).

At the other end of the spectrum are more empirical methods which utilise secondary properties which reflect more conventional terms, such as the atomic volume, electronegativity or some function of the enthalpy of evaporation (Darken and Gurry 1953, Hildebrand and Scott 1956, Mott 1968, Pauling 1960, Kaufman and Bernstein 1970). In many cases the desire for simplicity has led to allocation of a set of constant parameters to each atomic species, even though such properties are known to vary substantially with the geometric or chemical environment in which they are placed. This is probably adequate if such parameters are to be fed into a correspondingly simple regular solution model or line compound model, but will not be sufficient if there is a need for sub-regular solution parameters or if substantial directional bonding is involved. Many treatments have been modified by feedback to give better agreement with experimental trends. In some cases this has been achieved by introducing additional terms and in others by merely altering the numerical values that were originally tied rigidly to a measured property (Miedema 1976, Niessen *et al.* 1983).

6.6.1 The prediction of liquid and solid solution parameters

6.6.1.1 Empirical and semi-empirical approaches. The problem of making theoretical estimates for the interaction coefficients for the liquid phase has been tackled in different ways by various authors. Kaufman and Bernstein (1970) considered that the liquid state would exhibit the lowest repulsive forces of all the states of condensed matter and that a description of the interaction parameters for the liquid state would be the best basis for the prediction of interaction parameters for various solid phases.

Their expression for a liquid interaction parameter (L) follows Mott (1968) and starts with the simple sum of an attractive term, e_o, and a repulsive term, e_p,

$$L = e_o + e_p. \tag{6.29}$$

Kaufman and Bernstein (1970) derived e_o via the electronegativity values, φ_i and φ_2 (Pauling 1960)

$$e_o = -100\,(\varphi_1 - \varphi_2)^2. \tag{6.30}$$

Estimates for e_p were based on Hildebrand's solubility parameters, δ_{ij}, (Hildebrand and Scott 1950), which are related to the enthalpy of vaporisation ($H_{v(ij)}$) and the molar volume $V_{m(ij)}$ of elements i and j respectively so that

$$\delta_{(i,j)} = \left(-\frac{H_{v(i,j)}}{V_{m(i,j)}}\right)^{1/2}. \tag{6.31}$$

References are listed on pp. 173–178.

Making an adjustment for the effect of temperature finally leads to

$$e_p = 0.3\left(V_{m(i)} + V_{m(j)}\right)\left\{\left(\frac{-H_{v(i)}}{V_{m(i)}}\right)^{1/2} - \left(\frac{-H_{v(j)}}{V_{m(j)}}\right)^{1/2}\right\}. \tag{6.32}$$

Further parameters are then added to determine the interaction parameters for various crystal structures, e.g., the interaction parameter, B, for b.c.c. structure becomes

$$B = L + e_1 + e_2. \tag{6.33}$$

Following Kaufman and Bernstein (1970) the first of these is a strain-energy term depending on the volume difference between i and j which will always be a positive contribution and assumed to be proportional to $GV(\Delta V/V)^2$, where G is a modulus which, in the absence of data, can be approximated as $H_{v(ij)}/V$. The second term is based on the variation of $H^{L\to B}$ with group number across the periodic table reflecting the relation between e_o and the heat of vaporisation. Similarly, the interaction parameters E, for c.p.h. solutions, and A, for f.c.c. solutions, become

$$E = B + e_3 \tag{6.34}$$

and

$$A = E + e_4. \tag{6.35}$$

The strain energy term is thus assumed to be independent of crystal structure for the three major types of substitutional solid solutions.

By contrast, the 'macroscopic atom' model of Miedema (Miedema *et al.* 1975) starts with a descriptions of the solid state which is then modified to describe the liquid state (Boom *et al.* 1976a, 1976b). In their model the enthalpy of formation at 0.5 mole fraction, $H_{c=0.5}$ is given to a first approximation by:

$$H_{c=0.5} \approx \left[-P(\Delta\phi^*)^2 + Q(\Delta {n_{ws}}^{1/3})^2 - R\right]. \tag{6.36}$$

Here n_{ws} is an electron density based on the volume of Wigner–Seitz atomic cells, V_m, and it is assumed that differences in electron density Δn_{ws} between different species of atoms will always lead to local perturbations that give rise to a positive energy contribution. On the other hand, ϕ^* is a chemical potential based on the macroscopic work function ϕ, so that differences, $\Delta\phi^*$, at the cell surfaces between different species of atoms lead to an attractive term, analogous to the gain in energy from the formation of an electric dipole layer. P, Q and R are empirically derived proportionality constants. P and Q were initially taken to be adjustable parameters, but turned out to be almost universal constants for a wide variety of atomic combinations, especially amongst the transition metals. The parameter R was introduced as an arbitrary way of adjusting for the presence of atoms with p

electrons and takes on values that increase regularly with the valency of the B-group element. In contrast to the Kaufman model (Kaufman and Bernstein 1970), Eq. (6.36) contains no parameters which refer to crystal structure and therefore the heats of solution of f.c.c., b.c.c. and c.p.h. structures are predicted to be, a priori, identical. The same conclusion can also be expected for liquid solutions, and indeed the suggested parameters for liquid and solid solutions are very similar. The constants P and Q are practically the same, although it was necessary to introduce different values of R.

***6.6.1.2* Ab initio *electron energy calculations*.** While there are many methods for predicting the relative stability of ordered structures, electron energy calculations for predicting interaction parameters for the liquid is still a major problem. Calculations of the heat of solution for disordered solutions falls in an intermediate category. It is a surprising fact that it is at present still impossible to calculate the melting point, or the entropy and enthalpy of fusion of the elements to any reasonable degree of accuracy, which poses a major challenge to a full calculation of any phase diagram by FP methods. One method to overcome this problem for liquids is to assume that it will exhibit *sro* parameters based on the predominant solid state structure(s) in the phase diagram (Pasturel *et al.* 1992).

Pasturel *et al.* (1985) and Colinet *et al.* (1985) have used a tight-binding model which considers the moments of the density of states. The model provides an estimate for the *d* electron transfer between the elements in an alloy/compound by using the concept of partial density of states. The model is, however, simplified so that neither atomic position or crystal structure is calculated in detail. The results can therefore be considered to provide a good general prediction for disordered phases but is independent of crystal structure. The reason why this works reasonably well is because the magnitude of the fundamental electronic *d*-band effect for many such alloys is substantially larger than the effect arising from differences in crystal structure. More accurate results probably require the incorporation of directional bonding (Pettifor *et al.* 1995) which can lead to highly composition-dependent interaction parameters.

6.6.2 The prediction of thermodynamic properties for compounds

6.6.2.1 The concept of counter-phases. When a stable compound penetrates from a binary into a ternary system, it may extend right across the system or exhibit only limited solubility for the third element. In the latter case, any characterisation also requires thermodynamic parameters to be available for the equivalent metastable compound in one of the other binaries. These are known as *counter-phases*. Figure 6.16 shows an isothermal section across the Fe–Mo–B system (Pan 1992) which involves such extensions for the binary borides. In the absence of any other guide-

References are listed on pp. 173–178.

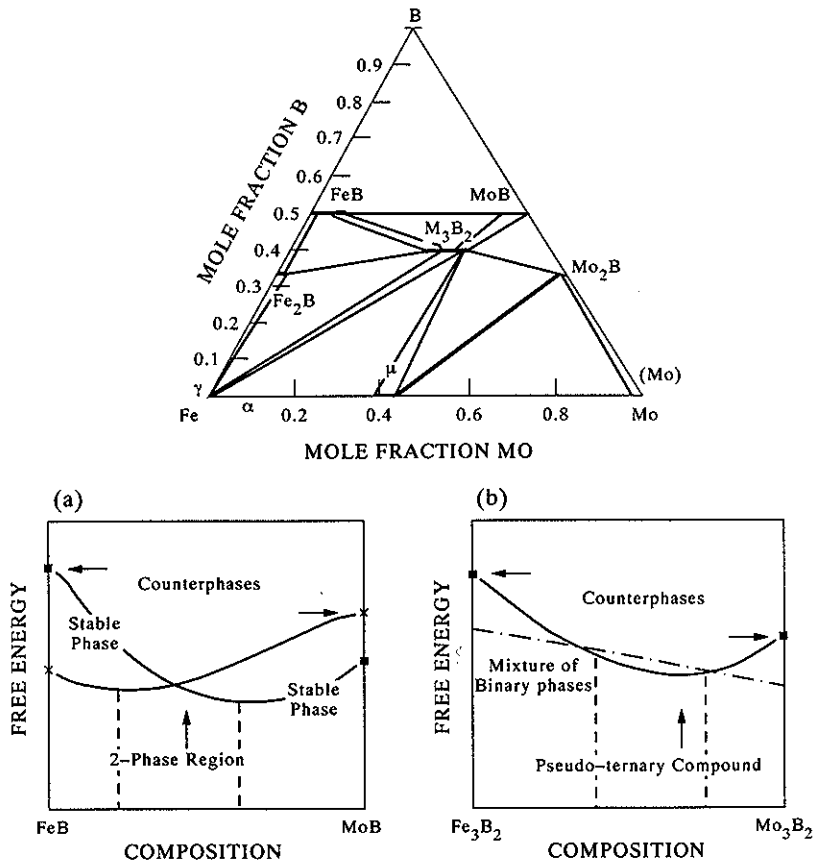

Figure 6.16. Counter phases in the Fe–Mo–B system: (a) the section FeB–MoB and (b) the section Fe_3B_2–Mo_3B_2 (from Pan 1992 and Miodownik 1994).

lines it is necessary to use empirical methods, which have been well documented in Kaufman and Bernstein (1970), and constitute a useful fitting procedure. Accurate results can be obtained if there are some prior phase-boundary data for the ternary system which can be used to validate the assumed thermodynamics of the counter-phase. However, problems arise when there is little or no experimental information and when the extension of the compound into the ternary is small. Further, when multiple sublattice modelling is used (see Chapter 5) it may be necessary to input thermodynamic properties for compounds which are compositionally far away from the area of interest in the CALPHAD calculation. It is therefore desirable to have a method of *predicting* the thermodynamic properties of as many counter-phases as possible.

6.6.2.2 Structure maps. Attempts have been made to chart the occurrence of particular structures in relation to familiar parameters such as size, electronegativity and electron concentration (Darken and Gurry 1953, Villars *et al.* 1989). Some of these schemes have only limited applicability to particular areas of the periodic table, but more recently there has been greater success through structure maps which are based on the concept of a Mendeleev number (Pettifor 1985a). These have been extended to ternary compounds (Pettifor 1985b) and give considerable insight into the choice of structures which may be significant competitors in a given multicomponent situation. Calculations which give more detailed energies of various competing structures in particular regions of the map, such as for the Laves phases (Ohta and Pettifor 1989) are now emerging with increased frequency.

6.6.2.3 The Miedema model and other semi-empirical methods. The Miedema model was originally devised as a tool for merely predicting the *sign* of the heat of solution at the equiatomic composition. Therefore Eq. (6.36) does not contain any concentration-dependent terms (Miedema 1973, Miedema *et al.* 1973). However, the treatment was extended in subsequent publications, and modifications were made to include ordering contributions and asymmetric effects (Miedema *et al.* 1975, de Boer *et al.* 1988). Additional functions $f(c_A^s, c_B^s)$ and $g(c_A, c_B, V_{mA}, V_{mB})$ were kept very simple and did not include additional parameters other than (V_m), which had already been used to determine (n_{ws}).

$$\Delta H(c_A, c_B) = f(c_A^s, c_B^s)\, g(c_A, c_B, V_{mA}, V_{mB}) \left[-P(\Delta\phi^*)^2 + Q\left(\Delta {n_{ws}}^{1/3}\right)^2 - R\right] \tag{6.37}$$

where $f(c_A^s, c_B^s) = c_A^s c_B^s(1 + 8(c_A^s c_B^s)^2)$ and c_A^s, etc., are surface concentrations. These arise from the concept that in their 'macroscopic atom' model the enthalpy effects are generated at the common interface of dissimilar atomic cells. Such an expression contains only a limited degree of asymmetry and essentially use a very primitive ordering model that does not even consider nearest-neighbour interactions but assumes that $H_{\text{ord}}/H_{\text{disord}}$ is virtually a constant. Since there is no provision for any crystallographic parameters it is impossible to make any predictions about the relative stability compounds with different crystal structures at the same stoichiometry. A quantum-mechanical rationale of the Miedema approach has been published by Pettifor (1979a), outlining its strengths and weaknesses.

Machlin (1974, 1977) developed a semi-empirical treatment which used a constant set of nearest-neighbour interactions and was one of the earliest semi-empirical attempts to obtain the relative enthalpies of formation between different crystal structures. This successfully predicted the correct ground states in a substantial number of cases, but the treatment was generally restricted to transition metal combinations and a limited number of crystal structures.

References are listed on pp. 173–178.

6.6.2.4* Ab initio *electron energy calculations. Some of the earliest electron energy calculations were made for transition metals where it was noted that trends in cohesive energy could be approximated to a very reasonable degree by considering only the *d*-band electrons (Friedel 1969, Ducastelle and Cyrot-Lackman 1970). Various means of representing the density of states were then applied in an attempt to quantify this. Van der Rest *et al.* (1975) utilised the coherent potential approximation (CPA) method with off-diagonal disorder to compute the density of states curve. This method was employed by Gautier *et al.* (1975) and Ehrenreich and Schwartz (1976) for extensive calculations of transition metal alloys. Later work by Pettifor (1978, 1979b), Varma (1979) and Watson and Bennett (1981) extended the *d*-band concept further and comparison with experimental enthalpies of formation for equi-atomic compounds were quite reasonable, although there is a clear tendency for the predictions to be too exothermic. They are also limited because they are insensitive to crystal structure and, subsequently, give no predictions for metastable compounds. Pseudo-potential calculations are also a method by which heats of formation can be predicted (Hafner 1989, 1992). These work better for sp-bonded compounds such as the alkali metal Laves phases (Hafner 1987) where nearly free electron theory is well suited, but they are not so applicable to *d*-band calculations which are necessary for transition metal alloys.

Electron energy calculations utilise methods which solve the Schrödinger equation and start with the specification of the lattice space group taking into account a wide variety of interatomic forces. It is therefore possible to make calculations for a large group of ordered structures and calculate the difference in enthalpy that arise from any specified change in crystallography at a given composition for any combination of elements (Pettifor 1985a, Finnis *et al.* 1988). Such calculations incorporate the effects of changes in band width, the centre of gravity of the bands, various forms of hybridisation and can also include directional bonding (Pettifor 1989, Phillips and Carlsson 1990, Pettifor *et al.* 1995).

Although there are inherent approximations in any electron energy calculation, it is significant that this route now has a high success rate in predicting the correct ground state amongst a large range of competing structures (Gautier 1989, Sluiter and Turchi 1989, Nguyen-Manh *et al.* 1995). In order to shorten the calculation time these are often limited to those structures thought most likely to occur. This can potentially lead to the omission of other contenders but algorithms have recently been developed which can markedly extend the number of structures sampled and remove such arbitrary limitations (Lu *et al.* 1991).

Electron energy calculations now offer a coherent explanation of trends observed both across and down the periodic table and the grouping and overlaps observed in structure maps. Of particular importance are the marked changes that occur on moving to elements of higher atomic number, which means that some of the earlier assumptions concerning similarities of behaviour for compounds of the 3*d*, 4*d*, and 5*d* elements (Kaufman and Bernstein 1970) have had to be revised. Quantum

mechanical effects also lead to significantly greater sinusoidal variations in stability with atomic number and hence also to markedly greater asymmetry in the variation of enthalpy of formation of similar structures in a given binary system.

6.7. SUMMARY

Despite a sometimes turbulent history a series of standard and effective lattice stability values are now readily available for the majority of elements. Most of the remaining areas of controversy concern structures which seem to be elastically unstable or where the magnetic structure is uncertain. The relative stability of different compounds seems to be taking a similar route, but clearly involves a much wider range of structures. The availability of many different calculation routes has led to numerous comparisons being made between the various calculated results and whatever experimental information is available for the stable phases (Kaufman 1986, Birnie *et al.* 1988, Colinet *et al.* 1988, Watson *et al.* 1988, de Boer *et al.* 1988, Aldinger *et al.* 1995). Figure 6.17 shows that there is often good general agreement for a given class of structures so that it is now possible to make a better estimate for the enthalpies of unknown metastable compounds.

The success of earlier empirical schemes in predicting the sign and magnitude of the enthalpy of formation can in part be attributed to making predictions for *AB* compounds. This can hide asymmetrical effects which are more apparent when other stoichiometries are considered. The empirical and semi-empirical schemes do

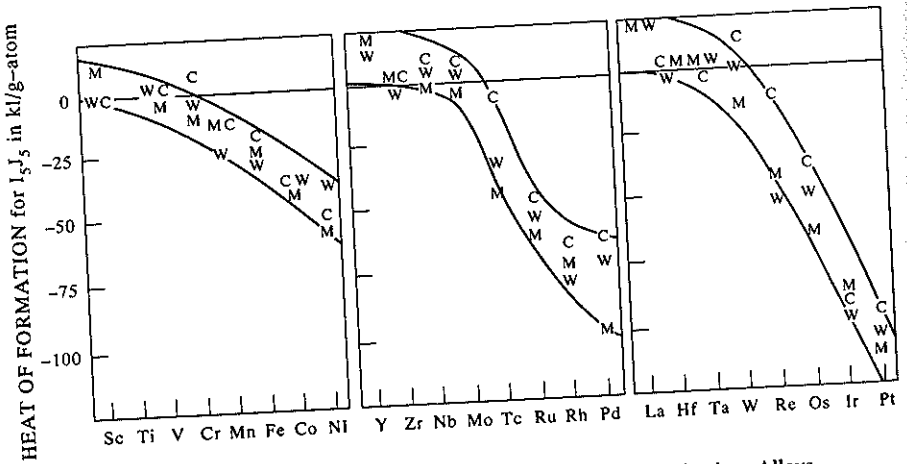

Figure 6.17. Comparison of enthalpies of formation for AB Titanium Alloys M=predictions of Miedema (de Boer *et al.* 1988), W=predictions of Watson and Bennett (1984) and C=predictions of Colinet *et al.* (1985). Figure from Aldinger *et al.* (1995).

References are listed on pp. 173–178.

not have the capacity to handle a wide range of bonding characteristics without the introduction of many additional parameters with arbitrary numerical values. This much diminishes their predictive value as far as defining the relative stability of counter-phases is concerned. The more sophisticated electron energy calculations are now undoubtedly a better guide for the relative enthalpy of a much wider range of structures and should be increasingly used as input data in any CALPHAD optimisation. However, such calculations cannot predict the relative entropies of the competing structures and this is still an area where an empirical approach is required for the present.

REFERENCES

Achar, B. S. and Miodownik, A. P. (1974) Report on Phase Equilibria in Alloys, Report to Science Research Council (UK) under Contract B/RG/19175.

Ågren, J. (1979) *Met. Trans.*, **10A**, 1847.

Ågren, J., Cheynet, B. Clavaguera-Mora, M. T., Hack, K., Hertz, J., Sommer, F. and Kattner, U. (1995) *CALPHAD*, **19**, 449.

Aldinger, F., Fernandez Guillermet, A., Iorich, V. S., Kaufman, L., Oates, W. A., Ohtani, H., Rand, M. and Schalin, M. (1955) *CALPHAD*, **19**, 555.

Anderson, J. O., Fernandez Guillermet, A. and Gustafson, P. (1987) *CALPHAD*, **11**, 365.

Ardell, A. J. (1963) *Acta. Met.*, **11**, 591.

Asada, T. and Terakura, K. (1993) in *Computer Aided Innovation of New Materials, Vol. 1*, eds Doyama, M. *et al.* (Elsevier Science, Amsterdam), p. 169.

Austin, J. B. (1932) *Ind. Chem. Engineering*, **24**, 1225.

Bendick, W. and Pepperhoff, W. (1982) *Acta. Met.*, **30**, 679.

Birnie, D., Machlin, E. S., Kaufman, L. and Taylor, K. (1982) *CALPHAD*, **6**, 93.

Blackburn, L. D., Kaufman, L. and Cohen, M. (1965) *Acta. Met.*, **13**, 533.

Boom, R., de Boer, F. R. and Miedema, A. R. (1976a) *J. Less Common Metals*, **45**, 237.

Boom, R., de Boer, F. R. and Miedema, A. R. (1976b) *J. Less Common Metals*, **45**, 271.

Brewer, L. (1967) in *Phase Stability in Metals and Alloys*, eds Rudman, P. S. *et al.* (McGraw-Hill, New York), p. 39.

Brewer, L. (1975) LBL-3720 Reprint on Contract W-7405-ENG-48.

Brewer, L. (1979) in *Calculation of Phase Diagrams and Thermochemistry of alloy phases* eds Chang, Y. A. and Smith, J. F. (AIME, Warrendale, PA), p. 197.

Bridgman, P. W. (1931) in *The Physics of High Pressure* (Bell, London).

Bundy, F. P. (1965a) *J. Appl. Physics*, **36**, 616.

Bundy, F. P. (1965b) ASTM Special Technical Publication Number 374.

Burton, B., Chart, T. G., Lukas, H. L., Pelton, A. D., Siefert, H. and Spencer, P. (1995) *CALPHAD*, **19**, 537.

Chalmers, B. (1959) in *Physical Metallurgy* (John Wiley), p. 85.

Chang, Y. A., Colinet, C., Hillert, M., Moser, Z., Sanchez, J. M., Saunders, N., Watson, R. E. and Kussmaul, A. (1995) *CALPHAD*, **19**, 481.

Chase, M. W., Ansara, I., Dinsdale, A. T., Eriksson, G., Grimvall, G., Höglund, L. and Yokokawa, H. (1995) *CALPHAD*, **19**, 437.

Chen, Y. G. and Liu, B. X. (1997) *J. Alloys & Compounds*, **261,** 217.
Cho, S. A. and Puerta, M. (1976) *J. Solid State Chem.*, **16,** 355.
Chuang, Y. Y., Schmid-Fester, R. and Chang, Y. A. (1985) *Met. Trans.*, **16A,** 153.
Colinet, C., Bessound, A. and Pasturel, A. (1988) *J. Phys. F*, **18,** 903.
Colinet, C., Pasturel, A. and Hicter, P. (1985) *CALPHAD*, **9,** 71.
Craievich, P. J., Weinert, M., Sanchez, J. and Watson, R. E. (1994) *Phys. Rev. Lett.*, **72,** 3076.
Craievich, P. J. and Sanchez, J. (1995) Unpublished research reported in Chang *et al.* (1995).
Crampin, S., Hampel, K., Vvedensky, D. D. and McLaren, J. M. (1990) *J. Mater. Res.*, **5,** 2107.
Darken, L. S. and Gurry, R. W. (1953) *The Physical Chemistry of Metals* (McGraw-Hill, New York).
Darken, L. S. and Smith, R. P. (1951) *Ind. Eng. Chem.*, **43,** 1815.
de Boer, F. R., Boom, R., Mattens, W. C. M., Miedema, A. R., and Niessen, A. K. (1988) in *Cohesion in metals: Cohesion and Structure, Vol. 1* (Elsevier Science, Amsterdam), p. 644.
de Fontaine, D. (1996) *MRS Bulletin*, **21,**(8), 16.
Dinsdale, A. T. (1991) *CALPHAD*, **15,** 317.
Domb, C. (1958) *Nuevo Cimento*, **9**(S1), 9.
Ducastelle, F. and Cyrot-Lackman, F. (1970) *J. Phys. Chem. Solids*, **31,** 1295.
Ducastelle, F. and Gautier, F. (1976) *J. Phys. F*, **6,** 2039.
Ehrenreich, H. and Schwartz, L. (1976) in *Solid State Physics*, eds Ehrenreich, H. *et al.* (Academic Press, New York), p. 149.
Einarsdotter, K., Sadigh, B., Grimwall, G. and Ozolins, V. (1997) Submitted to *Phys. Rev. Lett.*
Engel, N. (1964) *ASM Trans. Quarterly*, **57,** 619.
Fernandez Guillermet, A. and Gustafson, P. (1985) *High Temp.–High Press.*, **16,** 591.
Fernandez Guillermet, A. and Hillert, M. (1988) *CALPHAD*, **12,** 337.
Fernandez Guillermet, A. and Huang, W. (1988) *Z. Metallkde.*, **79,** 88.
Fernandez Guillermet, A. and Huang, W. (1990) *Int. J. Thermophys.*, **11,** 949.
Fernandez Guillermet, A., Gustafson, P. and Hillert, M. (1985) *J. Phys. Chem. Solids*, **46,** 1427.
Fernandez Guillermet, A., Ozolins, V., Grimwall, G. and Korling, M. (1995) *Phys. Rev. B*, **51,** 10,364.
Fernando, G. W., Watson, R. E., Weinert, M., Wang, Y. J. and Davenport, J. W. (1990) *Phys. Rev. B*, **41,** 11,813.
Finnis, M. W., Paxton, A. T., Pettifor, D. G., Sutton, A. P. and Ohta, Y. (1988) *Phil. Mag. A*, **58,** 143.
Friedel J. (1969) in *Physics of Metals*, ed. Ziman, J. (Cambridge Univ. Press), p. 340.
Friedel, J. (1974) *J. de Physique*, **75,** 59.
Gautier, F., Van der Rest, J. and Brouers, F. (1975) *J. Phys. F*, **5,** 1184.
Gautier, F. (1989) in *Alloy Phase Stability*, eds Stocks, G. M. and Gonis, A. (NATO ASI series E *Appl. Sci.*, **163,** Kluwer, Dordrecht), p. 321.
Gazzara, C. P., Middleton, R. M. and Weiss, R. J. (1964) *Phys. Lett.*, **10,** 257.
Gonis, A., Zhang, X. G, Freeman, A. J., Turchi, P. E. A., Stocks, G. M. and Nicholson (1987) *Phys. Rev. B*, **36,** 4630.

Goodwin, L., Skinner, A. J. and Pettifor, D. G. (1989) *Europhys. Lett.*, **9,** 701.
Grimwall, G. (1974) *Sol. State Comm.*, **14,** 551.
Grimwall, G. (1977) *Inst. Phys. Conf. Ser.* No 30.
Grimwall, G. (1997) Ringberg III to be published.
Grimwall, G. and Ebbsjo, I. (1975) *Physica Scripta*, **12,** 168.
Grimwall, G., Thiessen, M. and Fernandez Guillermet, A. (1987) *Phys. Rev. B*, **36,** 7816.
Gschneider, K. A. (1961) *Rare-Earth Alloys* (Van Nostrand, Amsterdam).
Gschneider, K. A. (1964) *Solid State Physics*, **16,** 275.
Gschneider, K. A. (1975) *J. Less Common Metals*, **43,** 179.
Gyorffy, B. L. and Stocks, G. M. (1983) *Phys. Rev. Lett.*, **50,** 374.
Hafner, J. (1987) *From Hamiltonians to Phase Diagrams* (Springer, Berlin).
Hafner, J. (1989) *Cohesion and Structure: Vol. 2*, eds Pettifor, D. G. and de Boer, F. R. (North Holland, Amsterdam).
Hafner, J. (1992) in *Electron Theory in Alloy Design*, eds Pettifor, D. G. and Cotttrell, A. H. (Inst. Materials, London), p. 44.
Haglund, J., Grimwall, G. and Jarlborg, T. (1993) *Phys. Rev. B*, **47,** 9279.
Hasegawa, H. and Pettifor, D. G. (1983) *Phys. Rev. Lett.*, **50,** 130.
Heine, V. and Weaire, D. (1971) *Solid State Physics*, **24,** 247.
Hildebrand, J. H. and Scott, R. L. (1956) *The Solubility of Non-Electrolyes* (Reinhold, New York).
Hilliard, J. (1963) *Trans. A.I.M.E.*, **223,** 429.
Ho, K. M. and Harmon, B. N. (1990) *Mat. Sci. Eng. A*, **127,** 155.
Hume-Rothery, W., Reynolds, P. W. and Raynor, G. V. (1940) *J. Inst. Metals*, **66,** 191.
Inden, G. (1975) *Z. Metallkunde*, **66,** 577.
Jansen, J. F. and Freeman, A. J. (1984) *Phys. Rev.*, **B30,** 561.
Johannson, C. H. (1937) *Arch. Eisenhuttenw.*, **11,** 241.
Kaufman, L. (1959a) *Acta. Met.*, **7,** 575.
Kaufman, L. (1959b) *Bull. Amer. Phys. Soc.*, **4,** 181.
Kaufman, L. (1967) in *Phase Stability of Metals and Alloys*, eds Rudman, P. S. *et al.* (McGraw-Hill, New York), p. 125.
Kaufman, L. (1972) in *Metallurgical Thermochemistry* (NPL-HMSO, London), p. 373.
Kaufman, L. (1974) in *Materials under Pressure*, Honda Memorial Series on Materials Science No. 2 (Maruzen, Tokyo), p. 66.
Kaufman, L. (1986) in *Computer Modelling of Phase Diagrams*, ed. Bennett, L. H. (Met. Soc. AIME, Warrendale, PA), p. 237.
Kaufman, L. (1991) *Scand. J. Met.*, **20,** 32.
Kaufman, L. (1993) *CALPHAD*, **17,** 354.
Kaufman, L. and Bernstein, H. (1970) *Computer Calculations of Phase Diagrams* (Academic Press, New York).
Kaufman, L. and Cohen, M. (1956) *Trans. AIME*, **206,** 1393.
Kaufman, L. and Cohen, M. (1958) *Progr. Metal Physics*, **7**(3), 165.
Kaufman, L. and Nesor, H. (1973) *Z. Metallkde.*, **64,** 249.
Kaufman, L., Clougherty, E. V. and Weiss, R. J. (1963) *Acta. Met.*, **11,** 323.
Klement, W. and Jayaraman, A. (1966) *Progress in Solid State Chemistry*, **3,** 289.
Kmetko, E. A. and Hill, H. H. (1976) *J. Phys. F*, **6,** 1025.
Kouvetakis, J. and Brewer, L. (1993) *J. Phase Equilibria*, **14,** 563.

Chapter 8
The Role of Magnetic Gibbs Energy

8.1. INTRODUCTION

In paramagnetic materials there is no polarisation of electron spins and therefore it is unnecessary to consider a magnetic contribution to the Gibbs energy if this condition is taken to be the standard state. However in ferromagnetic, anti-ferromagnetic and ferri-magnetic materials, there is also competition between different spin arrangements and the enthalpy of certain transition metals, rare earths and their associated alloys and compounds are lowered by specific forms of spin polarisation. This includes the technologically important elements Fe, Ni and Co and their alloys and the effect can be of sufficient magnitude to have a major effect on phase transformation.

There are many different forms of spin polarisation. The *ferromagnetism* exhibited by b.c.c. Fe is probably the best-known variant. Here the coupling between atoms favours parallel spin configurations between nearest neighbours and the critical ordering temperature is known as the Curie temperature (T_c). In other materials the exchange forces favour anti-parallel spins between nearest neighbours. If there is only one species of atoms this is known as *anti-ferromagnetism* and the critical ordering temperature is known as the Neel temperature (T_n). If the anti-parallel coupling involves more than one species of atoms with different values of spin, there will be a net spin in one particular direction. Such a material, e.g., Fe_3O_4, is considered to be *ferri-magnetic* and again behaves like a ferromagnetic with a Curie temperature.

Many other subtle differences can occur, such as periodic changes in the crystallographic direction in which the spins are orientated, but these details are rarely considered in thermodynamic terms. In the treatments which follow, it is sufficient to note that the quantum number $s = +½$ or $-½$ defines the spin-up or spin-down direction for individual electrons, while the magnitude of any magnetic effects depends on the number of electrons that are being polarised. The unit magnetic moment associated with spin ½ is equal to a Bohr magneton (μ_B) and the number of magnetic electrons/atom is defined by the symbol β, so that $\beta = 2s$ (Bozorth 1956).

Unlike chemical ordering, which can only occur in alloys, magnetic ordering can occur in unary systems and the magnetic Gibbs energy turns out to be sufficiently large to cause fundamental changes in structure. For example, the high-temperature

form of solid Fe is δ which has a b.c.c. structure and transforms to γ-Fe with the more close-packed f.c.c. structure at 1394°C. Both of these phases are paramagnetic at these elevated temperatures, but the onset of ferromagnetism in the b.c.c. phase causes this phase to reappear at 912°C as α-Fe. This makes Fe a unique element in that the high-temperature allotrope reappears at low temperatures, and it should be noted that the thermodynamic effect due to short-range magnetic order is already sufficient to cause the re-appearance of the b.c.c. form; α-Fe only becomes ferromagnetic below its Curie temperature at 770°C. At 0 K the magnetic enthalpy ($\approx$9000 J mol^{-1}) is an order of magnitude larger than was involved in the $\delta-\gamma$ high temperature transformation ($\approx$900 J mol^{-1}).

The change in Gibbs energy with temperature of Fe, with respect to the paramagnetic form δ-Fe, is shown in Fig. 8.1(a). This can be correlated directly with the value of the magnetic specific heat (Fig. 8.1(b)) (Nishizawa *et al.*. 1979), which in turn is related to a corresponding change in the saturation magnetisation, β, (Fig. 8.1(c)) (Nishizawa 1978). The critical magnetic ordering temperature, the Curie temperature (T_c), is defined either by the peak in C_p^{mag} or by the maximum rate of change in the variation of β with T. The situation is made more complex on alloying as both T_c and β vary with composition.

It has already been mentioned in the previous chapter that the Ising model, which underlies the formalism used for most chemical ordering treatments, was originally used to describe magnetic transitions. It is, however, technically only valid if the various magnetic states correspond to multiples of the unit magnetic spin, s. Early attempts to describe the associated thermodynamic functions within formal ordering theory were by Saito *et al.* (1959), Arita (1978) and Moran-Lopez and Falicov (1979). More recent examples of the combination of chemical and magnetic ordering, as applied to b.c.c. Fe-base alloys, have been given by Inden and Pitsch (1991) and Kosakai and Miyazaki (1994). The BWG treatment appears to be a reasonable assumption in such systems because the saturation magnetisation of Fe (2.2 μ_B) is close to the integral value $\beta = 2$ which is equivalent to $s = 1$. However, the concentration dependence of the saturation magnetisation, and the important role played by magnetic short-range order, makes it difficult to use such a treatment in the general case and it has been necessary to devise alternative methodologies to describe the magnetic Gibbs energy of alloy systems.

8.1.1 Polynomial representation of magnetic Gibbs energy

While acknowledging that the 'Gibbs energy anomaly' was associated with magnetism, early attempts to characterise the behaviour of Fe, did not derive G^{mag} explicitly from ferromagnetic parameters such as β. Instead, G^{mag} was derived either by the direct graphical integration of C_p^{mag} or simply incorporated into the overall Gibbs energy difference between the γ- and α-phases in Fe by means of a global polynomial expression such as used by Kaufman and Nesor (1973)

References are listed on pp. 256–258.

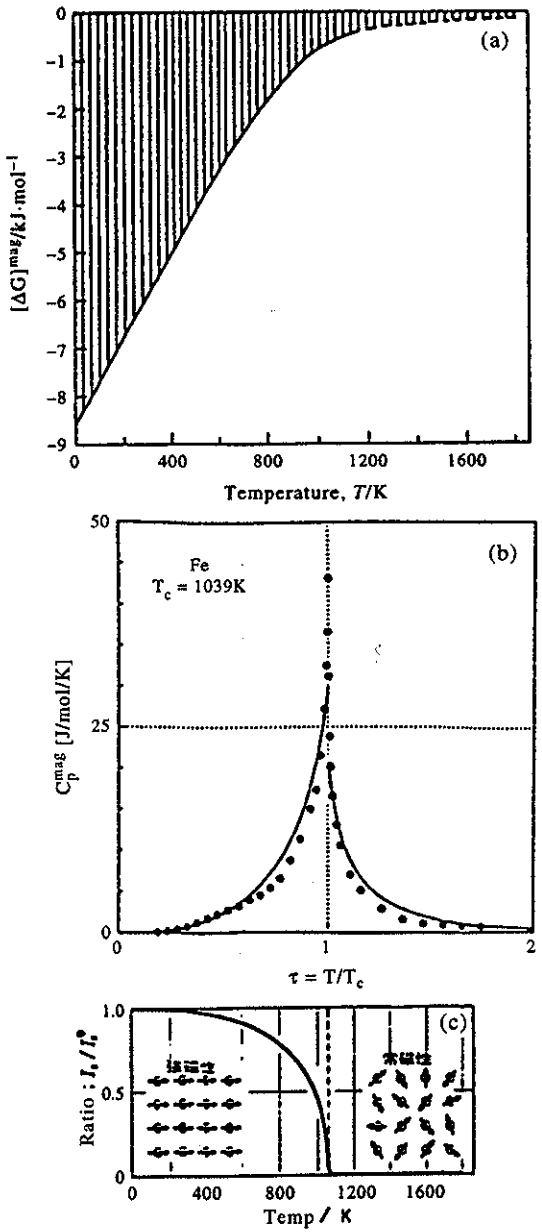

Figure 8.1. Correlation between (a) magnetic Gibbs energy, (b) magnetic specific heat (from Nishizawa 1992) and (c) change of saturation magnetisation for pure Fe (from Nishizawa 1978).

$$300 < T < 1100K \qquad G^{\gamma\to\alpha} = 6109 - 3.462T - 0.747217 \times 10^{-2}T^2 + 0.5125 \times 10^{-5}T^3. \tag{8.1}$$

Different temperature regions then required different sets of coefficients and, in specific systems, the coefficients had to be modified when used to describe the low-temperature martensitic transformation (Kaufman and Cohen 1956). It soon became evident that it was preferable to work with functions that properly reflected the physical origin of the extra Gibbs energy. This was also important when moving from pure Fe to increasingly complex steels, as specific heat measurements are not often as generally available as measurements of β or T_c.

8.1.2 Consideration of the best reference state

The first step is to consider the methods which can be used to represent the change of magnetisation with temperature, and how this can be translated into the corresponding change of G^{mag}. By analogy with configurational ordering, it would be reasonable to choose the ground state at 0 K as the fundamental reference point. This view was taken by Zener (1955) who may be considered the first author to try and obtain an explicit description of G^{mag}. However, many important phase changes are associated with the high-temperature behaviour, especially the region where short-range magnetic order is present. Starting at 0 K therefore presents certain problems. Firstly, an accurate representation of the temperature dependence of the magnetic parameters is required, and this can be highly non-linear. Secondly, anomalies can arise if there is a rapid variation of the magnetic ordering temperature with composition (Inden 1991). This is particularly true if T_c reaches zero in the middle of a system. Finally, it is necessary to devise a system which can take care of mixtures of magnetic and non-magnetic components.

In contrast to most treatments of configurational ordering, the high-temperature paramagnetic state has therefore been adopted as the best reference state. Objections to using this state on the grounds that it cannot be retained below T_c are unwarranted, as the situation can be considered analogous to using the liquid phase as a reference state at high temperatures.

8.1.3 Magnitude of the short-range magnetic order component

The magnetic specific heat shows a marked degree of short-range magnetic order above T_c which decreases asymptotically to zero when $T >> T_c$. Figure 8.2 illustrates how the equivalent values for Ni are obtained by careful subtraction of other components from the total specific heat (Hofmann *et al.* 1956). The importance of standardising this procedure has been emphasised by de Fontaine *et al.* (1995). The fraction (ϕ) of the total magnetic enthalpy retained above T_c is clearly always an important quantity and, by analysing experimental results, Inden (1976) obtained a

References are listed on pp. 256–258.

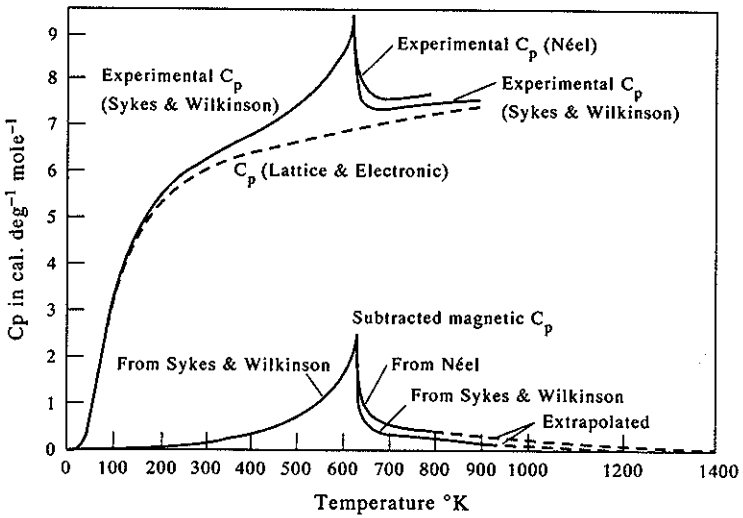

Figure 8.2. Extraction of magnetic specific heat from the total specific heat for pure Ni (from Hoffman *et al.* 1956).

value of $\phi = 0.27$ for both f.c.c. Ni and Co while the larger value of $\phi = 0.43$ was found for b.c.c. Fe. These values were subsequently assumed equally valid for all other f.c.c. and b.c.c. phases (Hillert and Jarl 1978, Inden 1981a). While this is a reasonable assumption for steels, it may not hold for atoms with larger magnetic moments (de Fontaine *et al.* 1995). This has been confirmed by a CVM treatment applied to Gd (Schon and Inden 1996). In order to incorporate this result into a semi-empirical treatment suitable for multi-component systems it may be worthwhile to revert to an earlier suggestion (Paskin 1957) that ϕ is a function of s and the nearest-neighbour co-ordination number, (z),

$$\phi = \frac{s+1}{s(z-1)}. \tag{8.2}$$

8.2. DERIVATION OF THE MAGNETIC ENTROPY

While it is important to partition the long-range and short-range magnetic components correctly, the maximum entropy contribution due to magnetism, S^{mag}_{max}, is an equally crucial factor.

8.2.1 Theoretical value for the maximum magnetic entropy

Despite the intrinsic complexity of magnetic phenomena, there is general agreement

$$300 < T < 1100\text{K} \qquad G^{\text{mag}} = 0.109 - 3.4021 \times 10^{-2}T + 0.74721 \times 10^{-5}T^2 + 0.5125 \times 10^{-5}T^3. \qquad (8.1)$$

Different temperature regions then required different sets of coefficients and, in specific systems, the coefficients had to be modified when used to describe the low-temperature martensitic transformation (Kaufman and Cohen 1956). It soon became evident that it was preferable to work with functions that properly reflected the physical origin of the extra Gibbs energy. This was also important when moving from pure Fe to increasingly complex steels, as specific heat measurements are not often as generally available as measurements of β or T_c.

8.1.2 Consideration of the best reference state

The first step is to consider the methods which can be used to represent the change of magnetisation with temperature, and how this can be translated into the corresponding change of G^{mag}. By analogy with configurational ordering, it would be reasonable to choose the ground state at 0 K as the fundamental reference point. This view was taken by Zener (1955) who may be considered the first author to try and obtain an explicit description of G^{mag}. However, many important phase changes are associated with the high-temperature behaviour, especially the region where short-range magnetic order is present. Starting at 0 K therefore presents certain problems. Firstly, an accurate representation of the temperature dependence of the magnetic parameters is required, and this can be highly non-linear. Secondly, anomalies can arise if there is a rapid variation of the magnetic ordering temperature with composition (Inden 1991). This is particularly true if T_c reaches zero in the middle of a system. Finally, it is necessary to devise a system which can take care of mixtures of magnetic and non-magnetic components.

In contrast to most treatments of configurational ordering, the high-temperature paramagnetic state has therefore been adopted as the best reference state. Objections to using this state on the grounds that it cannot be retained below T_c are unwarranted, as the situation can be considered analogous to using the liquid phase as a reference state at high temperatures.

8.1.3 Magnitude of the short-range magnetic order component

The magnetic specific heat shows a marked degree of short-range magnetic order above T_c which decreases asymptotically to zero when $T >> T_c$. Figure 8.2 illustrates how the equivalent values for Ni are obtained by careful subtraction of other components from the total specific heat (Hofmann *et al.* 1956). The importance of standardising this procedure has been emphasised by de Fontaine *et al.* (1995). The fraction (ϕ) of the total magnetic enthalpy retained above T_c is clearly always an important quantity and, by analysing experimental results, Inden (1976) obtained a

References are listed on pp. 256–258.

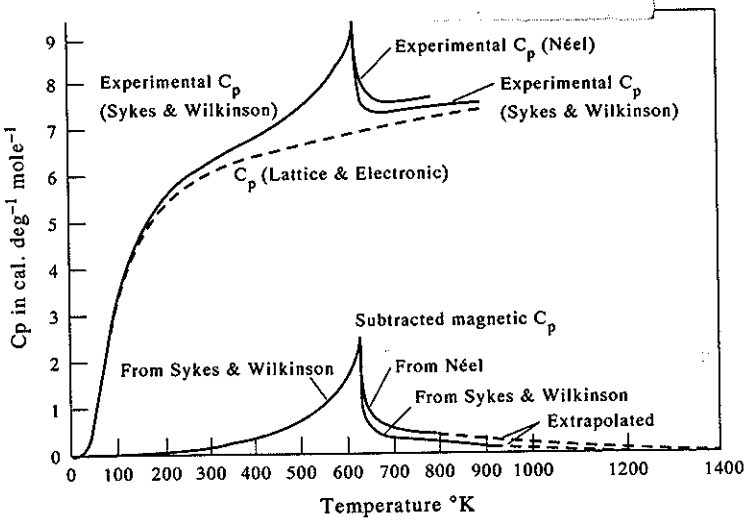

Figure 8.2. Extraction of magnetic specific heat from the total specific heat for pure Ni (from Hoffman *et al.* 1956).

value of $\phi = 0.27$ for both f.c.c. Ni and Co while the larger value of $\phi = 0.43$ was found for b.c.c. Fe. These values were subsequently assumed equally valid for all other f.c.c. and b.c.c. phases (Hillert and Jarl 1978, Inden 1981a). While this is a reasonable assumption for steels, it may not hold for atoms with larger magnetic moments (de Fontaine *et al.* 1995). This has been confirmed by a CVM treatment applied to Gd (Schon and Inden 1996). In order to incorporate this result into a semi-empirical treatment suitable for multi-component systems it may be worthwhile to revert to an earlier suggestion (Paskin 1957) that ϕ is a function of s and the nearest-neighbour co-ordination number, (z),

$$\phi = \frac{s+1}{s(z-1)}. \qquad (8.2)$$

8.2. DERIVATION OF THE MAGNETIC ENTROPY

While it is important to partition the long-range and short-range magnetic components correctly, the maximum entropy contribution due to magnetism, $S^{\text{mag}}_{\text{max}}$, is an equally crucial factor.

8.2.1 Theoretical value for the maximum magnetic entropy

Despite the intrinsic complexity of magnetic phenomena, there is general agreement

that the maximum entropy generated by the de-coupling of spins between atoms can be expressed by:

$$S_{\max}^{\text{mag}} = R\log_e(2s+1). \tag{8.3}$$

Technically, the values of s are theoretically restricted to integral multiples of s and one should consider the sum of each contributing species, but these values are not always available.

8.2.2 Empirical value for the maximum magnetic entropy

The saturation magnetisation β, in μ_B per atom, of many materials often corresponds to non-integral values of s. This is due to contributions other than s being involved, for example polarised conduction electrons. It is, therefore, general practice to substitute the experimental value of the saturation magnetisation at 0 K, β_0, for $2s$ in Eq. (8.3) which leads to (Miodownik 1977)

$$S_{\max}^{\text{mag}} = R\log_e(\beta_0+1). \tag{8.4}$$

8.2.3 Explicit variation in entropy with magnetic spin number and temperature

The magnetic entropy may be rigorously specified if the BWG mean-field approximation is combined with specific values of the magnetic spin. The expression for the magnetic entropy corresponding to $s = \frac{1}{2}$, as a function of the degree of order η, is identical to that already given in Eq. (7.2) of the previous chapter on configurational ordering

$$S_{\text{BWG}}^{\text{mag}} = -Nk_B\left[\left(\frac{1+\eta}{2}\right)\log_e\left(\frac{1+\eta}{2}\right)+\left(\frac{1-\eta}{2}\right)\log_e\left(\frac{1-\eta}{2}\right)\right]. \tag{8.5}$$

However, the permutation of permissible spins rapidly becomes more complicated with higher values of s. The equivalent expression for $s = 1$, as derived by Semenovskaya (1974) and used by Inden (1975, 1981), is given by

$$\begin{aligned} S_{\text{BWG}}^{\text{mag},s=1} = &- Nk_B\Big[\log_e(8-6\eta+2\sqrt{4-3\eta^2}) - (1-\eta)\log_e(2(1-\eta)) \\ &- (1+\eta)\log_e(\eta+\sqrt{4-3\eta^2})\Big]. \end{aligned} \tag{8.6}$$

Expressions corresponding to $s = 3.2$ and $s = 2$ are listed in Inden (1981).

8.3. DERIVATION OF MAGNETIC ENTHALPY, H^{MAG}

8.3.1 Classical derivation

The simplest case is to start with a situation where all the atoms have the same spin.

References are listed on pp. 256–258.

The general expression for the BWG (mean field) approximation then gives

$$H^{\text{mag}} = \frac{N}{2}\sum_k z^{(k)}J^{(k)}\eta^2 s^2. \tag{8.7}$$

This allows for a summation for magnetic interactions in successive (k-th) neighbouring shells but, unless J values can be derived from first-principles calculations, there is generally insufficient experimental data to allow anything other than a single nearest-neighbour interaction parameter to be used. This, then, must be taken to incorporate any other longer-range effects, and application to real alloy systems is also technically restricted by having to use multiples of $s = 1/2$. Much therefore depends on whether this realistically simulates experimental values of β, which fortunately seem to be the case in Fe-rich, Co-rich and Ni-rich alloys. However, this is less secure at higher solute concentrations, especially if there are transitions between different forms of magnetism in the system (see Fig. 8.4).

An equation which includes the effect of adding a magnetic term to the enthalpy of an ordered system has already been given in Section 7.3.2.3 of Chapter 7, but no details were given of how to determine the value of the magnetic interaction energy $M_{A,B}^{(1)}$. For a binary alloy $A_{1-x}B_x$ this involves the introduction of three magnetic interaction parameters $J_{AA}^{(1)}$, $J_{BB}^{(1)}$ and $J_{AB}^{(1)}$ which describe the strength of the coupling between nearest-neighbour atoms whose (magnetic) electrons have parallel spins as compared to anti-parallel spins. The magnetic interchange energy $M_{AB}^{(1)}$ is then obtained by combining these parameters to yield

$$M_{AB}^{(1)} = J_{AA}^{(1)} + J_{BB}^{(1)} - 2J_{AB}^{(1)}. \tag{8.8}$$

This is entirely analogous to the treatment of the chemical interaction energies V_{ij} treated in Chapter 7. Negative values of $J_{i,j}$ correspond to ferromagnetism while positive values correspond to anti-ferromagnetism. Positive values of $M_{i,j}$ imply that the strength of the ferro-magnetic coupling between unlike atoms is stronger than between like atoms. Most treatments do not consider magnetic interactions beyond the nearest-neighbour coordination shell.

The most convenient way of determining the interchange energies is from experimental values of the critical ordering temperature, which is designated the Curie temperature for ferromagnetic ordering The Curie temperature for alloys with two magnetic components having the same spin (1/2 or 1) can be written as follows:

$$\begin{aligned} T_c = \mu T_c^{\text{BWG}} = \\ \left\{\frac{-8K_s}{\alpha(1-x)+\beta x}\left[(1-x)\frac{J_{AA}^{(1)}}{k}+x\frac{J_{BB}^{(1)}}{k}-x(1-x)\frac{M_{A,B}^{(1)}}{k}-\eta^2\frac{M_{A,B}^{(1)}}{k}\right]\right\}. \end{aligned} \tag{8.9}$$

In this equation, μ is the magnetic analogue to the χ factor used in the chemical ordering case to compensate for the higher critical temperatures always generated by the BWG formalism (see Chapter 7). Comparing the results from the BWG treatment with those of other more sophisticated treatments leads to a value of $\mu = 0.8$ (Inden 1975) and the long-range ordering parameter η takes values between 0 and 1 as in the case of chemical ordering. In the magnetic case η equals the ratio of the mean spin value per atom at temperature T to the maximum value of s (at 0 K). K_s is a parameter which varies with the magnitude of the magnetic spin s such that $K_s = 1$ for $s = 1/2$ and $K_s = 2/3$ for $s = 1$. The coefficients α and β can be set either to 0 or 1 to cover various combinations of magnetic and non-magnetic components.

8.3.2 *Empirical derivation*

Given that S_{max}^{mag} can be described using Eq. (8.4), it may be asked whether a corresponding value for H_{max}^{mag} can be obtained by combining S_{max}^{mag} with T_c. If magnetic ordering was a first-order transformation with a critical temperature, T^*, it would then follow that (Fig. 8.3).

$$H_{max}^{mag} = T^* S_{max}^{mag}. \tag{8.10}$$

However, since magnetic ordering is a second-order transformation, this has to be

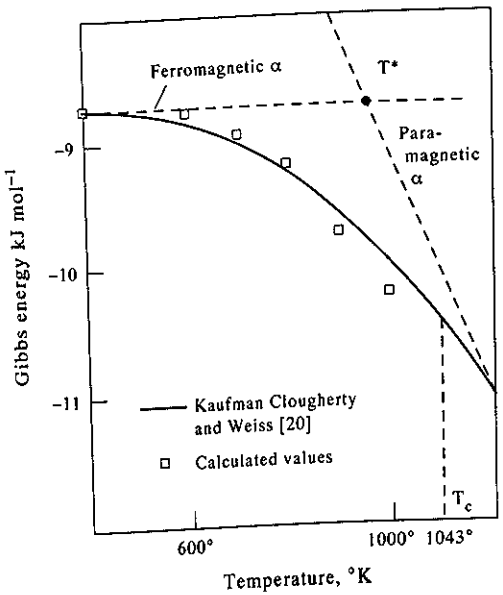

Figure 8.3. Relation of an effective first-order transformation temperature (T^*) to the real second-order Curie temperature (T_c) (from Miodownik 1977).

References are listed on pp. 256–258.

modified to take into account the proportion of short- and long-range order on either side of T_c (see Section 8.1.3). Miodownik (1977) assumed that $T^* \approx 0.9T_c$ for Fe, Co, Ni and their alloys. It then follows that

$$H_{max}^{mag} = 0.9T_c \log_e(\beta_0 + 1). \tag{8.11}$$

Weiss and Tauer (1958) made the alternative assumption that

$$H_{max}^{mag} \approx RT_c s^{1/3}. \tag{8.12}$$

Such equations have the advantage of simplicity but comparison with Eq. (8.2) implies that ϕ is totally independent of s and z. Whichever expression is used, the next step is to incorporate the effect of temperature on the alignment of the magnetic spins. In view of the other simplifications which have already been adopted, this can be achieved (Miodownik 1977, 1978a) by approximating the Brillouin–Langevin formalism for the number of aligned spins (β^T) remaining at $T < 0.9T_c$ through the following expression:

$$\beta^T = \beta_0[1 - \tau^6] \tag{8.13}$$

where τ defines the ratio (T/T_c). Assuming that the magnetic enthalpy scales as (β^T/β_0) this can then be combined with an arbitrary power function to account for short-range magnetic order for $T > 0.9T_c$)

$$\beta^T = \beta_0(1/2)^{[2+10(\tau-1)]}. \tag{8.14}$$

Equation (8.14) leads to a value for $\phi = 0.25$ at T_c, which is of comparable magnitude to the values assumed by Inden (1981a), although it clearly does not include any dependence on the co-ordination number z.

8.4. DERIVATION OF MAGNETIC GIBBS ENERGY

Even if magnetic interaction energies are available to define a magnetic enthalpy, the development of a viable Gibbs energy expression is difficult. As already noted in the preceding section, the expressions for the magnetic entropy in a BWG treatment become increasingly complicated when $s > 1/2$ and, indeed, may become inexact if the distribution of individual spins is not known. In practice their application also requires a series of nested Gibbs energy minimisation calculations which become costly in computing time. Also, of course, the BWG approximation does not take into account any short-range order except through empirical corrections.

Despite these drawbacks remarkably good results have been obtained in the equiatomic region of the Fe-Co system (Inden 1977) which are virtually indistinguishable from those obtained by CVM calculations (Colinet 1993). However, this

region deals only with A2/B2 equilibria where the BWG method is known to work well. It is otherwise inadequate to deal with f.c.c.–b.c.c. equilibria, notably in pure Fe or Fe-rich alloys, because of the very small differences in the free energies of the f.c.c. and b.c.c. allotropes. In such cases it is vitally important to include short-range magnetic order and find alternative means of defining the magnetic Gibbs energy.

8.4.1 General algorithms for the magnetic Gibbs energy

With expressions for the magnetic enthalpy and entropy it is now possible to build up an algorithm for G^{mag} at any temperature. The maximum magnetic entropy is taken as

$$S^{\text{mag}}_{\text{max}} = S^{\text{para}}_{T=\infty} - S^{\text{ferro}}_{T=0}. \tag{8.15}$$

In an analogous way the maximum magnetic enthalpy is

$$H^{\text{mag}}_{\text{max}} = H^{\text{para}}_{T=\infty} - H^{\text{ferro}}_{T=0}. \tag{8.16}$$

The magnetic entropy and enthalpy at a given temperature, S^{mag}_T and H^{mag}_T, respectively, are

$$S^{\text{mag}}_T, H^{\text{mag}}_T = f(T, T_c, \beta) \tag{8.17}$$

while the magnetic Gibbs energy G^{mag}_T at a given temperature is given by

$$G^{\text{mag}}_T = G^{\text{ferro}}_T - G^{\text{para}}_T. \tag{8.18}$$

8.4.2 Magnetic Gibbs energy as a direct function of β and T_c

Combining the expressions for magnetic entropy and enthalpy and assuming that the magnetic enthalpy scales as β^T/β_0

$$G^{\text{mag}}_T = -0.9RT_c \log_e(\beta_0 + 1)(\beta^T/\beta_0) - RT \log_e(\beta_0 - \beta^T + 1). \tag{8.19}$$

Here the first term represents H^{mag}_T and the second term the effect of S^{mag}_T. Eq. (8.19) represents one of the many empirical ways in which Eq. (8.18) can be made to work in practice (Miodownik 1977). However, this expression does not lend itself easily to a derivation of the associated value of C_p nor to an explicit formulation of $\delta\Delta G^{\text{mag}}/\delta T$. Therefore, most alternative expressions have been based on approximate analytical expressions for the magnetic specific heat. However, all such expressions also incorporate the functions $\log_e(\beta + 1)$ and τ and are a far cry from the original methods of graphical integration.

8.4.3 Magnetic Gibbs energy as a function of C_p^{mag} for ferromagnetic systems

8.4.3.1 The model of Inden. This approach was pioneered by Inden (1976) who developed the following empirical equations:

References are listed on pp. 256–258.

for $\tau < 1$ $$C_p^{\text{mag}} = K^{lro} R \log_e(1 + \tau^3)/\log_e(1 - \tau^3) \tag{8.20a}$$

for $\tau > 1$ $$C_p^{\text{mag}} = K^{sro} R \log_e(1 + \tau^5)/\log_e(1 - \tau^5) \tag{8.20b}$$

where K^{lro} and K^{sro} are empirically derived coefficients. At first sight these equations appear to differ substantially from Eq. (8.19), but the values of K^{lro} and K^{sro} are constrained by the need to correctly reproduce both the total entropy and take into account experimental values of ϕ. Since the total entropy is an explicit function of β, the net result is that this treatment also has a mixed dependence on the two key magnetic parameters β and T_c. Further, a relationship between K^{sro} and K^{lro} can be obtained by considering H_{mag}:

$$K^{sro} = 518/675(K^{lro} + 0.6K^{sro}) = \log_e(\beta + 1) \tag{8.21}$$

$$K^{lro} = 474/497[(1 - \phi)/\phi]K^{sro}. \tag{8.22}$$

A dependence on crystallographic parameters is introduced through making ϕ a function of z, as already indicated in Section 8.1.3. Introducing fixed values of ϕ appropriate to each crystal structure is a useful simplification as it is then possible to uniquely define the values of K^{lro} and K^{sro} (de Fontaine *et al.* 1995).

8.4.3.2 Model of Hillert and Jarl. In his original treatment, Inden (1976) used a complicated but closed expression for the enthalpy, but had to use a series expansion in order to calculate the entropy. Hillert and Jarl (1978) therefore decided to convert the C_p expression directly through a series expansion which substantially simplifies the overall calculation and leads to a maximum error of only 1–2 J/mol at the Curie temperature of Fe. The equivalent equations to those used by Inden (1976) are given by

for $\tau < 1$ $$C_p^{\text{mag}} = 2K^{lro} R(\tau^m + \tfrac{1}{3}\tau^{3m} + \tfrac{1}{5}\tau^{5m}) \tag{8.23a}$$

for $\tau > 1$ $$C_p^{\text{mag}} = 2K^{sro} R(\tau^{-n} + \tfrac{1}{3}\tau^{-3n} + \tfrac{1}{5}\tau^{-5n}). \tag{8.23b}$$

8.4.3.3 Alternative C_p models. Chuang *et al.* (1985) have developed alternative exponential functions to describe the C_p curves and applied this to various Fe-base alloys (Chuang *et al.* 1986)

for $\tau < 1$ $$C_p = K' R\tau \exp(-p(1 - \tau)) \tag{8.24a}$$

for $\tau > 1$ $$C_p = K'' R\tau \exp(-q(1 - \tau)). \tag{8.24b}$$

These equations have the advantage of greater mathematical simplicity, but it is still necessary to evaluate the constants K', K'', p and q.

8.4.3.4 Comparison of models for the ferromagnetic Gibbs energy. It is difficult to compare the various treatments described in Sections 8.4.3.1 to 8.4.3.3, because simultaneous changes were made in both the models and input parameters during their formulation. This is a perennial problem if different weightings are attached to magnetic and thermodynamic data (de Fontaine *et al.* 1995). The suggestion by Inden (1976) that values for m and n in Eqs (18.18a) and (18.18b) should be taken as 3 and 5 respectively has been preserved by Hillert and Jarl (1978). This is still the core assumption as far as $3d$ elements are concerned in current models. However, it may be necessary to relax this assumption in systems with larger magnetic spin numbers (de Fontaine *et al.* 1995)

8.4.4 Anti-ferromagnetic and ferri-magnetic systems

Providing there is no change in value of β_0 with temperature, Eq. (8.4) can also be used to determine the maximum magnetic entropy in anti-ferromagnetic and ferri-magnetic materials (Miodownik 1978a, Smith 1967, Hofmann *et al.* 1956). A comparison of predicted and experimental magnetic entropies and energies (Table 8.1) indicates that this is a reasonable assumption in most cases. If serious discrepancies remain between theoretical expectations and experimental results, it may be necessary to consider the existence of multiple magnetic states (see Section 8.7).

8.5. THE EFFECT OF ALLOYING ELEMENTS

The treatment of compounds and other end-members of fixed composition does not differ from that of the elements, but the next vital step is to consider the representation of these parameters for solid solutions.

Table 8.1. A comparison of predicted and experimental magnetic entropies and enthalpies.

Element	Exp. S^{mag}_{max} (J/mol/K)	Calc. (Eq. (8.4)) (J/mol/K)	Exp. H^{mag}_{max} (J/mol)	Calc. (Eq. (8.11)) (J/mol)
Ni	3.39	3.47	1757	1987
Fe	8.99	9.20	8075	8556
Gd	17.74	17.41	3372	4602
Dy	23.09	23.05	—	—
Ho	23.56	23.56	—	—
MnO_2	10.87	11.51	816	900
NiF_2	9.46	9.12	590	657
Cr_2O_3	22.72	23.22	5314	6255

References are listed on pp. 256–258.

8.5.1 Effect of changes in T_c and β with composition

The earliest derivation of G^{mag}_T was made by Zener (1955) who postulated that the effect of an alloying element was proportional to its effect on T_c. With the assumption that $\delta Tc/\delta x$ is a constant, it is then possible to write:

$$G^{mag}_{alloy}(T) = G^{mag}_{Fe}(T) - x\left(\frac{\delta T}{\delta x}\right) S^{mag}_{Fe} \tag{8.25}$$

where $T = T_c - x(\delta T/\delta x)$. The Zener method therefore depends totally on the assumption of a linear variation of $\delta T_c/\delta x$ and any associated changes in β are reflected in the change of T_c. It can, nevertheless, give reasonable results for dilute solutions and was extensively used by Hillert *et al.* (1967) in the period before the Inden formulation was more generally adopted in Europe. It, however, remained popular in Japan for the characterisation of Fe alloys, which was its original field of application (Nishizawa *et al.* 1979, Hasebe *et al.* 1985).

Zener's method does not explicitly take into account the effect of changes in β with composition but implicitly assumes that any changes in β are reflected in the changes in T_c. Clougherty and Kaufman (1963) considered how changes in β with composition might affect the terminal magnetic entropy of f.c.c. Ni–Zn alloys, but this did not lead to a generalised approach which was applicable across the whole system. Miodownik (1977) showed that values of T_c and β for alloys could be introduced into the same algorithm developed for the elements, but this was superseded by the advent of the Hillert–Jarl formalism. With the need to handle multi-component calculations it was then a natural step to develop (separate) Redlich–Kister polynomials for the variation of β and T_c with composition (Chin *et al.* 1987).

8.5.2 Systems whose end-members exhibit different forms of magnetism

8.5.2.1 Ferromagnetic to anti-ferromagnetic transition. When end-members exhibit different forms of magnetism there are often significant deviations from linearity in both T_c and β and these parameters may become zero in the middle of the system. One example is associated with a change from ferromagnetic to anti-ferromagnetic behaviour which occurs in a number of industrially important systems, such as Fe–Ni (Fig. 8.4(a)) and the related ternary system Fe–Ni–Mn (Fig. 8.4(b)). b.c.c. Fe–Cr, rare-earth and oxide systems can also exhibit similar complexity. In such situations special measures need to be taken to allow a Redlich–Kister-type polynomial to be used to describe T_c and β. Since ferromagnetism and anti-ferromagnetism are associated with values for $J_{i,j}$ of opposite sign, Weiss and Tauer (1956) suggested that a continuous change between these two forms of magnetic ordering could best be described by attaching a negative sign to Neel temperatures. These authors also suggested a semi-empirical

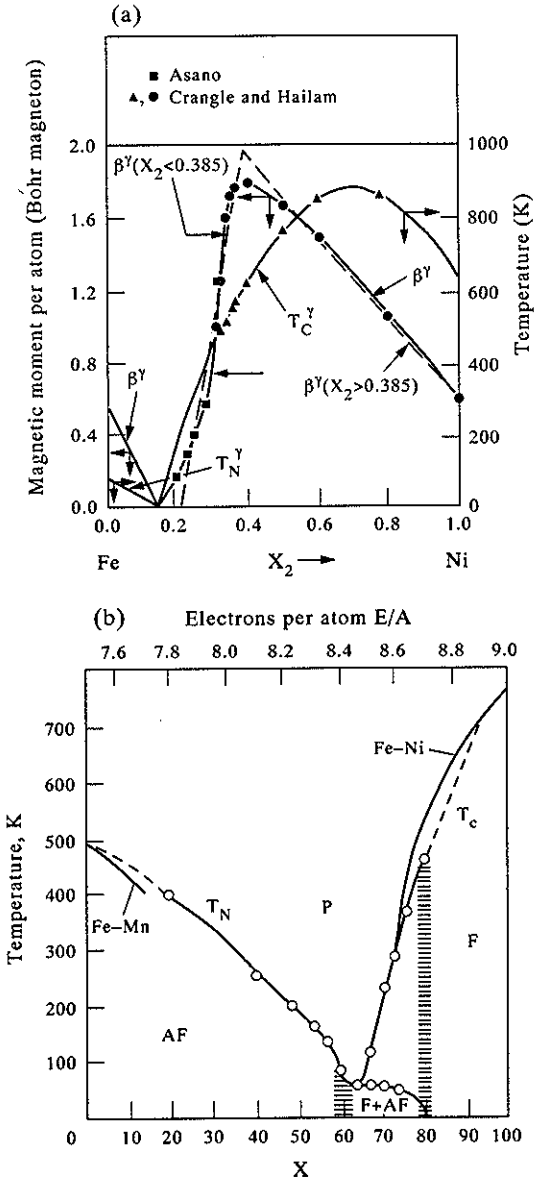

Figure 8.4. Variation of magnetic parameters T and β with composition in (a) Fe–Ni (from Chuang *et al.* 1986), (b) Fe–Ni–Mn alloys (from Ettwig and Pepperhoff 1974).

References are listed on pp. 256–258.

relation between T_{crit} and β which is useful if one or other of these parameters is not experimentally available.

$$T_{crit} = 113.5(Z\uparrow - Z\downarrow)\ln(\beta + 1). \tag{8.26}$$

Here the two parameters, $Z\uparrow$ and $Z\downarrow$, refer to the relative number of spins of opposite sign, which allows this equation to be used for both ferromagnetic and anti-ferromagnetic materials. One implication of Eq. (8.26) is that, for a given value of β and type of magnetism, the critical temperature is expected to be higher for f.c.c. materials than for b.c.c. materials, which accounts for the observation that $T_c^{Co} > T_c^{Fe}$ although $\beta^{Co} < \beta^{Fe}$. There are, however, problems when applying this simple empirical equation to anti-ferromagnetic BCC materials such as Cr and to structures with lower symmetry.

A more important conclusion of Eq. (8.26) is that, for a given value of β in an f.c.c. lattice, the value of T_n derived for an anti-ferromagnetic alloy will be 1/3 of the equivalent value of T_c in the ferromagnetic case. The utility of this approach has been verified by Chin *et al.* (1987) who, in order to optimise parameters for their Redlich–Kister polynomials for the critical temperatures of various binary alloy systems, converted positive values of T_n to negative values of T_c and were able to reproduce the critical temperature variation arising from the ferromagnetic/anti-ferromagnetic transition. These authors also used the same convention to differentiate ferromagnetic and anti-ferromagnetic values of β when adapting the Hillert–Jarl formalism into Thermo-Calc, although this must be considered purely as a mathematical convenience and has no theoretical justification.

Another simplification that has been made with respect to the implementation of magnetic algorithms into software packages, such as Thermo-Calc, relates to the composition at which T_c and β reach zero. One might expect that this would happen at one particular composition but Figs. 8.4(a) and (b) show that the situation may be much more complicated. In order to be consistent with a simplified magnetic model Chin *et al.* (1987) chose a set of parameters which effectively smoothed out the differences in the two critical compositions for binary alloys. This however precludes a proper prediction of regions of mixed magnetism, which is important in Invar alloys (Miodownik 1978b) as well as making it impossible to reproduce effects such as shown in Figs. 8.4(a) and (b).

8.5.2.2 Ferromagnetic–paramagnetic transition. In other cases, a zero T_c may be associated with the transition between ferromagnetism and paramagnetism. Even the use of higher-order Redlich–Kister polynomials cannot properly reproduce such a sudden change in slope and some smoothing of the measured variation of T_c and β has to be accepted in the vicinity of 0 K. As both enthalpy and entropy contributions scale approximately with T_c, at low temperatures, this will only lead to small errors on the overall Gibbs energy at such compositions. However, under certain circumstances spurious miscibility gaps have been predicted at high temperatures

in systems that exhibit abrupt changes in T_c with composition (Inden 1981). Care has, therefore, to be taken in deriving the input parameters to the Hillert–Jarl formalism in such cases. The fact remains that such miscibility gaps have never been observed in practice and it may, therefore, be that as T_c approaches zero some other effects, such as itinerant ferromagnetism (Wohlfarth 1974), may occur which essentially smooth out the variation of magnetic entropy. In this instance, the Redlich–Kister formalism may actually be a better approximation to reality than would be indicated by trying to reproduce a T_c or T_n obtained by linear extrapolation of experimental results to 0 K.

8.6. THE ESTIMATION OF MAGNETIC PARAMETERS

8.6.1 Magnetic versus thermochemical approaches to evaluating the magnetic Gibbs energy

In principle, the value of G_T^{mag} should be the same whether it is derived from knowledge of β or from the magnetic specific heat. Since the latter is derived by subtraction of other major terms from the total specific heat, such an agreement is a useful confirmation that the deconvolution process has been properly conducted. However, this is not always achieved. In some studies, e.g., for Cr (Andersson 1985), Co (Fernandez-Guillermet 1987) and Ni (Dinsdale 1991), the listed β values are 'effective thermochemical moments' which have been derived on the basis of a global thermochemical assessment rather than from magnetic measurements. Small differences will always arise when considering ways of averaging data and truncating series, but one should be cautious of a tendency for β to become an adjustable parameter. Such discrepancies will hopefully be reduced in the future by the incorporation of better magnetic models (de Fontaine *et al.* 1995).

8.6.2 Values of the saturation magnetisation, β

It should be emphasised that it is the rule rather than the exception for β to change markedly with crystal structure (Table 8.2). It is therefore unwise to assume that various metastable allotropes can be given the same value of β as for the stable structure. In some cases values of β can be extrapolated from stable or metastable alloys with the requisite crystal structure, but in others this is not possible. A significant development is that it is now possible to include spin polarisation in electron energy calculations (Moruzzi and Marcus 1988, 1990a, b, Asada and Terakura 1995). This allows a calculation of the equilibrium value of β_0 to be made in any desired crystal structure. More importantly, such values are in good accord with known values for equilibrium phases (Table 8.2). It has also been shown that magnetic orbital contributions play a relatively minor role (Eriksson *et al.* 1990), so calculated values of β for metastable phases should be reasonably reliable.

References are listed on pp. 256–258.

Table 8.2. Comparison of SGTE (*) first-principle and experimental magnetic moments for selected elements (adapted from de Fontaine *et al.* 1995)

Element	Source	Ferromagnetic moment (μB)			Anti-ferromagnetic moment (μB)		
		b.c.c.	f.c.c.	c.p.h.	b.c.c.	f.c.c.	c.p.h.
Cr	Chin *et al.* 1987*			0	0.4	0.82	0
Cr	Dinsdale 1991*			0	0.008	0.82	0
Cr	Asada 1993 (FP)	0	0	0	0/0.5	0/3.0	0
Cr	Moruzzi 1990 (FP)	0			0/0.6		
Cr	Weiss 1979				0/0.7		
Cr	Exp (β)				0.4 $f[T]$		
Cr	Exp (C_p)				0.0+		
Mn	Chin *et al.* 1987*						
Mn	Dinsdale 1991*				0.09	0.62	0
Mn	Asada 1993 (FP)	1.0	0/4	2.0	2.76	2.25	0.52
Mn	Moruzzi 1990 (FP)	0.9					
Mn	Weiss 1979		4.5			2.4/0	
Mn	Exp (β)	(1)			(1)	2.3	
Fe	Chin *et al.* 1987*	2.22		0		0.70	0
Fe	Dinsdale 1991*	2.22		0		0.70	0
Fe	Asada 1993 (FP)	2.32	2.56	2.56	1.55	1.21	0
Fe	Moruzzi 1990 (FP)	2.2	2.7		1.75	0.5/0	
Fe	Weiss 1979		2.6			0.40	
Fe	Exp (β)	2.22				0.70	
Fe	Chuang 1985 (C_p)	2.05				0.57	
Fe	Lytton 1964 (C_p)	1.03					
Co	Chin *et al.* 1987*	1.80	1.70	1.70			
Co	Dinsdale 1991*	1.35	1.35	1.35			
Co	Asada 1993 (FP)	1.80	1.70	1.61	1.0	0	1.2
Co	Moruzzi 1990 (FP)	1.70	1.80				
Co	Miodownik 1978	1.70	1.80			0	
Co	Exp (β)	2.00	1.80	1.70			
Co	Chuang 1985 (C_p)			0.89			
Co	Lytton 1964 (C_p)			1.21			
Ni	Chin *et al.* 1987*	0.85	0.62				
Ni	Dinsdale 1991*	0.85	0.52	0.52			
Ni	Asada 1993 (FP)	0.50	0.66	0.60	0	0.1	0.25
Ni	Moruzzi 1990 (FP)	0.30					
Ni	Weiss 1956		0.85				
Ni	Exp (β)		0.62				
Ni	Chuang 1985 (C_p)		0.25				
Ni	Lytton 1964 (C_p)		0.58				
Ni	Meschter 1981 (C_p)	0.53					

In addition to offering a comparison between theoretical and experimental values, Table 8.2 also indicates that there may be a significant difference between the β values that have been independently obtained by the deconvolution of C_p measurements and from magnetic measurements. There is also a significant spread between the β values obtained by using different methods to extract the magnetic

specific heat (Lytton 1964, Meschter *et al.* 1981, Chuang *et al.* 1985). Some of these differences can be rationalised by the occurrence of mixed magnetic states resulting from increasing temperatures, as most of the data in Table 8.2 essentially refers to 0 K. This is almost certainly the case for Cr and Mn (Weiss 1972, 1979, Moruzzi and Marcus 1990a, b). In the case of Co, the c.p.h. form, ε-Co, is a close competitor to the f.c.c. form, α-Co, near the Curie temperature. High stacking-fault densities may therefore also lead to unusual effects (Miodownik 1977). In the case of α-Mn, there is documented evidence for a considerable decrease in β on passing through T_n which could be associated with a transition from an anti-ferromagnetic to a 'non-magnetic state' (Gazzara *et al.* 1964, Weiss 1979). Nevertheless, a single temperature-independent value of β seems a useful starting point in the majority of cases, especially when no other data is available to predict values for metastable elements and solutions. It is noted that β is very sensitive to atomic volume (Moruzzi and Marcus 1990a, b) which is certainly one of the reasons for the non-linearity observed for the variation of β even in simple solid solutions.

8.7. MULTIPLE MAGNETIC STATES

It is not generally appreciated that there are many competing forms of magnetic ordering. When one particular magnetic ground state is substantially more stable than other alternatives, the conventional disordering of magnetic spins, as described in the previous sections, is the only scenario which needs to be considered. However, additional excitations at high temperatures can arise if another magnetic configuration with a comparable ground-state energy exists. Such a hypothesis was used to explain a number of anomalous experimental results in the case of metastable phases in various Fe, Ni and Co alloys and particularly in the case of Invar alloys (Weiss 1963, Chikazumi and Matsui 1978). Together with the switch from ferromagnetic to anti-ferromagnetic behaviour (Fig. 8.4) this makes compelling experimental evidence for the co-existence of two magnetic states in Fe–Ni and Fe–Co alloys (Miodownik 1978b). Weiss (1979) later extended this concept to other 3*d* elements.

8.7.1 Treatments of multiple states

The simplest way to describe the equilibrium between various competing states is to use a Shottky model (Weiss 1963) where

$$\alpha = \frac{f_{\gamma_1}}{f_{\gamma_2}} = \frac{g_2}{g_1} \exp\left(-\Delta E/RT\right). \tag{8.27}$$

Here α is the ratio of the fraction of atoms, f, corresponding to the two magnetic states, γ_1 and γ_2, and g_1 and g_2 are the corresponding degeneracies of the two states. Clearly if ΔE (the difference in energy between the two states) is large and/or the temperature is low, there is effectively only one state and one magnetic moment. However, as ΔE becomes smaller there can be changes in the effective magnetic moment, especially in the case of γ-Fe. Here the two states correspond to a ferromagnetic moment of $\approx 2.8\,\mu B$ and an anti-ferromagnetic moment of $\approx 0.5\,\mu B$, which leads to the *effective* moment being given by

$$\beta_T^{\max} = [2.8/(1+\alpha) + 0.5\alpha/(1+\alpha)]. \tag{8.28}$$

This contrasts with the assumption made in virtually all other magnetic models that the value of β is independent of temperature. Several variants of the Shottky model have been developed by Miodownik (1977, 1978a) to take into account the situation where one of the two states subsequently undergoes magnetic ordering (Fig. 8.5). In such cases it may also be necessary to consider a temperature-dependent ΔE (Miodownik and Hillert 1980).

8.7.2 Thermodynamic consequences of multiple states

One of the consequences of accepting the presence of multiple magnetic states is an additional contribution to the entropy and, therefore, several authors have considered the inclusion of multiple states in their description of low-temperature phase transformations in Fe and its alloys (Kaufman *et al.* 1963, Miodownik 1970, Bendick and Pepperhoff 1978). However, most authors have, in the end, preferred to describe the magnetic effects in Fe using more conventional temperature-independent values for the magnetic moments of the relevant phases. This is partly linked to the absence of any provision for the necessary formalism in current

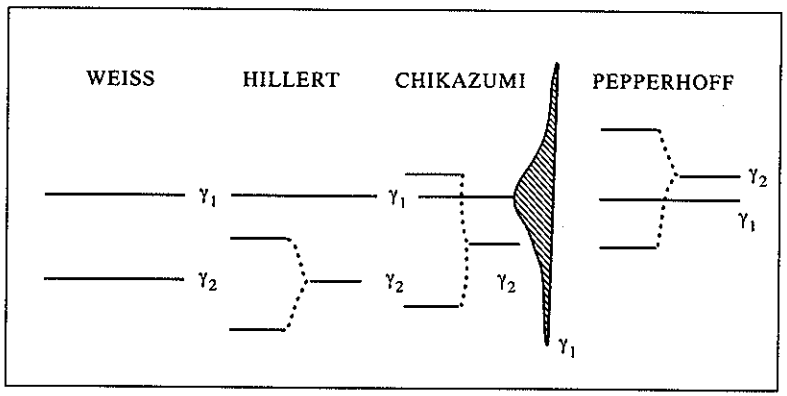

Figure 8.5. Schematic comparison of various two-state models (from Miodownik 1979).

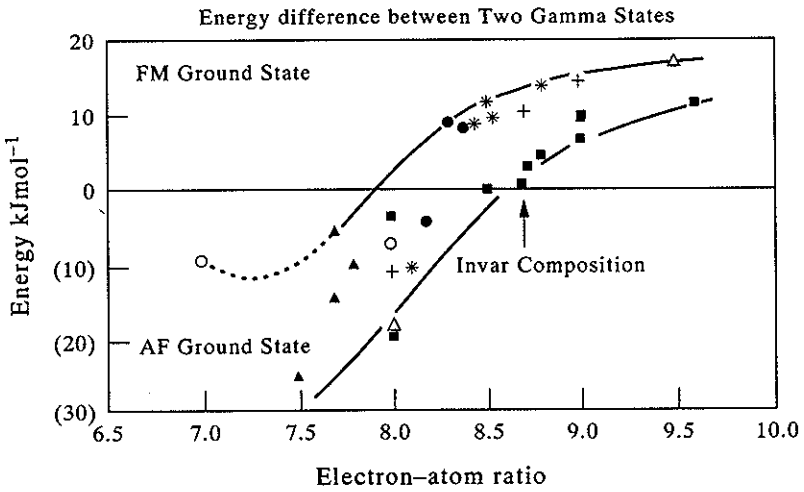

Figure 8.6. Variation of δE between two competing magnetic states with electron/atom ratio for some 3d elements (from de Fontaine *et al.* 1995). ■ Weiss (1963), ▲ Miodownik (1978b), • Bendick *et al.* (1977), * Bendick and Pepperhoff (1978), + Bendick *et al.* (1978), □ Moruzzi and Marcus (1990a), △ Moroni and Jarlsberg (1990), ○ Asada and Terakura (1995).

software packages for phase-diagram calculations, and also to the fact that, with the exception of Roy and Pettifor (1977), there was little theoretical backing for the concept of multiple states in its early stages of development.

It is interesting to note that recent electron energy calculations (Moroni and Jarlsberg 1990, Moruzzi and Marcus 1990a, b, Asada and Terakura 1995) have not only confirmed the necessary energetics for the existence of multiple states, but have also confirmed both the values of the moments (Table 8.2) and the energy gaps which had been previously inferred from experimental evidence (Fig. 8.6). It has therefore been suggested (de Fontaine *et al.* 1995) that future developments should make provision for the inclusion of multiple states. While having only a marginal effect on ΔG at high temperatures (Fig. 8.7a) such a model would lead to significant changes in the driving force for low-temperature (martensitic) transformations and, more importantly, should lead to better modelling of many associated changes in physical properties (Bendick and Pepperhoff 1978, Bendick *et al.* 1977).

8.8. CHANGES IN PHASE EQUILIBRIA DIRECTLY ATTRIBUTABLE TO G^{MAG}

The energy of magnetic transformations can be deceptively large, often exceeding that released by ordinary phase transformations. The following effects have been

References are listed on pp. 256–258.

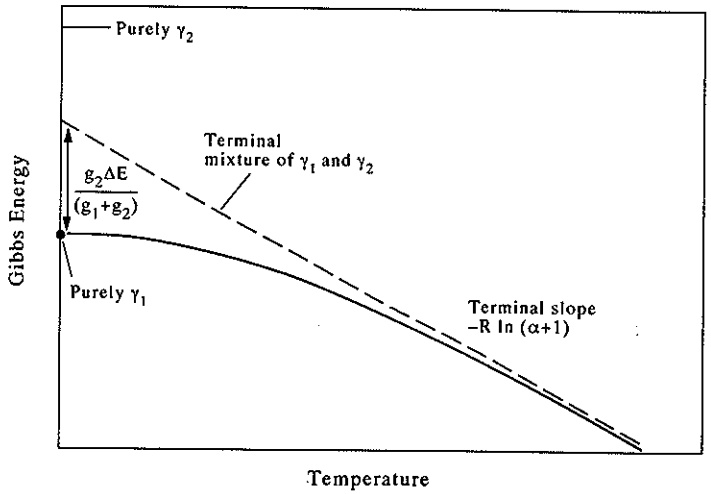

Figure 8.7. Variation of ΔG with temperature for a two-state model (from Miodownik 1977).

observed in various systems and confirmed by Gibbs energy calculations (Miodownik 1982).

A marked change in solid solubility. This occurs at the point where the solubility limit is intersected by the locus of magnetic transformation temperatures (Fig. 8.8). The magnitude of such effects obviously scales with the value of G^{mag}/dT and are most marked in Fe- and Co-rich alloys (Nishizawa *et al.* 1979, Hasebe *et al.* 1985). An interesting recent example is given by the Fe–Co–Zn system as the latter two elements have opposite effects on the Curie temperature of Fe (Takayama *et al.* 1995). In some early diagrams, such abrupt changes were inexplicable and deemed to be due to 'experimental error'.

Distortion of miscibility gaps. In the case of some miscibility gaps such intersections are accompanied by an even more marked distortion (Fig. 8.9). This is now often called the Nishizawa Horn, due to the extensive work of Nishizawa and coworkers (1979, 1992) on this effect, but it is interesting to note that the effect had previously been noted by Meijering (1963). Here, too, the apparent presence of more than one maximum in a miscibility gap was believed to represent experimental error before it was shown to have a sound theoretical foundation.

Continuous transition between first- and second-order transformations. When examined more closely, the Nishizawa Horn represents a situation where there is a continuous transition between a first- and second-order transformation. This remarkable situation is not restricted to systems which exhibit a miscibility gap (Inden 1981a) (Fig. 8.10), and it therefore remains to be seen whether it is possible to maintain a hard and fast distinction between these two types of transformation

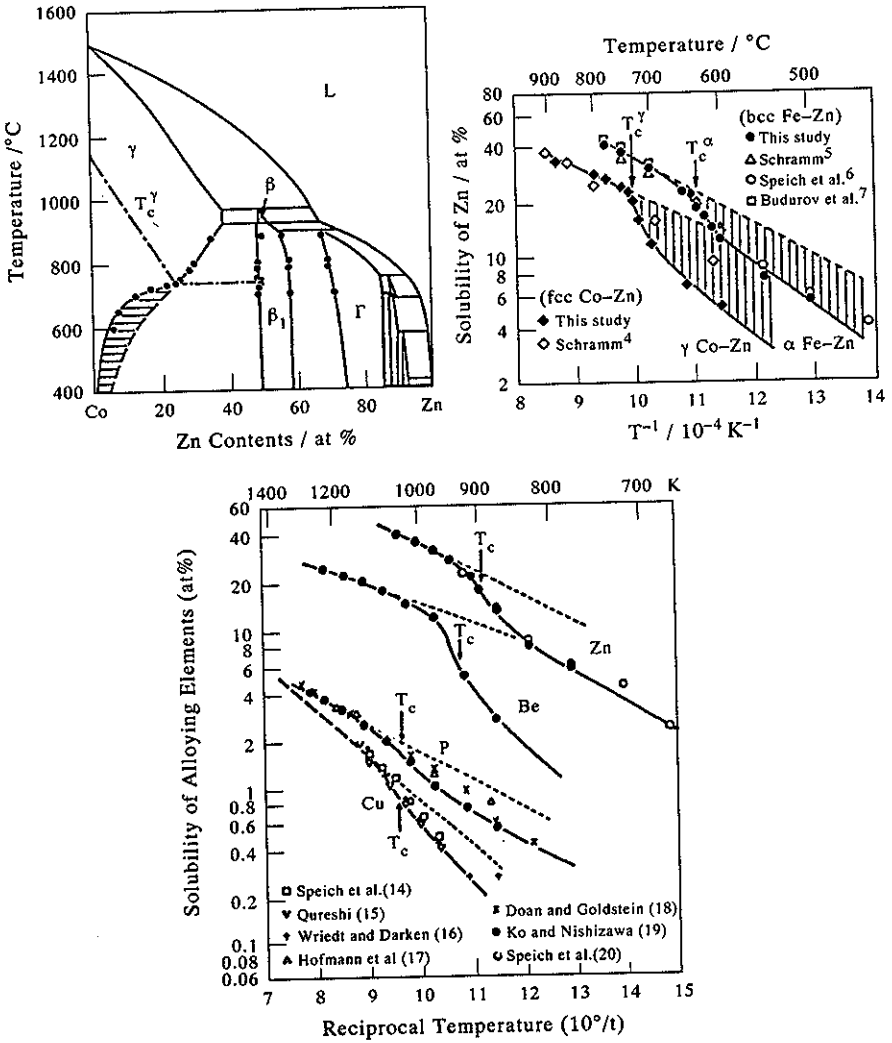

Figure 8.8. Change in solubility where a solubility transus is intersected by T_c (from Takeyama *et al.* 1995).

when faced with such well-documented effects (Hillert 1996).

Stabilisation of metastable phases by the magnetic Gibbs energy contribution. The allotropy of Fe represents an important example where, in the γ region of pure Fe, the Gibbs energy difference between b.c.c. Fe and f.c.c. Fe is small (50–60 J/mol). As a corollary, small changes in G_{mag} have an apparently disproportionate

References are listed on pp. 256–258.

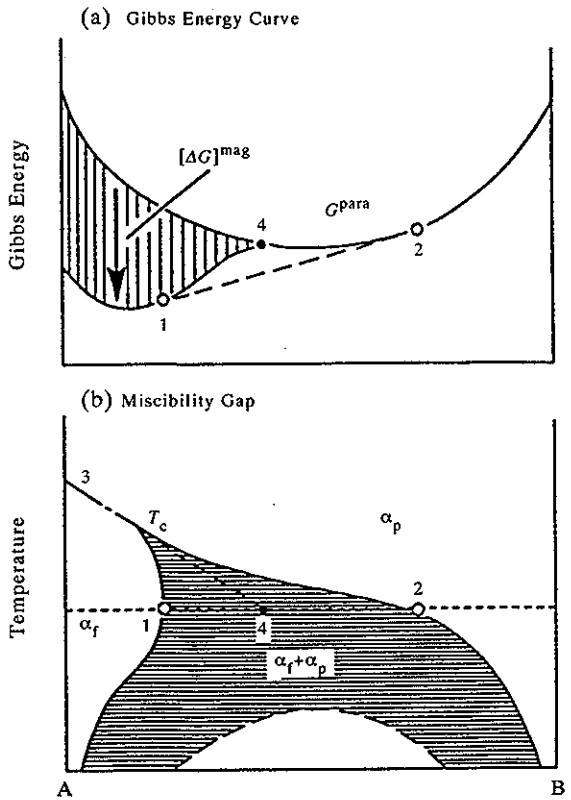

Figure 8.9. The formation of a Nishizawa Horn from the intersection of a magnetic transition and a miscibility gap (from Nishizawa 1992).

effect on the topography of the α/γ region in Fe-base alloys. Because of the location of the Curie temperature in pure Fe, the effect of magnetic forces on the A3 is much more pronounced than on the A4 and alloying additions can produce asymmetric effects on the two transitions (Zener 1955, Miodownik 1977, 1978a, b). Interestingly, although the Curie temperature of Co is much higher, the value of $G_{mag}^{f.c.c.-c.p.h.}$ is not as affected because the magnetic properties of both phases are similar (Miodownik 1977). However, because $S^{f.c.c.-c.p.h.}$ is also small, the allotropic transition temperature can be substantially reduced (Fig. 8.11).

Magnetic effects on metastable transformations. The underlying factor in all the above effects is the magnitude of the ratio (G^{mag}/G^{total}) and especially its variation with temperature. It follows that there can also be a substantial effect on the driving force for phase transformations, including shear transformations. Thus the martensite start temperature, $M_s^{\gamma\to\alpha}$, in most Fe alloys is dominated by the

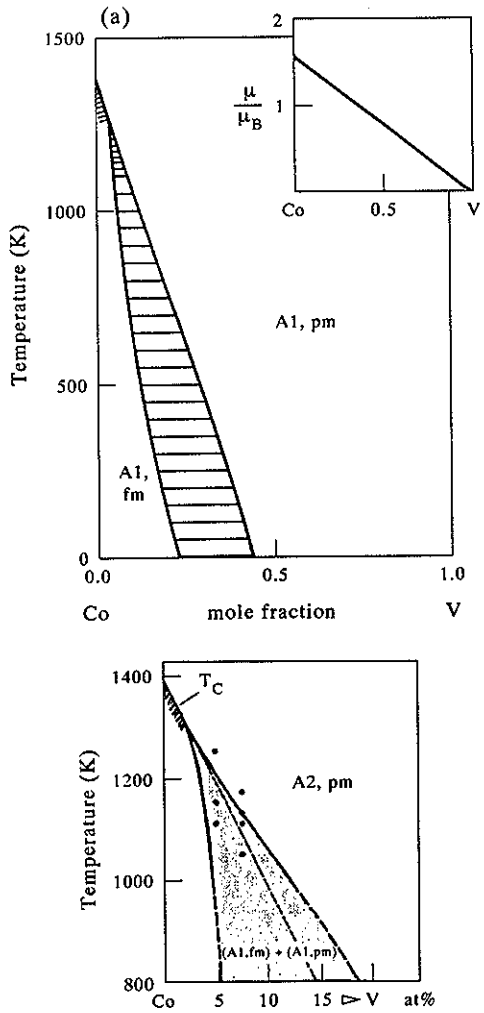

Figure 8.10. Continuous transition between first- and second-order transformations in Co–V alloys: (a) prediction and (b) experiment (from Inden 1985 and 1982).

ferromagnetism of the α phase while the $M_s^{\gamma\to\varepsilon}$ in Fe–Mn alloys is controlled by the anti-ferromagnetism of the γ phase (Miodownik 1982). Complex interactions can be expected in systems where the critical ordering temperatures for both chemical and magnetic ordering intersect (Inden 1982, Inden 1991, Skinner and Miodownik 1979), Fe–Si being a good example (Fig. 8.12).

Magnetic effects on stacking fault energy. As the width of a stacking fault in

References are listed on pp. 256–258.

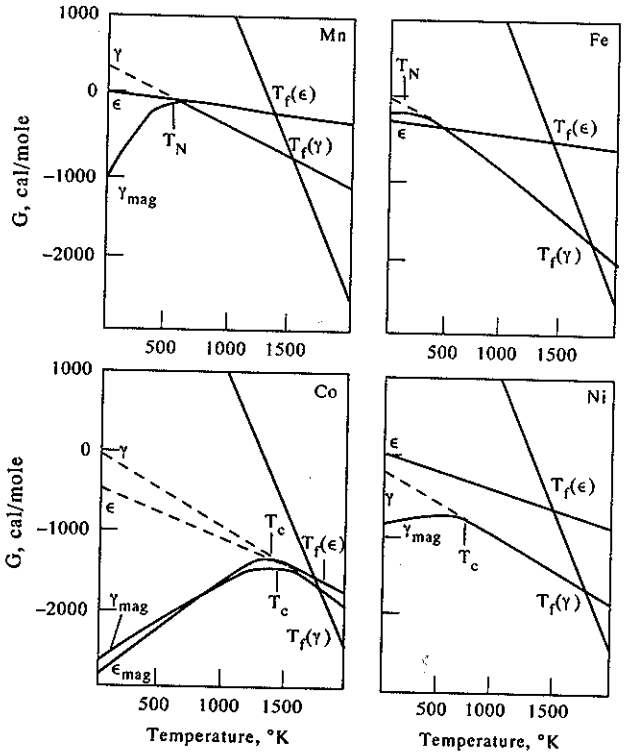

Figure 8.11. Effect of magnetic G on f.c.c.–c.p.h.-phase transitions in certain 3*d* elements (from Miodownik 1977).

f.c.c. lattices is a function of the Gibbs energy difference between f.c.c. and c.p.h. structures, this will also be affected by any magnetic component in either or both these structures (Fig. 8.11). This has been analysed by both Ishida (1975) and Miodownik (1978c). Although some of the parameters in both papers need to be re-examined in the light of more recent data, it is difficult to account for the observed trends without taking the magnetic Gibbs energy into consideration.

8.9. INTERACTION WITH EXTERNAL MAGNETIC FIELDS

All the effects noted above can be considered to arise from an *internal* magnetic field. But a Gibbs energy contribution, G_H^{mag}, is also generated if two phases differing in saturation magnetisation by an amount, ΔJ, are placed in an *external* magnetic field, **H**, and is given by

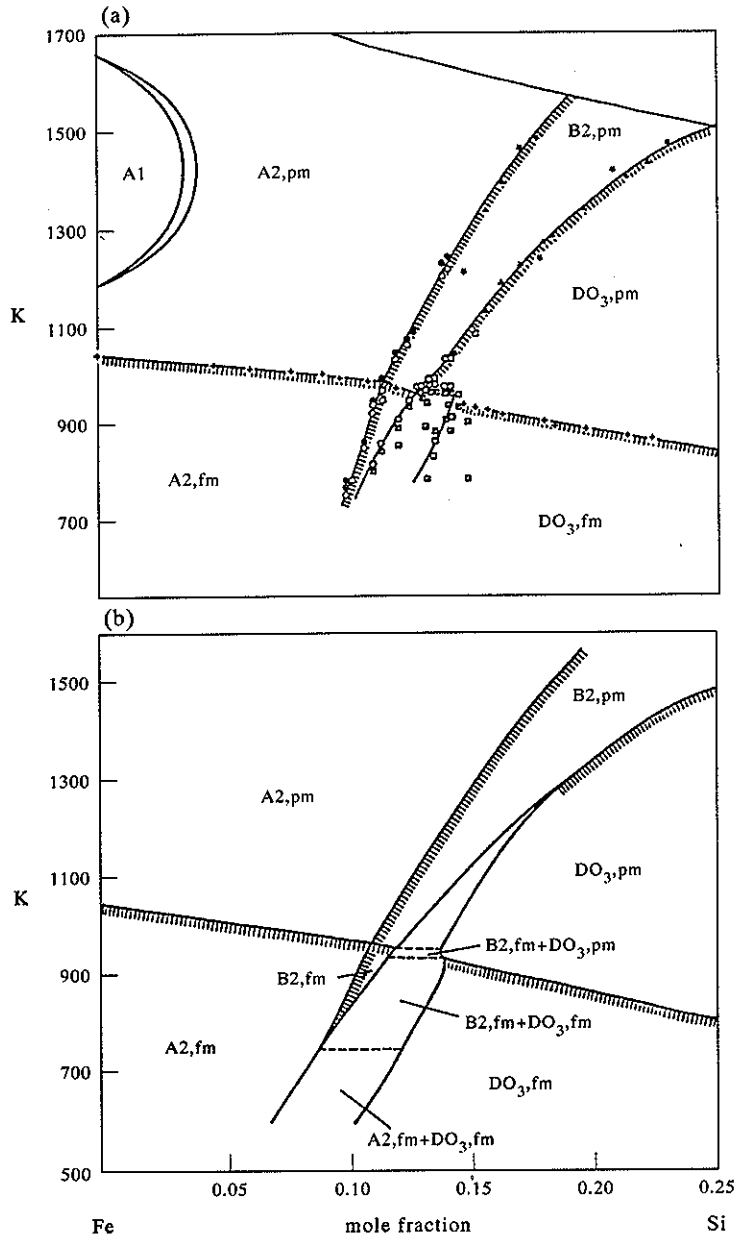

Figure 8.12. Equilibrium between magnetic and non-magnetic-ordered derivatives of b.c.c. Fe–Si alloys: (a) experimental and (b) calculated values (from Inden 1982).

References are listed on pp. 256–258.

$$G_{\mathbf{H}}^{\text{mag}} = \mathbf{H}\Delta J. \tag{8.24}$$

This term is entirely analogous to the more commonly recognised product $P\Delta V$ and is yet another constituent of the expression for the total Gibbs energy. The effect has been confirmed by many experiments and an external magnetic field can destabilise austenite during martensitic transformations, causing a rise in M_S temperature of approximately 3°K Tesla^{-1} (Sadovskiy *et al.* 1961, Fields and Graham 1976). This effect turns out to be directly proportional to the difference in entropy between the two phases (Satyanarayan *et al.* 1972). A magnetic field can also markedly alter the rate of transformation in isothermal martensite reactions (Peters *et al.* 1972, Kakeshita *et al.* 1993). While changes in M_S due to deformation are well known, the presence of high magnetic fields generated by superconductors at cryogenic temperatures can produce similar effects. Diffusion-controlled transformations are also prone to magnetic-field effects as the driving force for transformation is affected. Thus Fe–Co alloys can be converted from 100% austenite to 100% ferrite at elevated temperatures (Fig. 8.13) under the influence of a field generated by a conventional bench magnet (Peters and Miodownik 1973). The expansion of a miscibility gap and the precipitation of the σ phase in Fe–Cr alloys (Chen *et al.* 1983) are another example of effects that can be induced by an external field.

Although a magnetic field is not commonly applied, it has certain advantages in allowing a precise increment of Gibbs energy to be added instantaneously to a

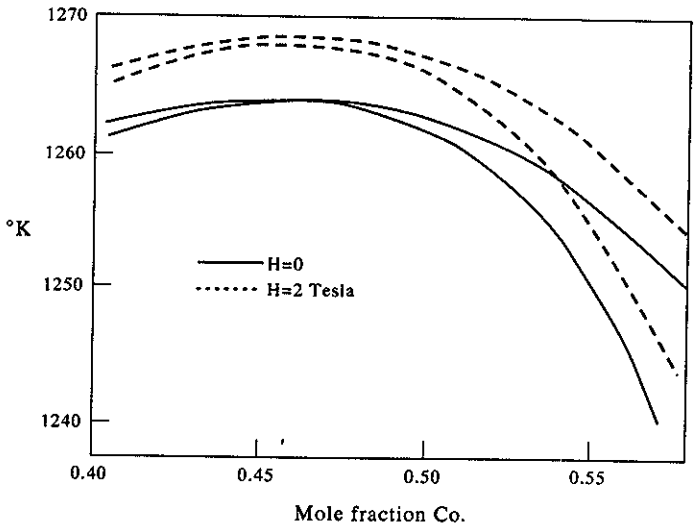

Figure 8.13. Effect of an external magnetic field on phase transformations in Fe–Co (from Peters and Miodownik 1973).

system simply by means of a field and without any requirement for direct contact with the specimen. It is also a salutary reminder that the Gibbs energy expressions in common use do not contain the complete range of terms implicit in Gibbs original formulation.

REFERENCES

Andersson, J.-O. (1985) *Int. J. Thermophysics*, **6**, 411.
Arita, M. (1978) *Acta Metall.*, **26**, 259.
Asada, T. and Terakura, K. (1995) in *Computer Aided Innovation of New Materials, Vol. 1*, eds Doyama, M. *et al.* (Elsevier Science, Amsterdam), p. 169.
Bendick, W. and Pepperhoff, W. (1978) *J. Phys. F*, **8**, 2535.
Bendick, W., Ettwig, H. H. and Pepperhoff, W. (1978) *J. Phys. F*, **8**, 2525.
Bendick, W., Ettwig, H. H., Richter, F. and Pepperhoff, W. (1977) *Z. Metallkde.*, **68**, 103.
Bozorth, R. M. (1956) in *Ferromagnetism* (Van Nostrand).
Chikazumi, S. and Matsui, M. (1978) *J. Phys. Soc. Japan*, **45**, 458.
Chin, C-P., Hertzman, S. and Sundman, B. (1987) TRITA-MAC 0203, Dept. Mat. Sci. Eng, Royal Institute of Technology, Sweden.
Chen, I-Wei, Faillace, E. and Miodownik, A. P. (1983) in *Ferritic Alloys for use in the Nuclear Energy Technologies*, eds Davis, J. W. and Michel, D. J. (AIME, Warrendale), p. 517.
Chuang, Y. Y., Schmid-Fester, R. and Chang, Y. A. (1985) *Met. Trans.*, **16A**, 153.
Chuang, Y. Y., Lin, J-C., Schmid-Fester, R. and Chang, Y. A. (1986) *Met. Trans.*, **17A**, 1361.
Clougherty, E. V. and Kaufman, L. (1963) *Acta. Met.*, **11**, 1043.
Colinet, C., Inden, G. and Kikuchi, R. (1993) *Acta. Metall.*, **41**, 1109.
de Fontaine, D., Fries, S. G., Inden, G., Miodownik, A. P., Schmid-Fetzer, R. and Chen, S. L. (1995) *CALPHAD*, **19**, 499.
Dinsdale, A. T. (1991) *CALPHAD*, **15**, 317.
Eriksson, O., Johansson, B., Albers, R. C. and Boring, A. M. (1990) *Phys. Rev. B*, **42**, 2707.
Ettwig, H. H. and Pepperhoff, W. (1974) *Phys. Sat. Solidi*, **23**, 105.
Fernandez Guillermet, A. (1987) *Int. J. Thermophysics*, **8**, 481.
Fields, R. and Graham, C. D. (1976) *Metall. Trans. A*, **7A**, 719.
Gazzara, C. P., Middleton, R. M. and Weiss, R. J. (1964) *Physics Letters*, **10**, 257.
Hasebe, M., Ohtani, H. and Nishizawa, T. (1985) *Metall. Trans.*, **16A**, 913.
Hillert, M. and Jarl, M. (1978) *CALPHAD*, **2**, 227.
Hillert, M., Wada, T. and Wada, H. (1967) *J. Iron and Steel. Inst.*, **205**, 539.
Hillert, M. (1996) Verbal communication at CALPHAD XXV, Erice, Sicily.
Hofmann, J. A., Paskin, A., Tauer, K. J. and Weiss, R. J. (1956) *J. Phys. Chem. Solids*, **1**, 45.
Inden, G. (1975) *Z. Metallkde.*, **66**, 577.
Inden. G. (1976) Proc. Calphad V (Dusseldorf) III-(4)-1.
Inden, G. (1977) *Z. Metallkde.*, **68**, 529.
Inden, G. (1981a) *Physica. B*, **103**, 82.
Inden, G. (1981b) *Scripta Metall.*, **15**, 669.
Inden, G. (1982) *Bull. Alloy. Phase. Diag.*, **2**, 412.

Inden, G. (1991) *Scand. J. Met.*, **20**, 112.
Inden, G. and Pitsch, W. (1991) in *Materials Science and Technology, Vol. 5*, ed. Haasen, P. (VCH Verlagsgeselleschaft, Weinheim), p. 497.
Ishida, K. (1975) *Phil. Mag.*, **32**, 663.
Kakeshita, T., Kuroiwa, K., Shimizu, K., Ikeda, T., Yamagishi, A. and Date, M. (1993) *Mat. Trans. Jap. Inst. Met.*, **34**(5), 415.
Kaufman, L. and Cohen, M. (1956) *Trans. AIME*, **206**, 1393.
Kaufman, L. and Cohen, M. (1958) *Progress in Metal Physics*, **7**(3), 165.
Kaufman, L. and Nesor, H. (1973) *Z. Metallkde.*, **64**, 249.
Kaufman, L., Clougherty, E. V. and Weiss, R. J. (1963) **11**, 323.
Ko, M. and Nishizawa, T. (1979) *J. Japan. Inst. Metals*, **43**, 126.
Kosakai, T. and Miyazaki, T. (1994) *Iron and Steel Inst. Japan*, **34**, 373.
Lytton, J. L. (1964) *J. Appl. Phys.*, **35**, 2397.
Meschter, P. J., Wright, J. W. and Brooks, C. R (1981) *J. Phys. Chem. Sol.*, **42**, 861.
Meijering, J. L. (1963) *Philips Res. Report*, **18**, 318.
Miodownik, A. P. (1970) *Acta Met.*, **18**, 541.
Miodownik, A. P. (1977) *CALPHAD*, **1**, 133.
Miodownik, A. P. (1978a) in *Honda Memorial Volume on Metal Science and Metallurgy*, in *Physics and Application of Invar Alloys*, ed. Saito, H. (Maruzen) **3**(18), p. 429.
Miodownik, A. P. (1978b) in *Honda Memorial Volume on Metal Science and Metallurgy*, in *Physics and Application of Invar Alloys*, ed. Saito, H. (Maruzen) **3**(12), p. 288.
Miodownik, A. P. (1978c) *CALPHAD*, **2**(3), 207.
Miodownik, A. P. and Hillert, M. (1980) *CALPHAD*, **4**, 143.
Miodownik, A. P. (1982) *Bull. Alloy. Phase. Diag.*, **2**, 406.
Moran-Lopez, J. L. and Falicov, L. M. (1979) *Sol. Stat. Comm.*, **31**, 325.
Moroni, E. G. and Jarlsberg, T. (1990) *Phys. Rev. B*, **41**, 9600.
Moruzzi, V. L. and Marcus, P. L. (1988) *Phys. Rev. B*, **38**, 1613.
Moruzzi, V. L. and Marcus, P. L. (1990a) *Phys. Rev. B*, **42**, 8361.
Moruzzi, V. L. and Marcus, P. L. (1990b) *Phys. Rev. B*, **42**, 10,322.
Nishizawa, T. (1978) *Bull. Japanese Inst. Metals*, **17**, 780.
Nishizawa, T. (1992) *Mat. Trans. Japanese Inst. Metals*, **33**, 713.
Nishizawa, T., Hasebe, M., and Ko, M. (1979) *Acta. Met.*, **27**, 817.
Paskin, A. (1957) *J. Phys. Chem. Solids*, **2**, 232.
Peters, C. T. and Miodownik, A. P. (1973) *Scripta Met.*, **7**, 955.
Peters, C. T., Bolton, P. and Miodownik, A. P. (1972) *Acta Met.*, **20**, 881.
Roy, D. M. and Pettifor, D. G. (1977) *J. Phys. F*, **7**, 183.
Sadovskiy, V. D., Rodigin, L., Smirnov, L. V., Filonchik, G. M. and Fakidov, I. G. (1961) *Phys. Met. Metallography*, **12**(2), 131.
Saito, H., Arrott, A. and Kikuchi, R. (1959) **10**, 19.
Satyanarayan, K. R., Eliasz, W. and Miodownik, A. P. (1972) *Acta. Met.*, **16**, 877.
Schon, C. G. and Inden, G. (1996) *Scripta Mater. Met.*, **30**, 000.
Semenovskoya, S. V. (1974), *Phys. Stat. Sol. B*, **64**, 291.
Skinner, D. and Miodownik, A. P. (1979) in *Proc. Int. Symp. on Martensitic Transformations: ICOMAT II*, eds Cohen, M. and Owen, W. (MIT, Boston), p. 259.
Smith, D. (1967) *Scripta Met.*, **1**, 157.
Takayama, T., Shinohara, S., Ishida, K. and Nishizawa, T. (1995) *J. Phase Equilibria*, **16**, 390.